

2012

Investigation of Premature Distress Around Joints in PCC Pavements: Parts I & II

Maria del Mar Arribas-Colón
Maria.Arribas-Colon@nrc.gov

Mateusz Radliński
mradlinski@exponent.com

Jan Olek
Purdue University - Main Campus, olek@purdue.edu

Nancy Whiting
Purdue University - Main Campus, whiting@purdue.edu

Recommended Citation

Arribas-Colón, M., M. Radliński, J. Olek, and N. Whiting. *Investigation of Premature Distress Around Joints in PCC Pavements: Parts I & II*. Publication FHWA/IN/JTRP-2012/25 & FHWA/IN/JTRP-2012/26. Joint Transportation Research Program, Indiana Department of Transportation and Purdue University, West Lafayette, Indiana, 2012. doi: 10.5703/1288284315019.

JOINT TRANSPORTATION RESEARCH PROGRAM

INDIANA DEPARTMENT OF TRANSPORTATION
AND PURDUE UNIVERSITY



INVESTIGATION OF PREMATURE DISTRESS AROUND JOINTS IN PCC PAVEMENTS: PARTS I & II

Maria del Mar Arribas-Colón

Graduate Research Assistant
School of Civil Engineering, Purdue University

Mateusz Radliński

Graduate Research Assistant
School of Civil Engineering, Purdue University

Jan Olek

Professor of Civil Engineering
Construction Materials Engineering
School of Civil Engineering, Purdue University
Corresponding Author

Nancy M. Whiting

Concrete Research Scientist
Applied Concrete Research Initiative
School of Civil Engineering, Purdue University

SPR-3016

Report Numbers: FHWA/IN/JTRP-2012/25 & FHWA/IN/JTRP-2012/26

DOI: 10.5703/1288284315019

RECOMMENDED CITATION

Del Mar Arribas-Colón, M., M. Radliński, J. Olek, and N. M. Whiting. *Investigation of Premature Distress Around Joints in PCC Pavements: Parts I & II*. Publication FHWA/IN/JTRP-2012/25 & FHWA/IN/JTRP-2012/26. Joint Transportation Research Program, Indiana Department of Transportation and Purdue University, West Lafayette, Indiana, 2012. doi: 10.5703/1288284315019.

CORRESPONDING AUTHOR

Professor Jan Olek
School of Civil Engineering
Purdue University
(765) 494-5015
olek@purdue.edu

JOINT TRANSPORTATION RESEARCH PROGRAM

The Joint Transportation Research Program serves as a vehicle for INDOT collaboration with higher education institutions and industry in Indiana to facilitate innovation that results in continuous improvement in the planning, design, construction, operation, management and economic efficiency of the Indiana transportation infrastructure.

https://engineering.purdue.edu/JTRP/index_html

Published reports of the Joint Transportation Research Program are available at: <http://docs.lib.purdue.edu/jtrp/>

NOTICE

The contents of this report reflect the views of the authors, who are responsible for the facts and the accuracy of the data presented herein. The contents do not necessarily reflect the official views and policies of the Indiana Department of Transportation or the Federal Highway Administration. The report does not constitute a standard, specification or regulation.

1. Report No. FHWA/IN/JTRP-2012/25 FHWA/IN/JTRP-2012/26		2. Government Accession No.		3. Recipient's Catalog No.	
4. Title and Subtitle Investigation of Premature Distress Around Joints in PCC Pavements: Parts 1 and 2				5. Report Date October 2012	
				6. Performing Organization Code	
7. Author(s) Maria del Mar Arribas-Colón, Mateusz Radliński, Jan Olek, Nancy Whiting				8. Performing Organization Report No. FHWA/IN/JTRP-2012/25 FHWA/IN/JTRP-2012/26	
9. Performing Organization Name and Address Joint Transportation Research Program Purdue University 550 Stadium Mall Drive West Lafayette, IN 47907-2051				10. Work Unit No.	
				11. Contract or Grant No. SPR-3016	
12. Sponsoring Agency Name and Address Indiana Department of Transportation State Office Building 100 North Senate Avenue Indianapolis, IN 46204				13. Type of Report and Period Covered Final Report	
				14. Sponsoring Agency Code	
15. Supplementary Notes Prepared in cooperation with the Indiana Department of Transportation and Federal Highway Administration.					
16. Abstract <p>Some of the Indiana concrete pavements constructed within the last 10-20 years have shown signs of premature deterioration, especially in the areas adjacent to the longitudinal and transverse joints. This deterioration typically manifested itself as cracking and spalling of concrete combined with the loss of material in the direct vicinity of the joint. In addition, in some cases "bulb-shaped" damage zones were also observed under the sealed parts of the joints.</p> <p>The objective of this study was to investigate possible causes of this premature deterioration. To reach this objective, the characteristics of the concrete in and near the deteriorated joints were compared and contrasted to the concrete characteristics in the non-deteriorated sections of pavement. The study was conducted in two different phases (Phase I and Phase II), and the findings are presented as a two-part report.</p> <p>The investigation started with a detailed inventory of selected areas of affected pavements in order to identify and classify the existing types of distresses and select locations for collection of the cores. During the Phase I of the study a total of 36 concrete cores were extracted from 5 different pavements.. During Phase II of the study a total of 18 cores were retrieved from five different pavement sections and subject to examination. The cores were subjected to eighth different tests: air-void system determination, Scanning Electronic Microscopy (SEM) analysis, X-ray diffraction (XRD) analysis, sorptivity test, freeze-thaw & resonance frequency test, resistance to chloride ion penetration (RCP) test and chloride profile (concentration) determination.</p> <p>The test results identified several cases of in-filling of the air voids (especially smaller air bubbles) with secondary deposits. These deposits were most likely the result of the repetitive saturation of air voids with water and substantially reduced the effectiveness of the air voids system with respect to providing an adequate level of freeze-thaw protection. Specifically, it was observed that the existing air void system in the concrete from panels near the deteriorated longitudinal joint had neither spacing factors nor specific surface values within the range recommended for freeze-thaw durability. Contrary to this, nearly all the concrete in lanes without damage had an adequate air void system at the time of sampling. In addition, the affected concrete often displayed an extensive network of microcracks, had higher rates of absorption and reduced ability to resist chloride ions penetration.</p> <p>From the observation of the drains performed using the remote camera it was obvious that not all the drains were functioning properly and some were entirely blocked. However, more precise or direct correlations could not be made between the conditions of the drains and observed pavement performance.</p>					
17. Key Words Portland cement concrete pavements, joints, deterioration, chlorides, air voids, SPR-3016			18. Distribution Statement No restrictions. This document is available to the public through the National Technical Information Service, Springfield, VA 22161.		
19. Security Classif. (of this report) Unclassified		20. Security Classif. (of this page) Unclassified		21. No. of Pages 75	22. Price

INVESTIGATION OF PREMATURE DISTRESS AROUND JOINTS IN PCC PAVEMENTS

PART I

SPR-3016

Report Number: FHWA/IN/JTRP-2012/25

DOI: 10.5703/1288284315019

EXECUTIVE SUMMARY

INVESTIGATION OF PREMATURE DISTRESS AROUND JOINTS IN PCC PAVEMENTS: PART I

Introduction

Some of the concrete pavements constructed within the last 10 to 20 years have shown signs of premature deterioration, especially in the areas adjacent to the longitudinal and transverse joints. This deterioration typically manifested itself as cracking and spalling of concrete, combined with the loss of material in the direct vicinity of the joint. In addition, “bulb-shaped” damage zones were also observed under the sealed parts of the joints.

The objective of this study was to investigate possible causes of this premature deterioration. To reach this objective, the characteristics of the concrete in and near the deteriorated joints were compared and contrasted to the characteristics of the concrete in the non-deteriorated sections of pavement. The study was conducted in two different phases (Phase I and Phase II), and the findings are presented as a two-part report.

During the Phase I of the study, a total of 36 concrete cores were extracted from five different pavements. While Phase I provided important preliminary information as to the potential causes of deterioration, it also demonstrated the need for a more focused approach that would eliminate such variables as the age of the pavement, site-specific subgrade and environmental conditions, materials variability, and quality of construction.

These goals were accomplished in Phase II of the study, which provided the opportunity to directly compare sections that were (1) paved under one construction project by the same contractor, (2) that used similar mix designs and materials, and (3) were most likely exposed to similar environments and deicing practices but showed very different performances. Several pavement sections were in good condition, while one section showed significant deterioration at the longitudinal joints. During Phase II of the study a total of 18 cores were retrieved from five different pavement sections and examined. In addition, where feasible the base material was sampled and the drainage observed at each core hole.

Findings

In general, the cores that came from the mid-span of the slabs included in Phase I of the study had better air void systems than those extracted from locations near the joints. They also had good resistance to freezing and thawing cycles, relatively low rates of absorption, and were classified as having low or very low resistance in the rapid chloride ion permeability test. The only exception was the core containing slag aggregates.

The cores that came from the undamaged joints showed marginal to substandard air void system parameters, higher rates of absorption than the mid-span cores, variable F-T durability (with most specimens having DF above 60%) and low to moderate resistance in the rapid chloride permeability test. The cores that exhibited higher rates of absorption also exhibited lower durability factors (freeze-thaw test). Moreover, it was noted that cores from undamaged joints contained a considerable quantity of small (~10 µm) air voids filled with either ettringite, Friedel’s salt, or a combination of both. However, numerous empty air voids were also present in these cores.

The cores that came from the damaged joints mostly exhibited a poor air void system, showed evidence of some of the highest rates

of absorption, displayed moderate to high chloride ion penetrability, and achieved relatively low values of the F-T durability factors. Additionally, it was noted that these cores contained numerous microcracks and infilled air voids (both small and large). The secondary (infilling) deposits contained ettringite, Friedel’s salt, or a combination of both.

In general, the observed microstructural and chemical changes in Phase I cores were consistent with the appearance of concrete undergoing prolonged saturation (through-solution mechanism for creating deposits in the air voids).

Similar to those observed in Phase I of the study, the concrete samples collected in Phase II also contained a certain amount of infilling of the air void system by secondary deposits. Furthermore, it was observed that the existing air void system in the concrete from panels near the deteriorated longitudinal joint had neither spacing factors nor specific surface values within the range recommended for freeze-thaw durability. Contrary to this, nearly all of the concrete in lanes without damage had an adequate air void system at the time of sampling.

From the observation of the drains performed by the remote camera it was evident that not all of the drains were functioning properly and some were entirely blocked. However, more precise or direct correlations could not be made between the functioning of the drains and observed pavement performance.

Finally, the data collected during this study were limited and thus not sufficient to definitely and unambiguously determine the single cause of joint deterioration. Rather, the results seem to indicate that the observed deterioration is most likely caused by combination of several variables that may include type of deicers used, type of subgrade, structural design of the pavement, and type of the sealant in the joint.

Implementation

This study provided the Indiana Department of Transportation (INDOT) with first-of-its-kind data regarding the changes in the microstructure of pavement concrete in the vicinity of joints affected by premature deterioration. These data strongly suggest that the high degree of saturation in the vicinity of the sealed joints contributed to their failure by reducing the freeze-thaw resistance of concrete. In addition to saturating the concrete, the constant presence of the high levels of moisture also resulted in significant infilling of the existing air void systems with secondary deposits, thus reducing their effectiveness.

Considering the limited nature of this study, the following implementation actions can be suggested:

1. Necessary steps should be taken to ensure an adequate air void system in the hardened concrete, especially in the vicinity of the joints. The commonly accepted measures of the quality of the air void system needed to ensure of the freeze-thaw resistant concrete include the specific surface area of the air bubbles of at least 600 in.²/in.³ and a spacing factor not greater than 0.008 in. Although having an elevated content of air voids in fresh concrete does not guarantee the quality of the air void system in the hardened concrete, a larger amount of air will generally help. This points to the importance of generating a sufficient quantity of air bubbles in the fresh concrete as some air will be lost due to transport, paving, and consolidation operations. Recent data collected from the SR 26 project in Lafayette, Indiana, indicated that the air content in hardened concrete may be as much as 3% lower than the air content of fresh concrete (measured right after concrete has been discharged from the mixer).

2. Serious consideration should be given to reducing the penetration of water into the concrete at the joints. Water trapped under the sealer will keep the concrete saturated and thus more susceptible to freezing and thawing damage. Furthermore, the degree of saturation will increase in the presence of deicers. Potential solutions may involve applying water repelling penetrating sealers to the surface of the joints, a more rigorous inspection and maintenance program for the sealers in the joints, or use of the unsealed joint in combination with the penetrating sealers.
3. INDOT should consider construction of the test sections to verify some of the solutions proposed in Part II of this report.

It would be useful to establish a data base that can collect information from future paving projects with respect to characteristics of materials used, deicing practices, weather conditions, sealer conditions, and quality of the air void system in the hardened concrete. Having such a database will be very beneficial in addressing future maintenance needs of concrete pavements.

The benefits of this research include:

- Assemblage of detailed field data on the conditions of concrete in the vicinity of the deteriorated joints, which would be useful to INDOT maintenance personnel in the process of selection of rehabilitation and preservation treatments.
- Generation of fundamental information regarding the potential mechanism of deterioration (damage resulting from freezing and thawing of saturated concrete, potentially enhanced by the lack of an adequate air void system, trapping of moisture under the partially damaged seal, and use of deicing chemicals).
- Increased level of awareness among INDOT's engineers and contractors of the factors contributing to observed deterioration, which, if confirmed by additional studies, will lead to changes in specifications with respect to concrete performance requirements and design, construction, and deicing practices.

CONTENTS

1. INTRODUCTION.....	1
2. CORING AND TESTING.....	1
2.1 Coring.....	1
2.2 Testing.....	3
3. RESULTS.....	3
3.1 Hardened Concrete Air Void Analysis.....	3
3.2 Infilling of Air Voids—Optical Microscopy Evidence.....	5
3.3 Infilling of Air Voids—Scanning Electron Microscope (SEM) Evidence.....	5
3.4 Sorptivity.....	6
3.5 The Freeze-Thaw Test.....	6
3.6 Resistance to Chloride Penetration Test.....	7
3.7 Chloride Ion Concentration with Depth.....	7
4. SUMMARY AND CONCLUSIONS.....	8
4.1 Summary.....	8
4.2 Discussion.....	9
4.3 Conclusions.....	9
REFERENCES.....	9

LIST OF TABLES

Table	Page
Table 2.1 Summary of number of cores obtained from specific pavement areas	2
Table 3.1 Air void system characteristics, voids infilling, F-T resistance and RCP data	4

LIST OF FIGURES

Figure	Page
Figure 1.1 Condition of the EB pavement at W. 86 th St.	1
Figure 1.2 Examples of water accumulation in the longitudinal joints	1
Figure 2.1 Specific pavement areas from which cores were collected	2
Figure 2.2 Schematic of the location of test specimen cut from each core	2
Figure 3.1 Example of the existing air content and spacing factor (US 67 cores)	5
Figure 3.2 Typical appearances of the infilled voids (a) and empty air voids (b) as seen using optical microscopy	6
Figure 3.3 SEM image from a specimen from SR 67 showing an air void completely filled with mixture of ettringite (spectrum, left) and Friedel's salt (spectrum, right)	6
Figure 3.4 Numerous large air voids filled with ettringite (left and right) and some cracks in the matrix (right)	7
Figure 3.5 Chloride ion concentration profile for mid-span cores	8
Figure 3.6 Chloride ion concentrations profiles (from joint faces inward) for undamaged joints (left) and damaged joints (right)	8

1. INTRODUCTION

Some of the Indiana concrete pavements constructed within the last 10 to 20 years have recently shown signs of premature deterioration, especially in the areas adjacent to the longitudinal and transverse joints. This deterioration typically manifests itself as cracking and spalling of concrete combined with the loss of material in the direct vicinity of the joint (see Figures 1.1a and 1.1b) (1). In addition, “bulb-shaped” damage zones were also observed under the sealed parts of the joint (see Figure 1.1c).

The in-situ evaluation of the affected areas of the pavements revealed that, in many cases, the longitudinal joints continued to hold water long after the wetting event (see Figure 1.2).

The objective of this study was to examine the changes in the microstructure and chemistry of concrete extracted from several pavements (and from different

locations within the slabs of each pavement) affected by this premature deterioration. It is hoped that the results of this investigation will help with the development of improved construction and maintenance guidelines aimed at preventing and eliminating this type of distress in future projects.

2. CORING AND TESTING

2.1 Coring

The location of specific sections of pavements for retrieval of the cores used in the examination was established in cooperation with the Indiana Department of Transportation (INDOT) and the Indiana Chapter of the American Concrete Pavement Association (ACPA). These locations were as follows:

- SB lanes of I-65 near downtown Indianapolis (5 cores)
- SR 933 near South Bend (3 cores)



Figure 1.1 Condition of the EB pavement at W. 86th St. (east of the intersection with N. Payne Rd. in Indianapolis, Indiana, referred to as AL location): (a) general view, (b) close-up of damaged region near the intersection of transverse and longitudinal joints and (c) example of bulb-shaped damage zone under the joint sealant (1).

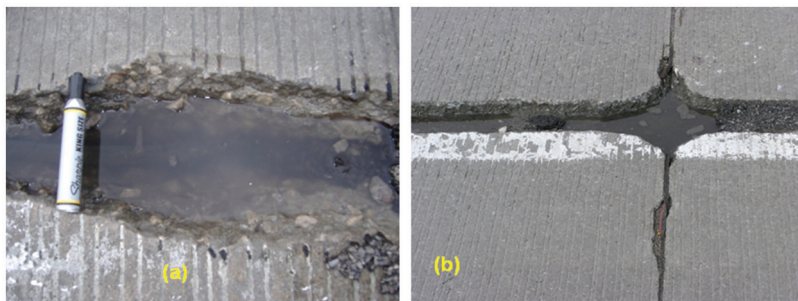


Figure 1.2 Examples of water accumulation in the longitudinal joints: (a) close-up of the longitudinal joint, (b) intersection of the longitudinal and transverse joints.

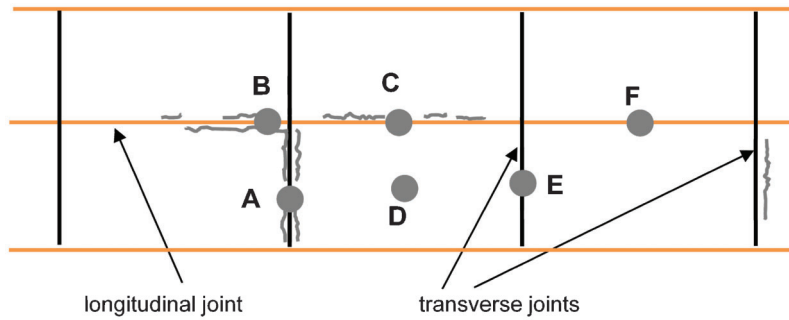


Figure 2.1 Specific pavement areas from which cores were collected (I).

- EB lanes of 86th St. at the intersection with Payne Rd., Indianapolis (17 cores) (NOTE: this location included two different sections: one located west of the traffic lights at the intersection (BL) and one located east of the traffic lights at the intersection (AL))
- EB ramp from US 67 to I-465 E, SW Indianapolis (11 cores)

At all of these locations an attempt was made to obtain at least one core from the specific areas of the pavement shown in Figure 2.1 (I). These specific areas included:

- A**—damaged area of the transverse joint
- B**—damaged area of the longitudinal joint near the transverse joint

- C**—damaged area of the longitudinal joint away from the transverse joint
- D**—mid-span of the slab, undamaged section
- E**—undamaged transverse joint adjacent to the damaged transverse joint
- F**—undamaged area of the longitudinal joint

The number and types of cores retrieved from each project site are detailed in Table 2.1. In total, thirty-six 6-in. cores were collected for examination.

Test specimens were cut from each of the collected cores as shown in Figure 2.2 (I). In cases where the core was excessively damaged, the cutting scheme had to be modified, thus effectively eliminating some of the test specimens.

TABLE 2.1
Summary of number of cores obtained from specific pavement areas

Location	Mid-span of the Slab (D)	Joints		Total
		Transverse	Longitudinal	
Ramp, US 67	4 (D)	2 (A), 2 (E)	3 (F)	11
W 86 th St., west of the traffic light @ N. Payne Rd. (BL)	6 (D)	—	—	6
W. 86 th St., east of the traffic light @ N. Payne Rd. (AL)	6 (D)	1 (A), 1 (E)	2 (C), 1 (B)	11
SR 933	2 (D)	1 (E)	—	3
I-65	—	—	3 (C), 1 (B), 1 (F)	5

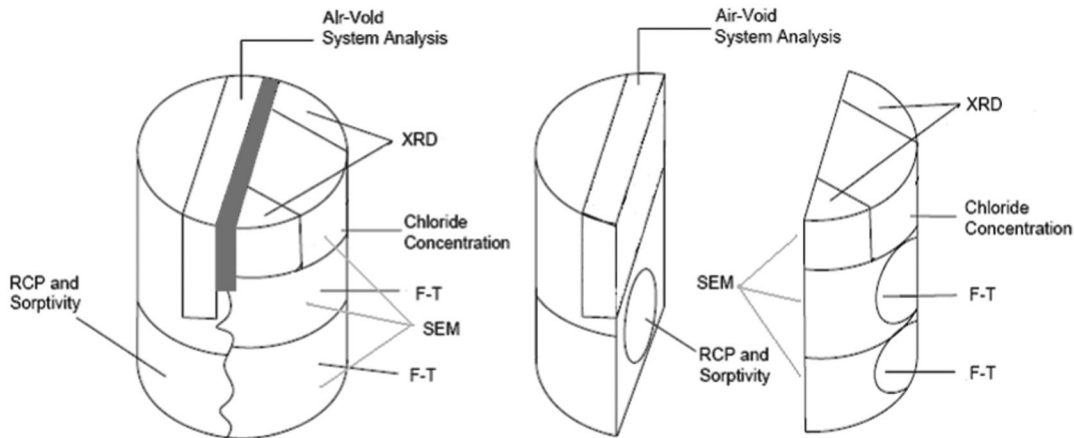


Figure 2.2 Schematic of the location of test specimen cut from each core.

2.2 Testing

To characterize the concrete and try to identify the cause of deterioration the cores were subjected to the following examinations:

- Analysis of air void system in hardened concrete (ASTM C457)
- Scanning Electronic Microscopy (SEM) analysis of concrete microstructure and energy dispersive spectroscopy (EDS) analysis of secondary deposits in the air bubbles
- X-ray Diffraction (XRD) analysis of powdered concrete
- Evaluation of water sorptivity
- Evaluation of freeze-thaw resistance (modified ASTM C666)
- Evaluation of resistance to chloride ions in press by ASTM C1202 chloride ion penetration (RCP) test
- Determination of chloride profile (concentration)

3. RESULTS

3.1 Hardened Concrete Air Void Analysis

The complete summary of the air void system parameters obtained by examining cores from each of the previously mentioned locations is provided in Table 3.1 (I). It should be noted that the typical target air void parameters recommended for adequate freeze-thaw protection of concrete are a spacing factor of less than 0.008 in. and specific surface of 600 in.²/in.³ or greater.

In northern climates, the concrete used for construction of pavements is typically air-entrained to prevent frost damage. This damage is the result of destructive pressure that can build up inside the wet concrete exposed to freezing temperatures (2,3). The Indiana DOT has a target total air value for concrete pavement of $6.5\% \pm 1.5\%$. Although the total air content is typically not a good indicator of the freezing and thawing resistance of concrete (4,5), it is nevertheless used as such in the specifications as it is measureable during construction. When specifying the target percent air value, it is assumed that an adequate amount of small entrained air bubbles have been produced within concrete microstructure to ensure an appropriate dispersion (spacing) of the air bubbles. The dispersion of the air bubbles (characterized by their spacing factor) and their average size (characterized by the parameter called the “specific surface area”) are considered to be much better indicators of the freezing-thawing resistance of concrete than the total percent of entrained air. This is because both of these parameters directly influence the length of the path the water in the freezing concrete has to travel before being able to escape to an empty air void. As such, these parameters directly control the extent of the internal pressure built up.

As an example, Figure 3.1 shows the analysis of air voids system for cores removed from SR 67. In this example, the *total* (entrained plus entrapped) air content for 7 of the 10 cores fell within the range

required by INDOT’s specifications ($6.5 \pm 1.5\%$). However, with the exception of three cores (SR67_5F, SR67_7F and SR67_9D), the *existing entrained air content* was lower than 4%.

While this finding seems to imply that perhaps the concrete did not contain sufficient amount of entrained air, the reader should be aware of the following limitations of the study: (a) only the voids that appeared empty when examined under the optical microscope (at magnification of 60X) were counted in determining the air content and (b) the distinction between the entrained and entrapped air while based on a predetermined criteria (shape and size of the void) was inherently arbitrary. It is also interesting to note that in all three cases when the entrained air content was higher than 4% the cores came from the undamaged parts of the pavement (locations D and F in Figure 2.1).

As already mentioned, all values reported in Table 3.1 are based exclusively on those voids that appeared empty when observed at the magnification of 60x using the optical microscope. This approach was adopted for two reasons: (a) the air voids which were infilled with the secondary deposits were very difficult to distinguish from the matrix itself and (b) it was assumed that (if present) the deposits in the voids will severely restrict (or totally eliminate) the ability of these voids to offer freeze-thaw protection to concrete. As a result, the total observed values of air content listed in Table 3.1 will *always be lower* than the air content values present in the same concrete at the time of construction.

The results presented in Table 3.1 indicate that the US 67 Ramp had existing entrained air content ranging from 6.2% to 2.1% and spacing factors ranging from 0.004 to 0.025. Approximately half of the cores had spacing factors well above 0.008 in., the maximum value recommended to provide F-T resistance (lowest total air) suggesting an inadequate air void system. The cores that had acceptable air void parameters were all from either the mid-span or from undamaged joints. Not surprisingly, cores from damaged joints had relatively high spacing factors of 0.015 and 0.025 in., respectively. However, some undamaged joints and mid-span cores also had spacing factors as high as 0.020 in.

For specimens obtained from W. 86th St. BL (west of light @ N. Payne Rd.) location, the total air content was (in general) in the range of about 3.0–5.0%, below the specified $6.5 \pm 1.5\%$. However, the spacing factor ranged from 0.004 in. to 0.006 in., which is well within the ≤ 0.008 in. recommendation. It should also be pointed out that no joint damage was observed at this particular site and that all cores were extracted from the middle of the slab (location D in Figure 2.1).

The entrained air content of all cores obtained from W. 86th St., AL BL (east of light @ N. Payne Rd.) location was relatively low and varied from 2.5% to 4.7%. The spacing factor values showed a high degree of scatter, ranging from 0.008 in. to 0.025 in. with a spacing factor of 0.015 in. or higher in all damaged cores.

TABLE 3.1
Air void system characteristics, voids infilling, F-T resistance and RCP data

Hwy	Core	% paste	Total % air (target 5%-8%)	Observed entrained % air	Specific surface (in. ² /in. ³) (target: >600)	Spacing factor (in) (target: < 0.008)	Infilled voids		Ft % df (avg)	Chloride ion penetrability (rcp)	From deteriorated joint
							Optical microscopy (60x)	SEM (~400-1400x)			
US 67	1A	26.8	5.8	3.83	291	0.015	Y	Y	53.2		Y
	2F	32.8	5.2	3.50	367	0.014	Y	Y			
	3E	29.0	5.2	3.05	381	0.013	Y	Y			
	4D	24.0	5.3	3.13	534	0.008	Y	Y	90.3	Low	
	5F	24.4	6.3	5.49	803	0.007	Y	Y	89.1	Mod	
	6D	29.5	4.0	2.12	271	0.020	NN	NN			
	7F	27.9	5.5	4.20	592	0.008	N	N	5.5		Y
	8A	31.4	4.3	2.44	224	0.025	Y	Y			
	9D	24.0	6.4	6.21	788	0.005	N	N			
	10D	31.6	3.8	3.48	1434	0.004	N	N			
	1D	25.5	3.4	3.06	1291	0.004	N	Y		VLow	
	2D	25.6	6.3	4.86	686	0.006	N	N			
	3D	26.9	4.2	4.13	1021	0.005	N	N			
	4D	28.4	4.5	4.35	917	0.006	N	N			
	5D	22.9	4.9	4.50	708	0.006	N	N			
	6D	25.5	5.4	5.26	812	0.006	N	N			
86 AL (east of light)	1D	29.4	3.7	3.68	505	0.011	N	N		Low	
	2D	29.1	4.1	2.54	251	0.022	N	N			
	3D	31.9	5.2	3.73	640	0.008	Y	Y			
	4D	30.0	4.3	2.54	412	0.013	Y	Y			
	5D	30.5	5.3	4.15	445	0.011	Y	Y			
	6D	27.1	5.2	4.40	450	0.010	N	N			
	7A	29.1	3.5	2.88	233	0.025	Y	Y	82.0	Mod	Y
	8B	28.9	4.7	3.83	316	0.016	Y	Y	26.2	High	Y
	9C	28.5	3.8	3.16	266	0.021	Y	Y	55.1	High	Y
	10E	27.4	6.0	4.74	363	0.012	Y	Y	60.1	High	Y
	11C	30.0	4.1	4.14	355	0.015	Y	Y	70.1	High	
	0D	4.5	4.5	3.66	356	0.016	Y	Y	64.3	Low	
	1D	29.6	4.6	4.42	607	0.009	N	N	99.9	VLow	
	2E	26.9	5.7	4.16	409	0.011	N	N	98.2	Low	
	2C	13.7	5.9	5.27	197	0.012	N	N			Y
	3B	23.2	4.9	3.88	172	0.026	N	N	55.2	Low	Y
4C	19.2	4.0	2.69	278	0.016	N	N			Y	
5C	22.6	5.1	3.71	254	0.017	N	N			Y	
6F	22.2	7.9	6.06	223	0.013	Y	Y	45.0*	Mod	Y	

NOTES:
 *Sample taken from core showing unusual cracking damage.
 % DF = Durability factor (target DF >60).
Boldface = Met target values.
 Mod = Moderate.
 VLow = Very low.
 NN = None noticed (i.e., very small voids not visible).

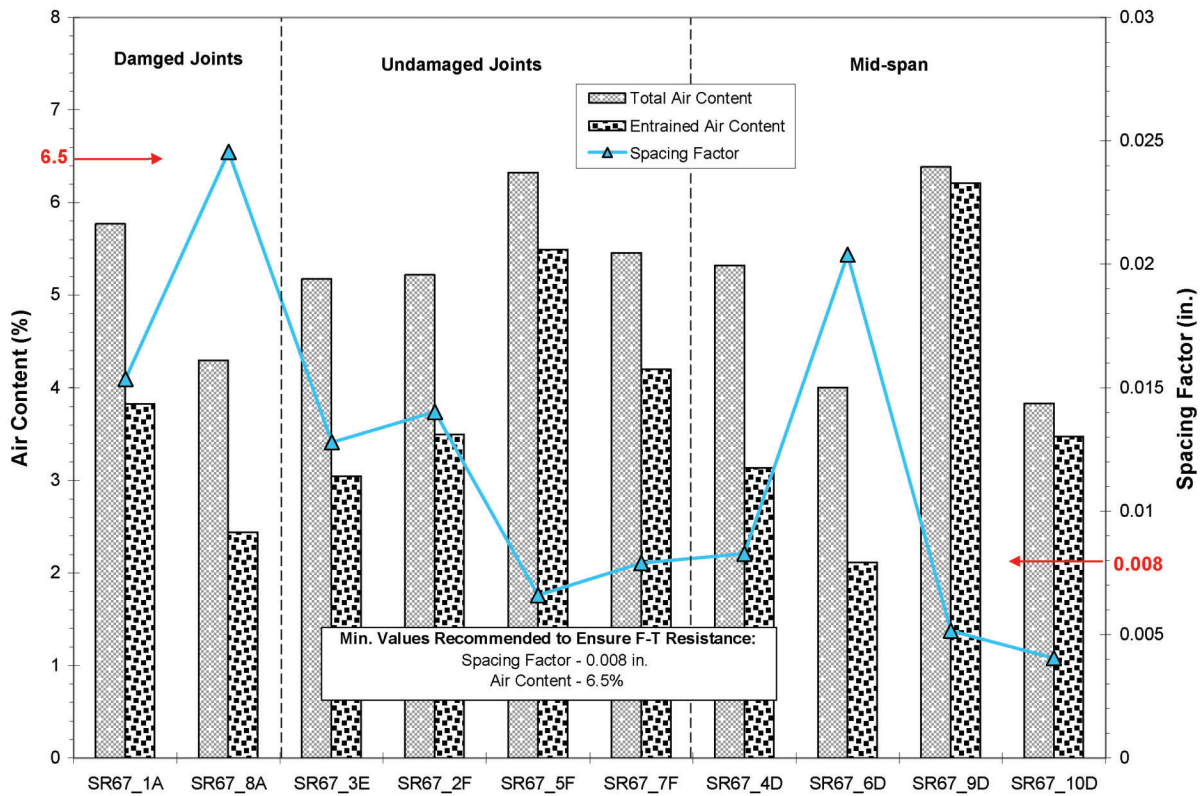


Figure 3.1 Example of the existing air content and spacing factor (US 67 cores). (NOTE: Only empty air voids were included in the count) (1).

The entrained air content of all three samples from SR933 was approximately 4.0%. The spacing factor ranged from 0.009 to 0.016 in.

In the specimens obtained from I-65 location the entrained air content ranged from 6.1% (in the core from an undamaged joint) to as low as 2.7%. However, the spacing factor in all cores was above the recommended limit and ranged from 0.016 to 0.20 in., implying that the effectiveness of this air void system with respect to F-T protection will likely be limited.

3.2 Infilling of Air Voids—Optical Microscopy Evidence

While several of the air void system values shown in Table 3.1 appear to be considerably below the target values, it should be noted that only the empty voids were counted. The microscopic examination of polished slabs from the cores at 60x magnification identified several cases of infilling of the air voids with secondary mineral deposits (especially the smaller air bubbles) as shown in Figure 3.2 (1). Further examination using the SEM and XRD identified some degree of infilling in all cores.

In summary, all examined concrete obtained from damaged joints shows evidence of a poor existing air void system. Concrete from some mid-spans and some undamaged joints also had a poor existing air void system. Although it is not possible to prove this with absolute certainty, it can probably be argued that some

of this concrete actually met the requirements for the standard entrained air content of $6.5\% \pm 1.5\%$ at time of placement (even though it is not clear what was the original quality of the air voids system in concrete from damaged joints). Furthermore, the strong evidence of infilling the existing air voids system obtained through optical observations puts in question its adequacy to resist damage from future freezing and thawing cycles. This is because the infilling of the smaller entrained air voids will significantly increase the air void spacing factor while it will only slightly decrease the total entrained air void volume (1,4,5).

3.3 Infilling of Air Voids—Scanning Electron Microscope (SEM) Evidence

The SEM images were collected in the backscattered mode and several of the observed microstructural features were further analyzed using energy dispersive x-ray analysis (EDXA). In particular, the EDXA method was used to identify the composition of the deposits presented in the infilled voids. Figures 3.3 and 3.4 (1) are examples of the numerous SEM analyses performed. The extremely small white square on the magnified part (right-hand side) of the images indicates the area analyzed with the EDXA. These EDXA spectra (or peaks) are shown at the bottom of each image and indicate that both ettringite (a) and Friedel's salt (b) were present as deposits in the void. The sulfate-

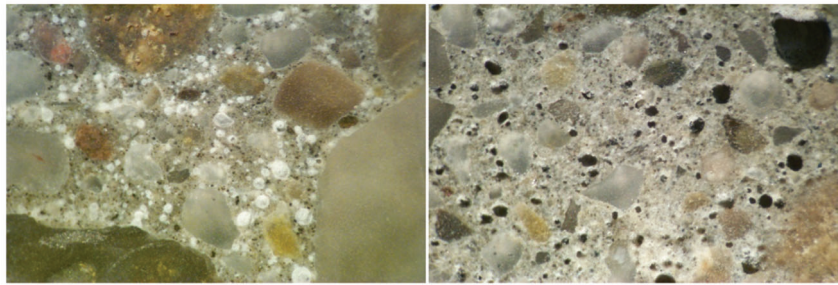


Figure 3.2 Typical appearances of the infilled voids (a) and empty air voids (b) as seen using optical microscopy (1).

sensitive staining technique was used to examine the extent and distribution of the ettringite and to try to distinguish between ettringite and Friedel's salt over larger area of the sample (6). However, no pattern of infilling with ettringite or other compound was detected. Figure 3.4 shows numerous large (~50 μm) air voids completely filled with ettringite and several cracks in the matrix.

3.4 Sorptivity

The measurements of sorptivity (or rate of water absorption) were conducted on previously conditioned concrete discs removed from the cores (see Figure 2.2). The results of the sorptivity testing are rather mixed. But generally, most of the cores from joints showed higher water absorption rates than cores from the mid-span and the highest water absorption rates were from cores taken at damaged joints. One exception was the very high water absorption rates of the mid-span core that had slag coarse aggregate (SR933, #0D). Since many variables that were not identified in this study can strongly influence the results of the sorptivity test, a more detailed analysis of these results are not warranted.

3.5 The Freeze-Thaw Test

These tests were conducted on a total of 49 concrete discs (approximately 0.9-in. thick) cut from cores from each pavement. The relative dynamic modulus of elasticity, which relates to deterioration of the concrete, was monitored. The specimens were exposed to 305 to 326 freeze-thaw cycles using the modified ASTM C666 procedure. The results are summarized in Table 3.1 and are expressed in the form of a durability factor (DF). Although there are no establish criteria in the industry on the limiting value of the durability factor, when it falls within the range of 40 to 60% the performance of concrete with respect to freezing and thawing is considered to be doubtful.

The values of the DF for all but two discs obtained from mid-span cores were higher than 60%. The two discs with DF lower than 60% were extracted from the core that contained slag coarse aggregate (SR933, #0D). However, even for this core, the average value of the DF (calculated from 4 discs) was 64.3.

Of the four cores taken at undamaged joints (locations E and F in Figure 2.1) all disks from 2 cores (2E and 5F) passed, all disks from 1 core (6F) failed and disks from the fourth core (10E) had mixed results with

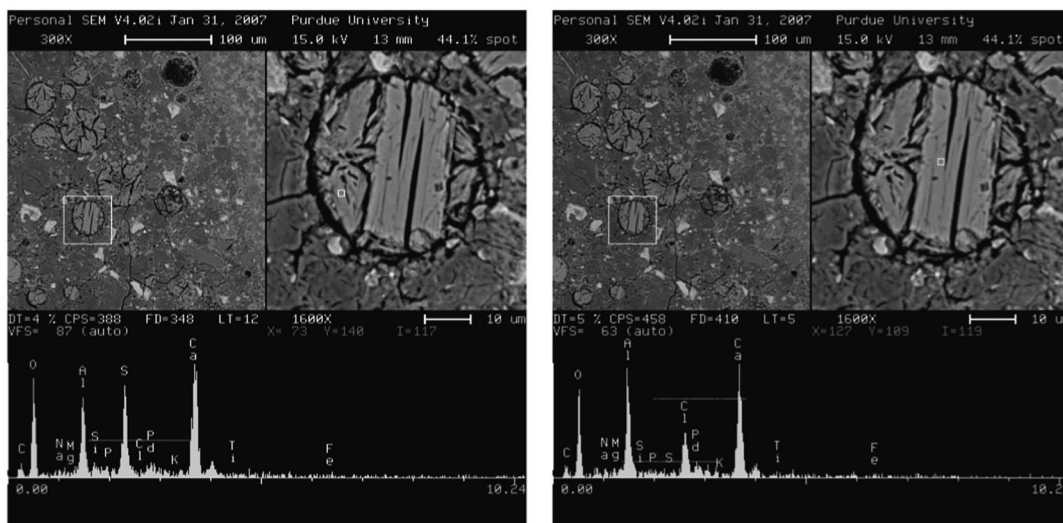


Figure 3.3 SEM image from a specimen from SR 67 showing an air void completely filled with mixture of ettringite (spectrum, left) and Friedel's salt (spectrum, right) (1).

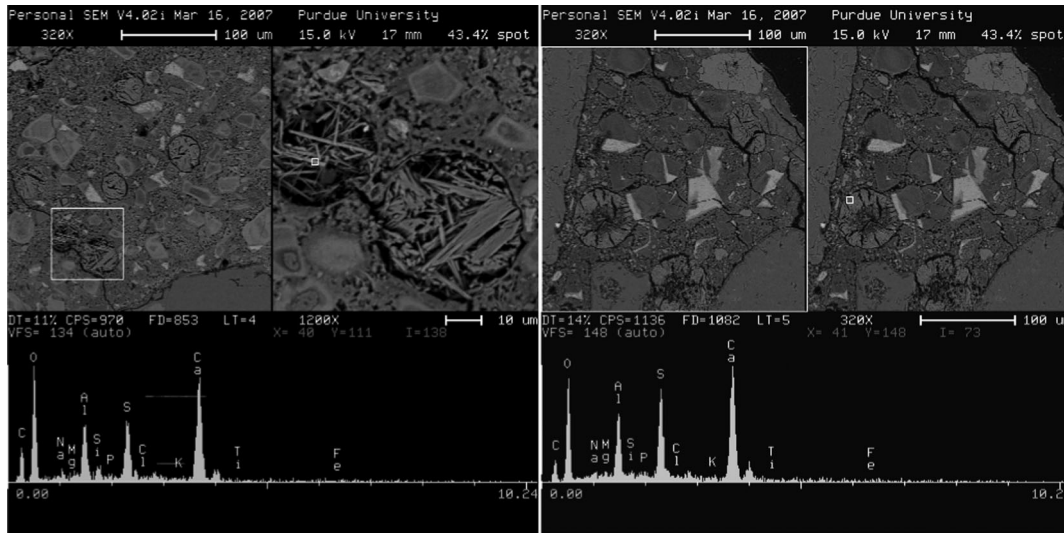


Figure 3.4 Numerous large air voids filled with ettringite (left and right) and some cracks in the matrix (right) (*l*).

an average $DF=60.1$ (barely passing). Of the 7 cores obtained from deteriorated joints all disks from 4 cores (1A, 8A, 8B and 9C) failed, all disks from 2 cores (7A and 11 C) passed and 1 core (3B) had varied results with an average DF of 55.2% (failing).

If we assume that the average performance of all the discs from the same core represents the performance of that core we can conclude the following:

- All of the mid-span cores passed the F-T test
- 3 of the 4 cores from undamaged joints passed the F-T test
- 5 of the 7 cores from damaged joints failed the F-T test

Although the data lacks a perfect relationship between F-T results and pavement deterioration, in many cases a chert inclusion in the coarse aggregate influenced the degree of distress in test specimens. Several specimens obtained from the damaged joints (locations A, B and C) experienced particularly severe forms of failure.

3.6 Resistance to Chloride Penetration Test

This test, often referred to as the rapid chloride permeability test (RCP) was used to measure the concrete's resistance to chloride ion penetration following ASSTHO T 277 standardized procedures. A total of thirteen specimens were tested. Although this is not a highly precise test, in general there was a good correlation between chloride ion penetrability and deterioration. The summary of the results and the classification of based on charge passed is presented in Table 3.1.

Specimens from all mid-span cores had very low to low chloride ion penetrability. Specimens from undamaged joints had low to moderate chloride ion penetrability. Specimens from damaged joints had low to high chloride ion penetrability.

3.7 Chloride Ion Concentration with Depth

To determine the changes in the amount of chlorides present in the specimens as a function of the depth from the exposed surface, concrete from individual layers of various cores was powdered and the amount of water soluble chloride ions was measured using the automated ion chromatography apparatus. The mid-span cores were tested with depth from the pavement surface downward. Cores taken at joints were tested from the joint face laterally inward, nominally parallel to the joint surface. The results are summarized in Figure 3.5 (for mid-span cores) and Figure 3.6 (for cores from undamaged and damaged joints) (*l*).

Although the chloride ion concentrations in mid-span cores were quite variable (ranging from 2 to 15 kg/m^3), they were highest in the top 10 mm of the pavement surface (see Figure 3.5) and then decreased significantly with depth, as expected. The chloride ion concentrations in cores from undamaged joints (left part of Figure 3.5) measured over the distance of about 25 mm from the joint surface were fairly uniform and ranged from approximately 2–6 kg/m^3 . In contrast, chloride ion profiles in cores from damaged joint varied significantly, with the lowest measurements near the joint surface (ranging from <0.5–6 kg/m^3), peak concentrations at depths of about 5–15 mm (ranging from approximately 6–11 kg/m^3) and relatively stable values of 4–6 kg/m^3 at distance of 22 mm or higher from the joint surface.

The elevated amounts of chloride ions observed few millimeters below the surface of the mid-span cores could most likely be attributed to the accumulation of deicing salts as these locations are not subjected to the direct wheel traffic. Similarly, the low (and uniform) levels of chlorides in the undamaged joints most likely reflect the lack of salt penetration due to protective action of the sealant. On the other hand, elevated levels of chlorides observed below

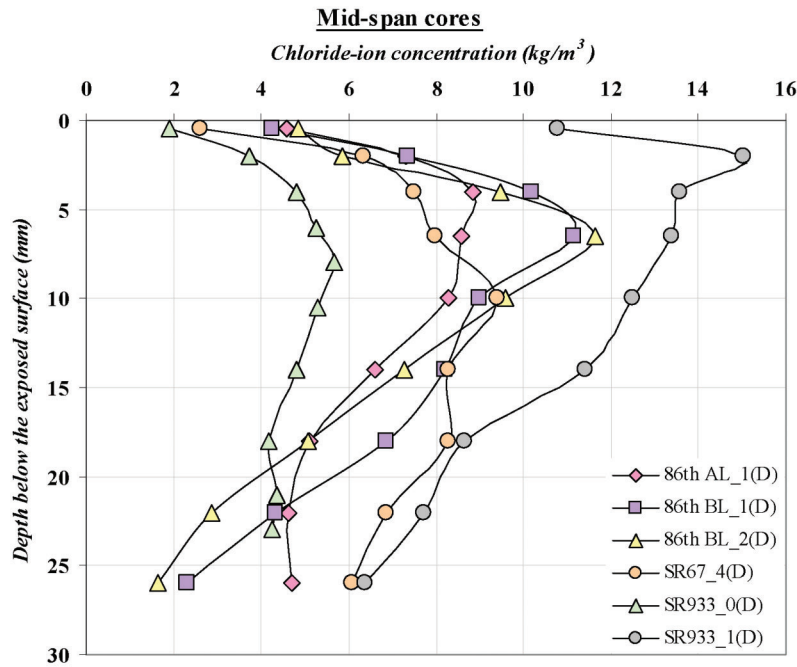


Figure 3.5 Chloride ion concentration profile for mid-span cores (I).

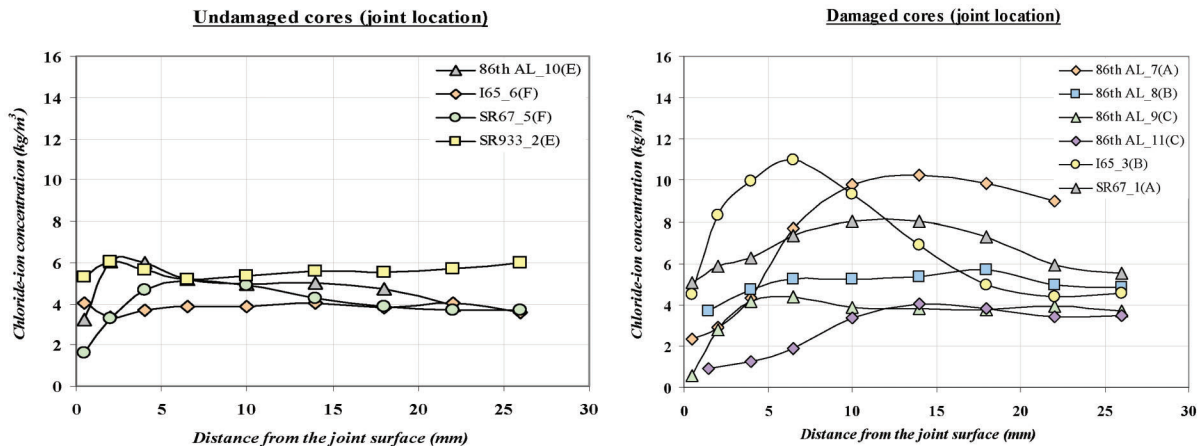


Figure 3.6 Chloride ion concentrations profiles (from joint faces inward) for undamaged joints (left) and damaged joints (right) (I).

surfaces of the damaged joints are indicative of prolonged chloride exposure which is likely the result of water standing in the joints due to sealer failure and lack of effective drainage. That accumulation of water is particularly damaging during the winter months as the presence of deicing salts depresses the freezing point and increases the effective degree of saturation. The increased saturation will, in turn, lead to higher probability of freezing and thawing damage of concrete.

4. SUMMARY AND CONCLUSIONS

4.1 Summary

In this study, a laboratory evaluation of the specimens extracted from deteriorating concrete pavements

was conducted to determine the causes of damage in the vicinity of the joints. A total of 36 cores were removed from five different concrete pavement locations (US 67, W 86th St., west of the intersection with Payne Rd. (BL), W 86th St., east of the intersection with Payne Rd. (AL), SR-933 and I-65). It has been observed that predominant type of pavement failure at these locations was cracking and spalling in the general area of the joint.

In general, the cores which came from the mid-span of the slabs (location D) had better air void systems than those extracted from locations near the joints. They also had good resistance to freezing and thawing cycles, relatively low rates of absorption and were classified as having low or very low resistance in the rapid chloride ion permeability test. The only exception was the core containing slag aggregates. The cores

which came from the undamaged joints (locations E and F) showed marginal to substandard air void system parameters, higher rates of absorptions than the mid-span cores, variable F-T durability (with most specimens having DF above 60%) and low to moderate resistance in the rapid chloride permeability test. The cores which exhibited higher rates of absorptions also exhibit lower durability factors (freeze-thaw test). Moreover, it was noted that cores from undamaged joints contained a considerable quantity of small (~10 µm) air voids filled with either ettringite, Friedel's salt or a combination of both. However, numerous empty air voids were also present in these cores.

The cores which came from the damaged joints (locations A, B and C) mostly exhibited a poor (existing) void system, showed evidence of some of the highest rates of absorption, displayed moderate to high chloride ion penetrability and achieved relatively low values of the F-T durability factors. Additionally, it was noted that these cores contained numerous microcracks and infilled air voids (both small and large). The secondary (infilling) deposits contained ettringite, Friedel's salt or a combination of both.

4.2 Discussion

The ettringite and Friedel's salt deposits found in many air voids were most likely the result of the repetitive saturation of air voids with mineral-laden water that left precipitates behind in the air voids. Secondary deposits filling the air voids are commonly seen in damaged concrete (4,7–9).

The evidence obtained from the cores indicates that all of the concrete has been air-entrained, although the quality of the existing air void system was variable. Although there is some correlation between the poor quality of the air void system and the observed damage (see Table 3.1), there is also evidence that the air void system alone can't be solely responsible for the observed deterioration (i.e., samples 1A, 2F and 3E from US 67 have similar spacing factors but only location of sample 1A was showing deterioration). Similar observations apply to samples 6D and 8A from US 67 with only sample 8A representing the deteriorated joint. This last case is particularly noteworthy as it highlights an important general trend—the specimens collected from the mid-span of the slabs (the "D" location) never exhibited any significant degree of infilling of the air voids or any other signs of deterioration. This observation indicates that concrete at the joints is clearly subject to conditions promoting higher degree of saturation and thus is more prone to freeze-thaw (FT) damage. Once initiated, the FT process will result in formation of microcracks in the concrete. The presence of microcracks would increase the degree of concrete saturation and facilitate the movement of moisture through the microstructure, thus leading to secondary mineral deposits in the air voids.

These deposits would, in turn, lead to further reduction of the effectiveness of the air voids system.

4.3 Conclusions

The results obtained from evaluation field specimens lead to the following conclusions:

1. Cores extracted from the damaged joint locations (type A, B and C) mostly exhibited poor (in-situ) air void system characteristic, numerous microcracking, infilling of the air voids, higher rates of absorption, high values of RCP and low values of F-T durability factors.
2. The residual freeze-thaw (FT) resistance of concrete with infilled air voids (mostly from the vicinity of the damaged joints) was lower than that of concrete with lesser degree of voids infilling (mid-span locations).
3. The observed microstructural and chemical changes were consistent with the appearance of concrete undergoing prolonged saturation (through-solution mechanism for creating deposits in the air voids).

REFERENCES

1. Arribas-Colon, M. "Investigation of Premature Distress around Joints in PCC Pavements." MSCE thesis, Purdue University, West Lafayette, Indiana, 2008.
2. Neville, A. M. *Properties of Concrete*, 4th ed. Longman Group, Ltd., London, 1995, 884 pages.
3. Kosmatka, S. H., B. Kerkhoff, and W. C. Panarese. *Design and Control of Concrete Mixtures*, EB001, 14th ed. Portland Cement Association, Skokie, Illinois, 2002, 372 pages.
4. Radlinski, M., J. Olek, M. del Mar Arribas, A. Rudy, T. Nantung, and M. Byers. Influence of Air-Void System Parameters on Freeze-Thaw Resistance of Pavement Concrete—Lessons Learned from Field and Laboratory Observation. *Proceedings of the 9th International Conference on Concrete Pavements*, San Francisco, August 17–21, 2008, pp. 824–835.
5. Olek, J., M. Radlinski, and M. del Mar Arribas. Premature Deterioration of Joints in Selected Indiana Portland Cement Concrete Pavements. *Proceedings of the XXIII Conference "Awaria Budowlane"*, M. Kaszynska, ed., Wydawnictwo Uczelniane Politechniki Szczecińskiej, 2007, pp. 859–868.
6. Poole, A. B., and A. Thomas. A Staining Technique for the Identification of Sulfates in Aggregates and Concretes. *Mineralogical Magazine*, Vol. 40, September 1975, pp. 315–316.
7. Stutzman, P. E. *Deterioration of Iowa Highway Concrete Pavements: A Petrographic Study*. National Institute of Standards and Technology (NIST), Gaithersburg, Maryland, December 1999.
8. Lee, H., A. M. Cody, R. D. Cody, and P. G. Spry. *PCC Pavement Deterioration and Expansive Mineral Growth*. Department of Geological and Atmospheric Sciences, Iowa State University, Ames, Iowa, 1998.
9. Sutter, L. L., K. R. Peterson, T. J. Van Dam, and K. Smith. Using Epifluorescence Optical Microscopy to Identify Causes of Concrete Distress. *Transportation Research Record: Journal of the Transportation Research Board*, No. 1798, Transportation Research Board of the National Academies, Washington, D. C., 2002, pp. 22–30.

INVESTIGATION OF PREMATURE DISTRESS AROUND JOINTS IN PCC PAVEMENTS

PART II I-94 NEAR MICHIGAN CITY

SPR-3016

Report Number: FHWA/IN/JTRP-2012/26

DOI: 10.5703/1288284315019

EXECUTIVE SUMMARY

INVESTIGATION OF PREMATURE DISTRESS AROUND JOINTS IN PCC PAVEMENTS: PART II

Introduction

Some of the concrete pavements constructed within the last 10 to 20 years have shown signs of premature deterioration, especially in the areas adjacent to the longitudinal and transverse joints. This deterioration typically manifested itself as cracking and spalling of concrete, combined with the loss of material in the direct vicinity of the joint. In addition, “bulb-shaped” damage zones were also observed under the sealed parts of the joints.

The objective of this study was to investigate possible causes of this premature deterioration. To reach this objective, the characteristics of the concrete in and near the deteriorated joints were compared and contrasted to the characteristics of the concrete in the non-deteriorated sections of pavement. The study was conducted in two different phases (Phase I and Phase II), and the findings are presented as a two-part report.

During the Phase I of the study, a total of 36 concrete cores were extracted from five different pavements. While Phase I provided important preliminary information as to the potential causes of deterioration, it also demonstrated the need for a more focused approach that would eliminate such variables as the age of the pavement, site-specific subgrade and environmental conditions, materials variability, and quality of construction.

These goals were accomplished in Phase II of the study, which provided the opportunity to directly compare sections that were (1) paved under one construction project by the same contractor, (2) that used similar mix designs and materials, and (3) were most likely exposed to similar environments and deicing practices but showed very different performances. Several pavement sections were in good condition, while one section showed significant deterioration at the longitudinal joints. During Phase II of the study a total of 18 cores were retrieved from five different pavement sections and examined. In addition, where feasible the base material was sampled and the drainage observed at each core hole.

Findings

In general, the cores that came from the mid-span of the slabs included in Phase I of the study had better air void systems than those extracted from locations near the joints. They also had good resistance to freezing and thawing cycles, relatively low rates of absorption, and were classified as having low or very low resistance in the rapid chloride ion permeability test. The only exception was the core containing slag aggregates.

The cores that came from the undamaged joints showed marginal to substandard air void system parameters, higher rates of absorption than the mid-span cores, variable F-T durability (with most specimens having DF above 60%) and low to moderate resistance in the rapid chloride permeability test. The cores that exhibited higher rates of absorption also exhibited lower durability factors (freeze-thaw test). Moreover, it was noted that cores from undamaged joints contained a considerable quantity of small (~10 µm) air voids filled with either ettringite, Friedel’s salt, or a combination of both. However, numerous empty air voids were also present in these cores.

The cores that came from the damaged joints mostly exhibited a poor air void system, showed evidence of some of the highest rates

of absorption, displayed moderate to high chloride ion penetrability, and achieved relatively low values of the F-T durability factors. Additionally, it was noted that these cores contained numerous microcracks and infilled air voids (both small and large). The secondary (infilling) deposits contained ettringite, Friedel’s salt, or a combination of both.

In general, the observed microstructural and chemical changes in Phase I cores were consistent with the appearance of concrete undergoing prolonged saturation (through-solution mechanism for creating deposits in the air voids).

Similar to those observed in Phase I of the study, the concrete samples collected in Phase II also contained a certain amount of infilling of the air void system by secondary deposits. Furthermore, it was observed that the existing air void system in the concrete from panels near the deteriorated longitudinal joint had neither spacing factors nor specific surface values within the range recommended for freeze-thaw durability. Contrary to this, nearly all of the concrete in lanes without damage had an adequate air void system at the time of sampling.

From the observation of the drains performed by the remote camera it was evident that not all of the drains were functioning properly and some were entirely blocked. However, more precise or direct correlations could not be made between the functioning of the drains and observed pavement performance.

Finally, the data collected during this study were limited and thus not sufficient to definitely and unambiguously determine the single cause of joint deterioration. Rather, the results seem to indicate that the observed deterioration is most likely caused by combination of several variables that may include type of deicers used, type of subgrade, structural design of the pavement, and type of the sealant in the joint.

Implementation

This study provided the Indiana Department of Transportation (INDOT) with first-of-its-kind data regarding the changes in the microstructure of pavement concrete in the vicinity of joints affected by premature deterioration. These data strongly suggest that the high degree of saturation in the vicinity of the sealed joints contributed to their failure by reducing the freeze-thaw resistance of concrete. In addition to saturating the concrete, the constant presence of the high levels of moisture also resulted in significant infilling of the existing air void systems with secondary deposits, thus reducing their effectiveness.

Considering the limited nature of this study, the following implementation actions can be suggested:

1. Necessary steps should be taken to ensure an adequate air void system in the hardened concrete, especially in the vicinity of the joints. The commonly accepted measures of the quality of the air void system needed to ensure of the freeze-thaw resistant concrete include the specific surface area of the air bubbles of at least 600 in.²/in.³ and a spacing factor not greater than 0.008 in. Although having an elevated content of air voids in fresh concrete does not guarantee the quality of the air void system in the hardened concrete, a larger amount of air will generally help. This points to the importance of generating a sufficient quantity of air bubbles in the fresh concrete as some air will be lost due to transport, paving, and consolidation operations. Recent data collected from the SR 26 project in Lafayette, Indiana, indicated that the air content in hardened concrete may be as much as 3% lower than the air content of fresh concrete (measured right after concrete has been discharged from the mixer).

2. Serious consideration should be given to reducing the penetration of water into the concrete at the joints. Water trapped under the sealer will keep the concrete saturated and thus more susceptible to freezing and thawing damage. Furthermore, the degree of saturation will increase in the presence of deicers. Potential solutions may involve applying water repelling penetrating sealers to the surface of the joints, a more rigorous inspection and maintenance program for the sealers in the joints, or use of the unsealed joint in combination with the penetrating sealers.
3. INDOT should consider construction of the test sections to verify some of the solutions proposed in Part II of this report.

It would be useful to establish a data base that can collect information from future paving projects with respect to characteristics of materials used, deicing practices, weather conditions, sealer conditions, and quality of the air void system in the hardened concrete. Having such a database will be very beneficial in addressing future maintenance needs of concrete pavements.

The benefits of this research include:

- Assemblage of detailed field data on the conditions of concrete in the vicinity of the deteriorated joints, which would be useful to INDOT maintenance personnel in the process of selection of rehabilitation and preservation treatments.
- Generation of fundamental information regarding the potential mechanism of deterioration (damage resulting from freezing and thawing of saturated concrete, potentially enhanced by the lack of an adequate air void system, trapping of moisture under the partially damaged seal, and use of deicing chemicals).
- Increased level of awareness among INDOT's engineers and contractors of the factors contributing to observed deterioration, which, if confirmed by additional studies, will lead to changes in specifications with respect to concrete performance requirements and design, construction, and deicing practices.

CONTENTS

1. INTRODUCTION	1
1.1 Background and Problem Statement	1
1.2 I-94 Project Construction Details	1
1.3 Preliminary field observations	3
2. OBJECTIVES	4
3. WORK PLAN	4
3.1 Collection of Cores	4
3.2 Test Specimens and Concrete Tests	5
3.3 Drainage Testing of Joints and Base/Subbase Sampling.	5
4. DATA COLLECTION AND ANALYSIS	6
4.1 Labeling Scheme	6
4.2 Drainage and Base Samples	6
4.3 Megascopic Exam of Cores	8
4.4 Chloride Analysis	9
4.5 Freezing and Thawing Test and Results.	9
4.6 Rapid Chloride Permeability Test (RPC)	10
4.7 Air Void System Analysis.	10
4.8 Scanning Electron Microscopy Analysis (SEM)	11
5. SUMMARY AND CONCLUSIONS.	13
REFERENCES	16
APPENDIX A. Drainage and Drainage Layer Observations and Testing	17
APPENDIX B. I-94 Pavement Cores	21
APPENDIX C. Tests and Testing Results	44
APPENDIX D. SEM Results	47

LIST OF TABLES

Table	Page
Table 1.1 Aspects of the various mixes and time of placement (per contractor)	2
Table 3.1 Summary of core locations	5
Table 4.1 Core locations with drainage and base conditions noted	7
Table 4.2 Summary of the condition of drains inspected	8
Table 4.3 Freezing and thawing test results	11
Table 4.4 Summary of existing air void system analysis	13
Table A.1 I-94 Michigan City drainage and base information	17
Table B.1 Core locations—a cross-reference of the preliminary numbering system and standardized system	21

LIST OF FIGURES

Figure	Page
Figure 1.1 Deteriorated longitudinal joint, I-94	1
Figure 1.2 Overview of the I-94 project area	1
Figure 1.3 Mixture design for mix 1	2
Figure 1.4 Core locations on site specific map	3
Figure 1.5 Occasional corner cracking in the EB lanes of eastern most portion of this project in the area with unsealed joints (identified as Section 5)	3
Figure 1.6 Sealer and backer rod at some joints: (a) sealer at variable depths, (b) sealer missing and backer rod exposed	4
Figure 4.1 Example of the core labels used	6
Figure 4.2 Map of core locations and corresponding drainage	6
Figure 4.3 Examples of some of the base material cemented into larger chunks (left and center), and cemented onto the bottom of the core (right)	7
Figure 4.4 Drain 1. Vegetation growing in the drain pipe (left); a small amount of water in the bottom of the drain (right)	8
Figure 4.5 The condition of the drain outlets varied	9
Figure 4.6 Surface appearance of a sealed joint (left) and unsealed joint (right)	9
Figure 4.7 Cores from sawn and sealed joints	10
Figure 4.8 Cores from unsealed sawn joints	10
Figure 4.9 View of sealed sawn joints in place, in the core hole	10
Figure 4.10 Examples of chloride concentrations in cores from Sections 1 and 4	11
Figure 4.11 Average DF of F-T specimens taken at the sawn joint compared to corresponding mid-span of the same panel	12
Figure 4.12 DF values for cores taken from pavement placed in 1997 (EB lanes) and 1998 (WB lanes)	12
Figure 4.13 Features observed in specimens analyzed using SEM	14
Figure 4.14 Presence of poorly hydrated cement grains (bright angular particles with strong Si and Ca peaks) common in the top 0–2 mm of many specimens and at the sawn joint face	15
Figure 4.15 Fly ash particles identified unexpectedly in specimens from Section 5 and specimen 3S (round particles inside red circles)	15
Figure A.1 Drainage layer samples from I-94, Section 1	18
Figure A.2 Aggregate drainage layer sampled at core holes in Sections 2 and 3	18
Figure A.3 Samples from drainage layer at core holes in Sections 4 and 5	19
Figure A.4 Drain 2. Initial PVC section completely submerged (left) and corrugated pipe further in with 1 in. of water (right)	19
Figure A.5 Drain 5 appears nearly clogged with sediment but still allows some water to pass	20
Figure A.6 Drain 6, at transition joint from corrugated to smooth PVC pipe approximately 10 ft into the pipe	20
Figure B.1 Standardized coring locations—revised	21
Figure B.2 Collection of cores	22
Figure C.1 Chloride analyses for cores taken in Sections 1 and 2	44
Figure C.2 Chloride analyses for cores taken in Sections 3, 4 and 5	45
Figure C.3 Freeze-thaw test results of all specimens tested.	46
Figure D.1 Specimen 1S	47
Figure D.2 Specimen 1W	49
Figure D.3 Specimen 3S	51
Figure D.4 Specimen 4D	53
Figure D.5 Specimen 5W	55

1. INTRODUCTION

1.1 Background and Problem Statement

The original JTRP project SPR-3016, *Investigation of Premature Distress around Joints in PCC Pavements*, referred to herein as *Part I*, examined and tested 36 concrete cores extracted from five different concrete pavements located in Indiana (ramp from SR 67 toward I-456 E in Indianapolis, I-65 SB lanes near MKL exit in Indianapolis, East and West of the traffic lights at the controlled intersection of W. 86th street at and N. Payne Rd. in Indianapolis and SR 933 near South Bend). The predominant type of concrete deterioration at these locations was cracking and spalling in the general area of the joint. In that study several valuable observations were made and preliminary conclusions reported that critical saturation of the joints contributed to the problem (*I*). However, important information was missing and may have varied from site to site making some comparisons tenuous. Information such as age of pavement; construction information; mixture design; subbase design, construction and condition; and deicing practices were not available for all the pavements and not within the scope and budget of the project. Much of this information was available for the concrete pavement placed along I-94 near Michigan City in 1997–1998, which offered an opportunity to take the investigation a step further and address some additional concerns.

A *Part II* Expansion of SPR-3016 was proposed to investigate I-94 near Michigan City that allowed an opportunity to investigate many concerns while at the same time, provided an opportunity to directly compare sections that were paved under one construction project by the same contractor, used similar mix designs and materials, were likely exposed to similar environments and deicing practices, but showed very different performances. Several sections were in good condition, while

one section of pavement showed significant deterioration at the longitudinal joints (as shown in Figure 1.1).

Prior to developing and executing the work plan background information was collected and the project site visited. The contractor still had many of the construction documents that included mix designs, paving dates and temperature, and acceptance test results, as detailed in the following section.

1.2 I-94 Project Construction Details

The focus of this investigation was a four-mile stretch of I-94 between the junctions with US 421 and US 20 (exits 34 and 40) near Michigan City (as shown in Figure 1.2). The eastbound lanes (EB) were paved from 9/19/97 through 12/18/97 and the westbound lanes (WB) were paved the following year from 6/22/98 through 10/10/98. Typically both the transverse and longitudinal joints on this job were sealed using a ¼-in. backer rod and silicon sealer. Because of the late-season paving in 1997, the joints in the EB lanes, east of STA 24+900, were left unsealed.

The research team is grateful for much of the construction information provided by Marc Diamente of Rieth-Riley who was present at the construction site for most of the 1997 and 1998 paving.

The paving sequence for both the EB and WB lanes was as follows (and diagrammed in Figure 1.3):

1. The two outside lanes were poured and both the transverse and longitudinal joints were created with a single-pass saw cut.
2. Then the inside lane and inside shoulder were poured as one and the longitudinal joint between these panels was created with a saw cut. This created a longitudinal cold joint between the inside lane and middle lane that was tied together using tie bars.
3. Next the outside shoulder was poured creating a cold joint that was tied to the outside lane.



Figure 1.1 Deteriorated longitudinal joint, I-94.

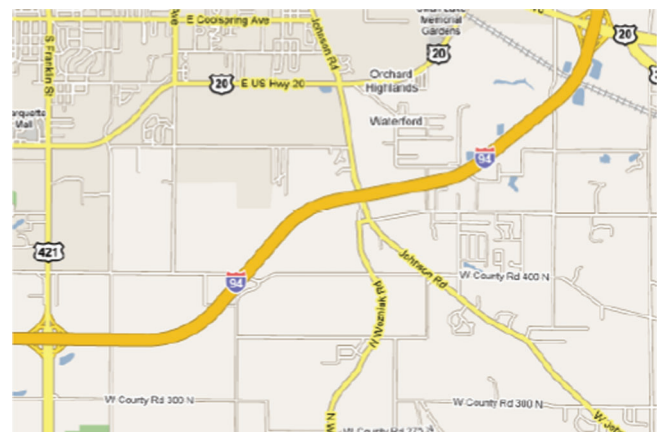


Figure 1.2 Overview of the I-94 project area.

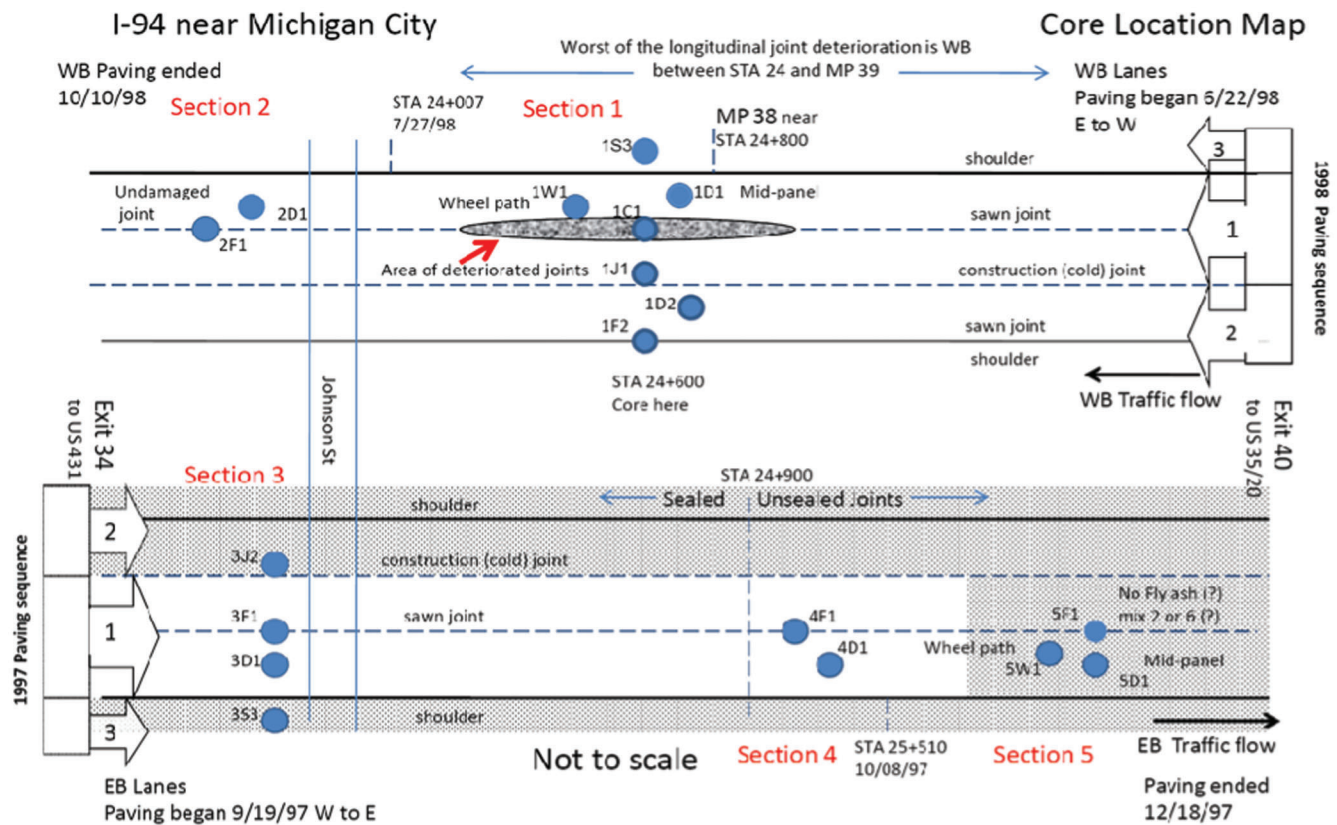


Figure 1.3 Core locations on site specific map.

4. Finally the concrete in the median adjacent to the barrier walls was poured last.

Figure 1.4 is the basic mix designs for Mix 1 and the target values for slump, unit weight and percent air. Mix 1 was the primary mix that contained fly ash and was used in 1997 (EB) until 10/10/97 and for the entire project in 1998. Mix 5 was identical to Mix 1 except a different fine aggregate was used and only used for a short stretch of the EB lanes. The mixes reportedly used for paving after mid-October no longer contained fly ash. These were Mix 2 and Mix 6 that were similar to Mix 1 and Mix 5 (respectively) but did not contain fly ash. Table 1.1 summarizes the mixes, their unique

characteristics and dates the contractor indicated they were used for paving. Much of this information is laid out on a site-specific map shown in Figure 1.3 and used as a basis for choosing the core locations. It should be noted that the SEM results obtained in the latter stages of this project indicate that, contrary to our understanding of the construction information, the concrete at Section 5 and in outside shoulder at Section 3 contained fly ash (see Figure 4.15 under SEM Analysis).

The mix water was well water; in 1997 a well was drilled on site specifically for the project and in 1998 an existing well that belonged to a nearby landowner was used (per verbal communication with Marc Diamente).

TABLE 1.1
Aspects of the various mixes and time of placement (per contractor)

Mix	Fly ash	Sand	Dates used for paving
1	Yes	BSS & G (Source 2489)	EB: 9/19 to 10/10/97 WB: 6/22 to 10/10/98 (entire project)
2	No	BSS & G (Source 2489)	EB:10/16 to 12/1/97, 12/17&12/18/97
5	Yes	Rieth Riley*	EB:10/10 to 10/14/97
6	No	Rieth Riley*	EB:12/3 to 12/16/97

*Rieth Riley sand was reportedly not washed well which lead to mixes with higher w/cm and lower strengths.

Mix Code			Description			
1			I-94 Paving Mix			
440-70						
Materials	Unit	Quantity	Supplier	Location	Source #	
Portland Cement	Kg	261.00	Lafarge	Alpena, MI	0020	
Flyash	Kg	42.00	AFA	Will Co., IL	0206	
-	-	-	-	-	-	
#8 Limestone	Kg	1097.00	Vulcan Mats	Francesville, IN	2461	
#23 Sand	Kg	798.00	BSS & G	Edwardsburg, MI	2489	
-	-	-	-	-	-	
VR	mL/100	130.40	Axim Technologies	Middlebranch, OH	8273	
1000N	mL/100	260.80	Axim Technologies	Middlebranch, OH	8273	
-	-	-	-	-	-	
Water	Kg	121.00	Rieth-Riley	Job Site	-	
Batch Weight	Kg/m ³	2319.00				
Strength Results						
Description	Unit	Results	7 Day Results	28 Day Results	Specimen	Unit
W/C Ratio1	-	0.40	-	-	S1	-
CA %1	-	58.00	-	-	S2	-
FA %1	-	42.00	-	-	Avg	-
Conc. Temp1	-	-				
Slump1	Cm	3.80				
Unit Wt1	Kg/m ³	2319.00				
Yield1	m ³	1.00				
Air Content1	%	6.50				

Figure 1.4 Mixture design for mix 1.

1.3 Preliminary Field Observations

During a site visit on July 7, 2008 it was noted that all the joints in the EB lanes appeared to be in good condition, however, in the WB lanes, some of the concrete was deteriorating primarily at longitudinal

joints (as shown in Figure 1.1). Some minor, infrequent corner cracking was observed in the outside driving lanes near the shoulder in the eastern-most portion of the EB lanes, identified as Section 5 (as shown in Figure 1.5). In this area the joints were not sealed, however, investigating the nature, extent and probable causes of the corner cracking was not part of this study.

Concrete deterioration was identified in a portion of the WB lane at the sawn and sealed longitudinal joint between the two outside driving lanes. The deterioration takes the form of spalling and loss of concrete at the joint resulting in the joint widening up to a few inches at the pavement surface (as shown in Figure 1.1). The worst of the deterioration was between RP 39 west to just east of the Johnson Street overpass, identified as Section 1 in Figure 1.4 (near STA 24). Before and after this section the joints appeared to be in good condition.

Several drain outlets for the edge and under drains were examined. Of those examined, the ones in the deteriorated section were dry, while water was either running freely from other drains, or the drains were plugged with sediment, precipitate or vegetation. Additional details are provided in the Drain Camera section and Appendix A.

Throughout the project in the WB lanes the joint sealer was not in good condition. It often was not at a consistent depth, appearing punched down an inch or more into the joint (as shown in Figure 1.6a), dislodged or missing altogether, exposing the backer rod (as shown in Figure 1.6b).



Figure 1.5 Occasional corner cracking in the EB lanes of eastern most portion of this project in the area with unsealed joints (identified as Section 5).

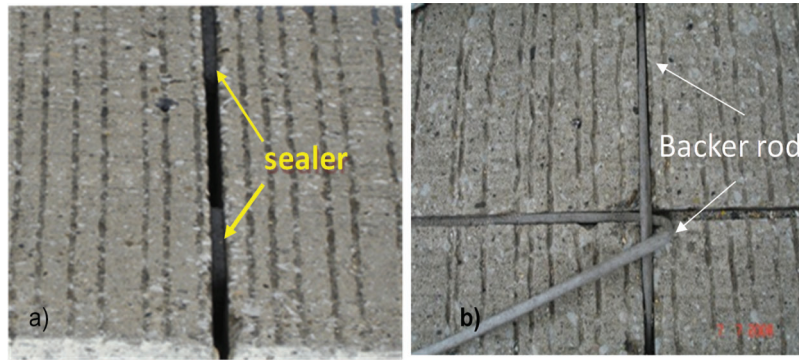


Figure 1.6 Sealer and backer rod at some joints: (a) sealer at variable depths, (b) sealer missing and backer rod exposed.

2. OBJECTIVES

The objectives of this study were to investigate the possible cause of premature distress observed in the concrete pavement found along the longitudinal joints in one section only along I-94 between exits 34 and 40 near Michigan City. To reach the objective the characteristics of the concrete in and near the deterioration were compared and contrasted to the concrete characteristics in the non-deteriorated sections of pavement in an effort to determine the cause of the deterioration. To the extent possible, the pavement structure, subbase, drainage and construction features in the distressed sections were compared to other sections in this segment of I-94 that were not exhibiting signs of premature distress.

In general the steps taken to meet these objectives included: examining construction documents provided by the contractor, discussing project details with the engineer who was present at the time of construction, examining the pavement surface and condition of the drain outlets in-situ, developing a detailed work plan and coring pattern, coring of both the distressed section and several other sections that appeared in good condition, examining and testing the cores, analyzing data to arrive at conclusions and recommendations.

3. WORK PLAN

The work plan for SPR-3016 Part II (Expansion) consisted of retrieving cores from very specific locations for testing and examination, similar to the original project, Part I. In addition, field observations of the drainage capabilities were performed; and edge and under drain inspected; and samples of the base material collected where possible.

3.1 Collection of Cores

A total of 18 cores were taken from various locations along I-94 between RP 34 and 40. The general coring locations and labeling scheme were similar to that shown in Figure 2.1 of Part I of this report, with the addition of cores taken at the outside shoulder (S), wheel path (W) and within 1 in. of construction joints (J). Specific details are provided in the Appendix A, Figure A.1.

Cores were taken at several different locations to capture several variables in the pavement sections: (1) structural variables included both sawn joints and cold/construction joints, (2) functional variables included shoulders, the far inside lane and the two primary outside driving lanes that possibly receiving different loads and deicer exposures (3) material-related variables included 4 different mixes, and (4) design variables including sealed and unsealed joints.

As previously identified, the worst of the deterioration was at the sawn longitudinal joint in Section 1, therefore the focus of the coring and investigation was in this area (7 cores), with 11 cores were taken from four other key areas for comparison with the deteriorated section and with features noted in the original study in order to better understand the mechanisms causing the distress. A total of 18 cores were retrieved (as detailed in Figure 1.4 and Table 3.1).

In all locations the non-joint cores were taken at least 2 ft away from any joints. Section 1 was in the WB lanes near STA 24+600, approximately 600 ft west of RP 38. In Section 1 the concrete was from Mix1, paved in July 1998 with ambient temperatures reportedly in the mid-80s (°F), all joints were sealed and the sawn longitudinal joint between the two outside driving lanes exhibited the most distress of any sections.

The concrete in Section 2 also was Mix 1, in the WB lanes near the west end of the study area, paved after Section 1, but has no visible signs of distress. Two cores were taken in this section; one at the longitudinal joint between the two outside driving lanes and one in the mid-span of the same panel of the outside driving lane. It was the same concrete mix, the same type of joints and most likely exposed to similar traffic and deicers as the most deteriorated section (1), and therefore provided a valuable comparison to the deteriorated section.

Section 3 was in the EB lanes with sealed joints. This section was paved the previous year (1997), using a different water source and ambient temperatures were reported to be milder at the time of paving (low to mid 70's). Mix 1 was used for the two outside driving lanes, and Mix 2 and/or 6, which did not contain fly ash, were reportedly used for the inside driving lane and shoulders at this location (however fly ash was found during the SEM examination of the core from the

TABLE 3.1
Summary of core locations

Core #	Section 1, Mix 1: WB deteriorated sawn longitudinal joint (near STA 24+600)
F	Spanning sawn longitudinal joint at inside shoulder
D2	Mid-panel in inside driving lane
D1	Mid-panel of outside driving lane
J	At construction (cold) joint (<1 in. from joint if possible)
C	Spanning deteriorated longitudinal joint
W	Wheel path nearest the deteriorated joint in the same panel as core 3
S	Shoulder
Core #	Section 2, Mix 1: B non-deteriorated sawn longitudinal joint (near STA 21+920)
F	Spanning sawn longitudinal joint between the two inside driving lanes
D	Mid-panel of outside driving lane
Core #	Section 3: EB lanes sealed joints (near Johnson St. overpass)
J	At construction (cold) joint (<1 in. from joint if possible) (Mix 2 or 6)
D	Mid-panel of the outside driving lane (Mix 1)
F	Spanning sawn longitudinal joint between the outside 2 driving lanes (Mix 1)
S	Shoulder (Thought to be Mix 2 or 6 at time of coring but found to contain fly ash)
Core #	Section 4, Mix 1: EB lanes unsealed joints (near STA 25)
F	Spanning sawn longitudinal joint between the outside 2 driving lanes
D	Mid-panel of outside driving lane
Core #	Section 5, Mix 2 EB lanes unsealed joints (paved 10/16/97 or later)
D	Mid-panel of outside driving lane
F	Spanning sawn longitudinal joint between the outside 2 driving lanes
W	Wheel path nearest the sawn longitudinal joint in the same panel as core 14

shoulder at this location). There was no evidence of deterioration in Section 3.

Section 4 was similar to Section 3 except the joints were not sealed. As with Section 3, it was thought that the two outside driving lanes in Section 4 were paved with Mix 1, similar also to Section 1, yet there was no evidence of deterioration. It was anticipated that the core from this unsealed joint would provide a valuable comparison to the cores from the sealed joints. The mid-span core was to provide good information about the original air void system and a valuable comparison to other mid-span concrete in other sections.

The three cores collected in Section 5, EB lanes, were in the outside two lanes in an area that the joints were not sealed, similar to Section 4 except the concrete was thought to be from Mix 2. Mix 2 is similar to Mix 1 except it did not contain fly ash. Therefore, Section 5 was cored with the intention that it had similarities to Section 1, except the concrete was paved late-season in 1997, did not contain fly ash, the joints were not sealed and the joints did not show signs of deterioration (see SEM Analysis section and Figure 4.5 for a discussion on fly ash in the mix).

3.2 Test Specimens and Concrete Tests

A total of 18 cores, 6 in. in diameter were retrieved for detailed examination and the following tests:

- Megascopic examination
- Chloride concentration profiles per ASTM C 1556
- Air void system analysis (ASTM C457)
- SEM
- Electrical Indication of Concrete's Ability to Resist Chloride Ion Penetration (RCP) (AASHTO 277, ASTM 1202)
- Freeze/thaw (F-T) Testing

All these tests were run on samples cut from the cores similar to the process described in Part I and shown in Figure 2.2 in Part I. Additional details on test procedures in Appendix C.

3.3 Drainage Testing of Joints and Base/Subbase Sampling

A measured amount of water was to be poured into each joint prior to coring and time to drain recorded. Because of the severe time restrictions on lane closures this was not practical at most sites. In the areas this test was completed some of the water often ran along the joint and it was difficult to measure the rate at which it actually penetrated the joint. Instead, more qualitative observations were made on the rate at which the drilling water drained from the core hole.

At several of the core locations it was intended that the base/subbase be sampled at least down through the drainage layer by scooping it out of the core hole and,

when possible, a sieve analyses completed. Again the severe time restrictions on lane closures made subbase sampling impractical at most sites, plus often the base in the core hole was not granular enough to scoop out. As much as possible the subbase was sampled by hand or a scoop and visually assessed in the lab.

Observations were made of the external condition of the drains near the coring locations. With INDOT's assistance and equipment, a drain camera with video-logging capabilities was used to inspect the internal condition of the drains where accessible.

4. DATA COLLECTION AND ANALYSIS

4.1 Labeling Scheme

The labeling of cores and specimens is similar to the scheme developed in Part I and is detailed in Figure 4.1.

4.2 Drainage and Base Samples

A sample of the drainable base material immediately under the pavement was retrieved at 12 of the 18 core locations. Photos of all the base samples are provided in Appendix A. Figure 4.2 shows a schematic of the core locations and the drainage conditions at these locations as well as the paving sequence.

Core Labels

1F2

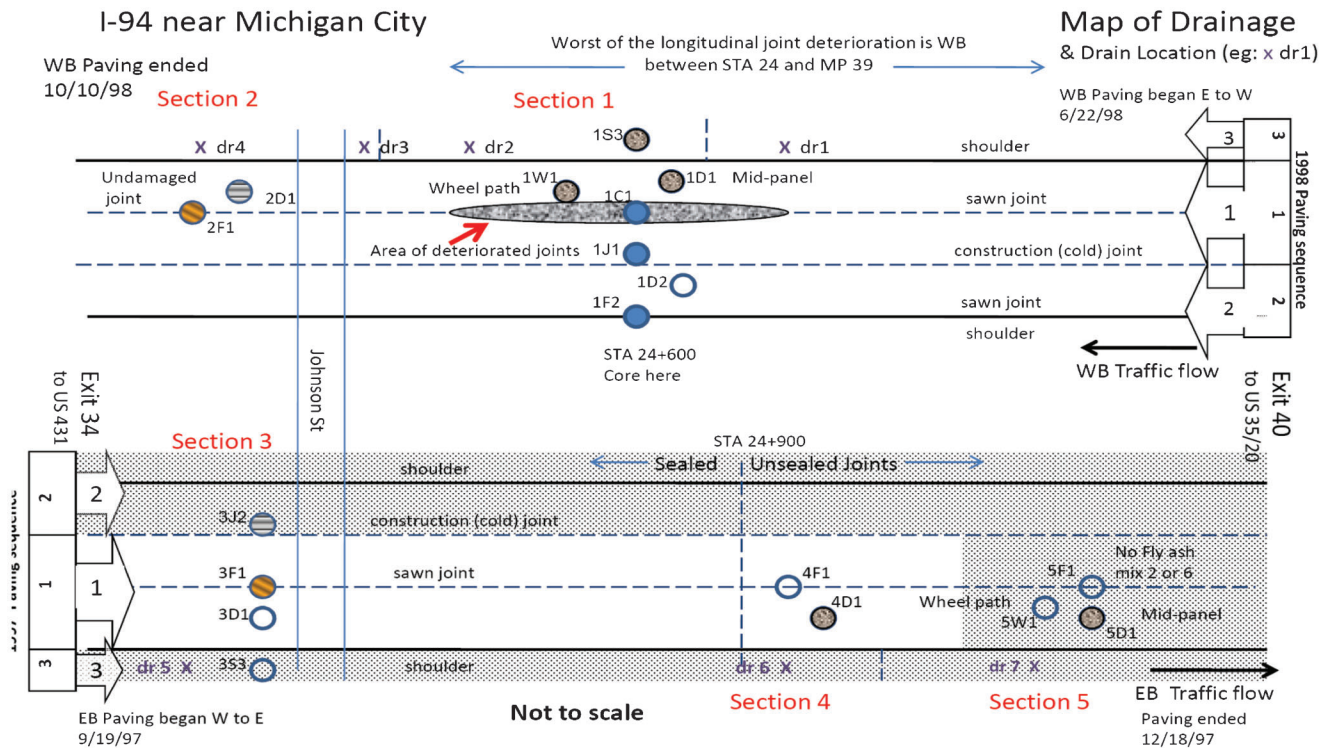
"1": The first number (1) refers to the section from which the cores were taken (1-5).

"F" The letter refers to the location in the panel (as shown in figure 5)

"2" The last number refers to the paving sequence and relates to the concrete mix.

Figure 4.1 Example of the core labels used.

The primary material used for this drainable base layer was a slag aggregate. However, at one core location the drainable base material was a quarried carbonate aggregate (core 3J2, EB lane). Core 3J2 represents the only location sampled from this paving sequence so the extent of the carbonate quarried aggregate base is uncertain. All remaining locations from which base material was retrieved had a slag aggregate for base. Sometimes the slag aggregate was granular, sometimes some of the slag was cemented into larger chunks, sometimes some of it was fused to the bottom of the core (examples shown in Figure 4.3 and Appendix B).



Based on the construction information: All of the WB lanes are Mix 1, EB lanes were paved with Mix 1 until 10/10/97. Mix 2 and Mix 6 did not contain fly ash and were used to pave the EB lanes from 10/16/97 until 12/18/97. Shaded area of EB lanes is where the construction information suggested were paved with mixes w/o fly ash. Contrary to the layout based on construction information (above), the SEM analysis indicates that concrete at Section 4 site did not have fly ash (probably Mix 2 or 6) and at Section 5 and at core 3S did have fly ash (probably mix 1).

- = good drainage
- = moderate drainage
- = moderately slow drainage
- = slow drainage
- = no drainage info

Figure 4.2 Map of core locations and corresponding drainage.



Figure 4.3 Examples of some of the base material cemented into larger chunks (left and center), and cemented onto the bottom of the core (right).

Sometimes the bottom of the core hole was hard and solid and no base material could be retrieved other than what was fused to the bottom of the core.

Based on the samples and drainage information collected, summarized and presented in Table 4.1 and Figure 4.2 it appears that where the base was a solid, fused mass the drainage was slow at the core hole and where the base was granular, with or without larger chunks, the drainage was moderate to very good. All core holes that had poor drainage were at joints. In Sections 1 and 2 where the drainage was measured at both joint and non-joint locations, the drainage was measurably reduced at the joints (1C, 1F, 1J, 2F)

compared to non-joint locations (1D, 1S, 1W, 2D). Unfortunately no drainage measurements were taken at unsealed joints due to traffic control concerns.

4.2.1 Drain Camera

On November 13, 2008 INDOT examined the edge-drains (running parallel to the pavement edge) and under-drains (that run under and perpendicular to the pavement and traffic direction) at the project site near the coring locations using a drain camera. The general locations of these drains are plotted on Figure 4.2 with an 'X' and 'dr #' (e.g. X dr1 = location of Drain 1, the

TABLE 4.1
Core locations with drainage and base conditions noted

Location	Established core no.	Drainage	Base condition	Notes
STA 24+600 WB lane	1F2	Very slow	NA	No base sampled
	1D2	NA	Granular	Granular slag aggregate; no notes about drainage
	1D1	Good	Granular	Quick drainage, granular base; nearby shoulder joint drained quickly
	1J1	Slow	± 2 in. granular then solid	± 2 in. of fine material in bottom of hole then hard layer that we could not penetrate w/hand or spoon
	1C1	Extremely slow	Hard, solid	No drainage noted in core hole after 20 min; chunks and some granular attached to core; material in hole too hard and solid to sample
	1W1 1S3	Good Good	Granular NA	Quick drainage Drained quickly; no water remained in hole after drilling
STA 23+900 WB lanes	2F1	Moderately slow	Pieces cement into large chunks	Moderately slow drainage (8 in. of water in hole after drilling, drop to 4.5 in. after 15 min); water poured at joint drained very slowly
	2D1	Moderate	NA	Moderate drainage; 5 in. of water in hole after drilling
STA 23+900 EB lanes	3J2	Moderate to good	Granular, limestone aggregate	Most of water drained from hole in 10 min
	3F1	Moderate to slow	Granular	4 in. of water in hole drained to 3.8 in. after 5 min; granular w/slag smell
	3D1	NA	Granular w/larger chunks	Granular with cemented chunks
	3S3	NA	Granular	
STA 25+000 EB lane	4F1	NA	Granular w/larger chunks	Larger chunks are smaller pieces cemented together
	4D1	Very good	Granular w/larger chunks	<1 in. water in hole after drilling
STA 125 EB lane	5F1	NA		
	5D1	Good	Granular	1–2 in. water in hole after drilling
	5W1	NA	Granular	Granular slag aggregate

TABLE 4.2
Summary of the condition of drains inspected

Near section	Drain no.	Location	Drain type	Condition		Comments
				Outlet	Drain	
1 WB	1	>100 ft either side of the deteriorated concrete section	E	~1 in. of sediment	W	~2 ft section submerged otherwise only a small amount of water and vegetation encountered (see Figure 4.4)
	2		U	Clear	W-S	63 ft long; water in drain from about 1 in. deep to completely submerged
	3		?	Clogged w/sediment	B	Impassible 3 ft in
2 WB	4	Near Section 2 cores	?	Clogged	B	Inaccessible because of water and vegetation in ditch
3 EB	5	Near Section 3 cores	?	Clogged w/sediment	W-B	Water was draining but cannot pass sediment visible w/camera at 5-6 ft
4 EB	6	Near Section 4	E	Clear	O	Cannot pass bend visible at 10 ft
5 EB	7	Near Section 5	U	Clear	S	First ~40 ft submerged, bend at 50ft

NOTES:

Drain type: U = under drain; E = edge drain; ? = unknown.

Drain condition: B = blocked; O= open; W= <1 in. water; S = submerged/filled with water.

first drain examined). There had been a light precipitation prior to our arrival.

The camera could not make the tight-angled turns from outlet to edge drain that were commonly built at the time of paving, so views of most of the edge drains were unattainable. Most of the areas examined were under-drains that ran perpendicular to the pavement and traffic direction.

A summary of the condition of the drains is provided in Table 4.2. Additional details and photos are presented in Appendix A. Figure 4.4 shows typical views of the drain with a small amount of vegetation (on the left) and a small amount of water (right) in the bottom of the drain. The condition of the drain outlets varied from clear and dry, to wet and clogged with sediment and precipitate or clogged with organics (as shown in Figure 4.5).

4.3 Megascopic Exam of Cores

A complete photo log of all 18 cores is provided in the Appendix B. Generally the concrete appeared

sound. More specific features also are presented in the appendix.

The pavement surface at most of the joints appeared in excellent condition, except for the deteriorated joints identified in Section 1 (as shown in Figure 4.6). However, looking at the vertical face of the core, perpendicular to the pavement surface, the profile of the sawn and sealed joints (as shown in Figure 4.7) look different than sawn joints that were not sealed (as shown in Figure 4.8)

The saw cut in the sealed non-deteriorated joints appeared smooth and distinct in the top ±2 in. then become more jagged and rough (1F, 2F and 3F in Figure 4.7), but the sawn surface of the unsealed joints is smooth and distinct for the entire 4-5 in. depth. It is interesting that joint deterioration in 1C also is in the top ±2 in. In some locations it appears that the rough surface begins just below the backer rod as seen in Figure 4.9 (right image) but at other locations it appears an inch or more below the backer rod (Figure 4.9, left image).

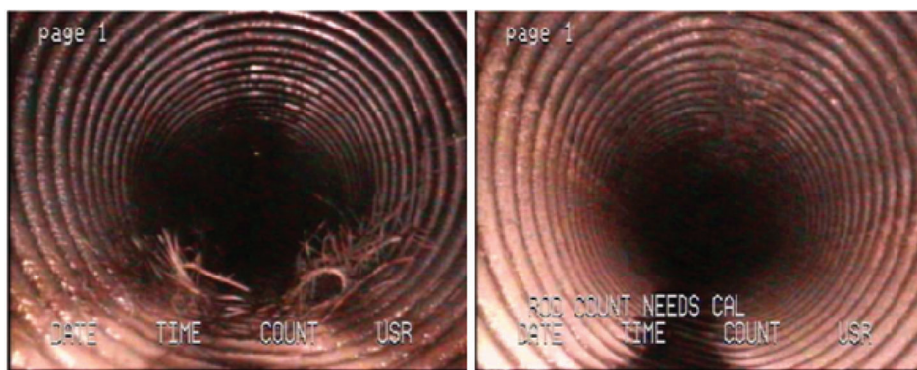


Figure 4.4 Drain 1. Vegetation growing in the drain pipe (left); a small amount of water in the bottom of the drain (right).



Figure 4.5 The condition of the drain outlets varied.

4.4 Chloride Analysis

Samples were prepared from the cores and analysis completed in the same manner and from similar intervals as described in the original Part I report (i.e., 9 or 10 distinct intervals from 0 to 25 mm [0–1 in.] depth, down from the pavement surface or in from the joint face). Powdered samples were tested for both water soluble chlorides by the INDOT Office of Research and acid soluble chlorides (total chlorides) by the INDOT Office of Materials and Test. The water soluble chlorides are chlorides that are easily removed from the concrete and not bound in a molecular matrix or complexed with other ions. The acid digest method will detect all chlorides whether ‘free’ or bound in a molecular structure of the paste, secondary deposit, minerals in aggregates or other compounds. Generally, the water soluble chlorides are primarily chlorides from deicing salts but some of these deicer derived chlorides may become part of secondary precipitates in the concrete (as seen as Friedel’s salt in this and the original investigation) (2).

In most samples the acid soluble chloride concentration was higher than and followed a similar pattern as the water soluble chlorides when plotted with depth (as shown in Figure 4.10). Generally the top 0–2 mm from the top of pavement or from the joint face had the lowest chlorides. (All the chloride concentration plots are shown in Appendix C.)

The chloride contents were compared at different core locations, and compared to the drainage, the time of construction (1997 and 1998), mixtures, pavements with and without sealed joints, traffic direction, and level of infilling in the air voids. A few minor patterns were observed:

- At the deteriorated joint the chlorides were the highest at depth; 1C had chlorides of 8.57 kg/m^3 at 18 mm while the chlorides measured at all other locations were below 8 kg/m^3 at this depth. However, the overall chloride content was fairly modest compared to other locations.
- The highest chlorides measured were from cores taken from the WB lanes (1S had 11.01 kg/m^3 ; 1D2 had 10.88 kg/m^3 ; 1W had 10.54) while the chloride measurement from cores from the EB lanes were 9.88 kg/m^3 (4D) or lower.
- Generally the sawn joint had lower chlorides than most other pavement locations and only changed slightly with distance from the joint face.
- The unsealed joints (4F and 5F) had slightly higher chlorides than sealed joints (2F and 3F) The deteriorated joint (1C), that was once sealed but subsequently exposed, and had the highest chloride content of all sawn joints.
- Cores 1C1, 1S3, 1W1 had a much larger difference between the water soluble and acid soluble chlorides measured than most other samples, as much as 5 kg/m^3 compared to 2 kg/m^3 for most other samples, suggesting a higher occurrence of chlorides tied up in compounds or crystallized structures.

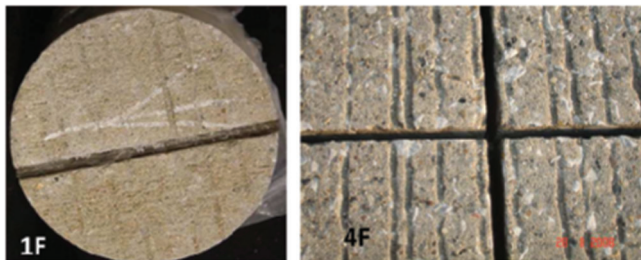


Figure 4.6 Surface appearance of a sealed joint (left) and unsealed joint (right).

4.5 Freezing and Thawing Test and Results

The freezing and thawing tests (F-T) were conducted as in the original Part I study, on three or four thin concrete discs cut from each core. The mass and the relative dynamic modulus were measured for each disc periodically during 300 F-T cycles and the average results are summarized in Table 4.3.

A durability factor (DF) was calculated using the final dynamic modulus as a percentage of the initial dynamic modulus measured at 0 cycles (per in ASTM C 666, *Standard Test Method for Resistance of Concrete to*

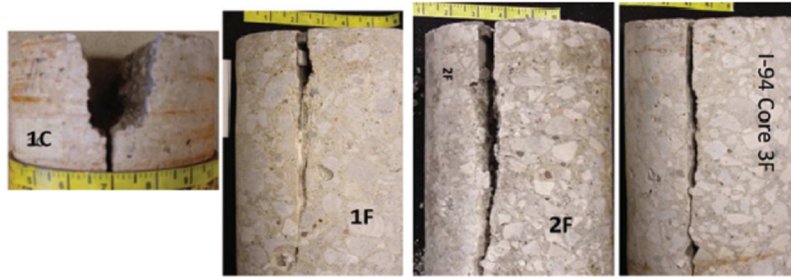


Figure 4.7 Cores from sawn and sealed joints (1C, 1F, 2F from WB lanes and 3F from EB lanes).

Rapid Freezing and Thawing). Although different agencies and contractors use different DF to identify concretes with satisfactory freezing and thawing performance, 60% is a common minimum acceptance value (2) and 80% or higher is usually considered F-T durable.

F-T specimens were not tested from the core retrieved from the deteriorated joint, 1C1. During the coring operation this core became wedged and stuck in the core barrel. The operators spent several hours trying to extricate the core from the barrel. In the process this core received repeated hard blows and pounding with hard objects, most likely inducing cracks to the concrete. Any test results that would be influenced by induced cracks, such as F-T cycling, would most likely not represent the in-place concrete.

As shown in Table 4.3 the average DF value for all cores was above 80 with all but one core (1F) greater than 90 suggesting all the concrete was F-T durable. The test results for all 66 discs tested are presented in Appendix C. Although all concrete had good F-T performance in the laboratory test there are some interesting trends.

As shown in Figure 4.11, the DF was lower for samples tested from cores taken at the joint (1-5F) compared to the corresponding mid-span (1-5D) the except in Section 3. This reduced DF at the joint is more pronounced in Sections 1 and 2, the WB pavement placed in 1998.

As shown in Figure 4.12, the DF factor tended to be a lower for the pavement sections placed in 1998 (WB lanes) compared to those placed a year earlier in 1997

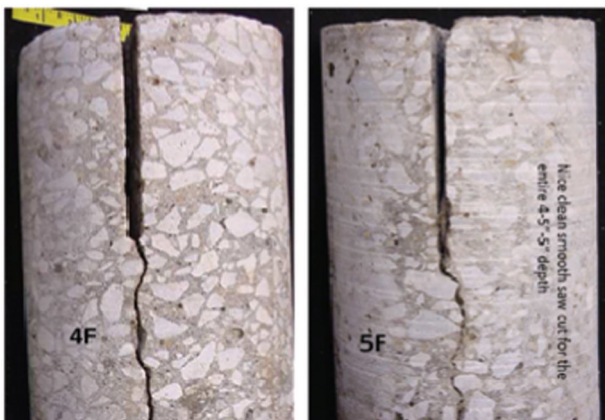


Figure 4.8 Cores from unsealed sawn joints.

(EB lanes). The lowest DF values came from concrete cores taken at sawn joints built in 1998 (1F2 and 2F1, WB lanes). The next lowest DF values came from the concrete panels that contained the deteriorated longitudinal joint (1D1, 1J1 and 1W1), placed in July 1998. All specimens tested from concrete poured in 1997 appear to have an excellent DF (higher than 94).

4.6 Rapid Chloride Permeability Test (RPC)

The RPC Test (ASTM C1202) samples were prepared and tested as describe in Part I using the equipment at the INDOT Office of Research. After all the tests were completed and results examined it was noted that many of the test results from the I-94 cores were oddly low. Upon closer inspection and testing of the electrical contacts for each cell it was discovered that some contacts had a very high resistance, possibly impeding some of the measurements. Unfortunately the tests could not be rerun and there was not enough of the concrete core remaining to produce another sample. This calls into question all the test results. Therefore all the RCP tests were disregarded and not considered in the final analysis.

4.7 Air Void System Analysis

Similar to the original Part I study, the air void system was analyzed using the ASTM C457 Modified Point Count Method. The process was completed manually for four slabs (1D1, 4F1, 5D1, 5F1). Polished slabs from 12 of the remaining 14 cores were processed, scanned and the images analyzed using software developed at Michigan Technological Institute

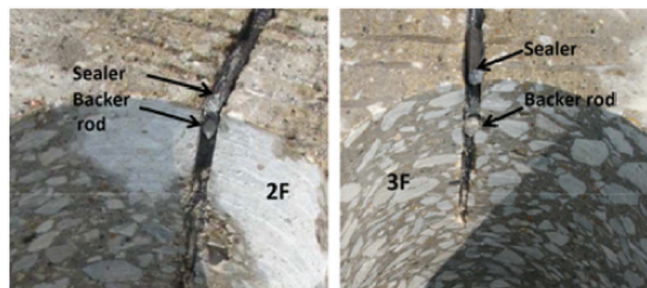


Figure 4.9 View of sealed sawn joints in place, in the core hole.

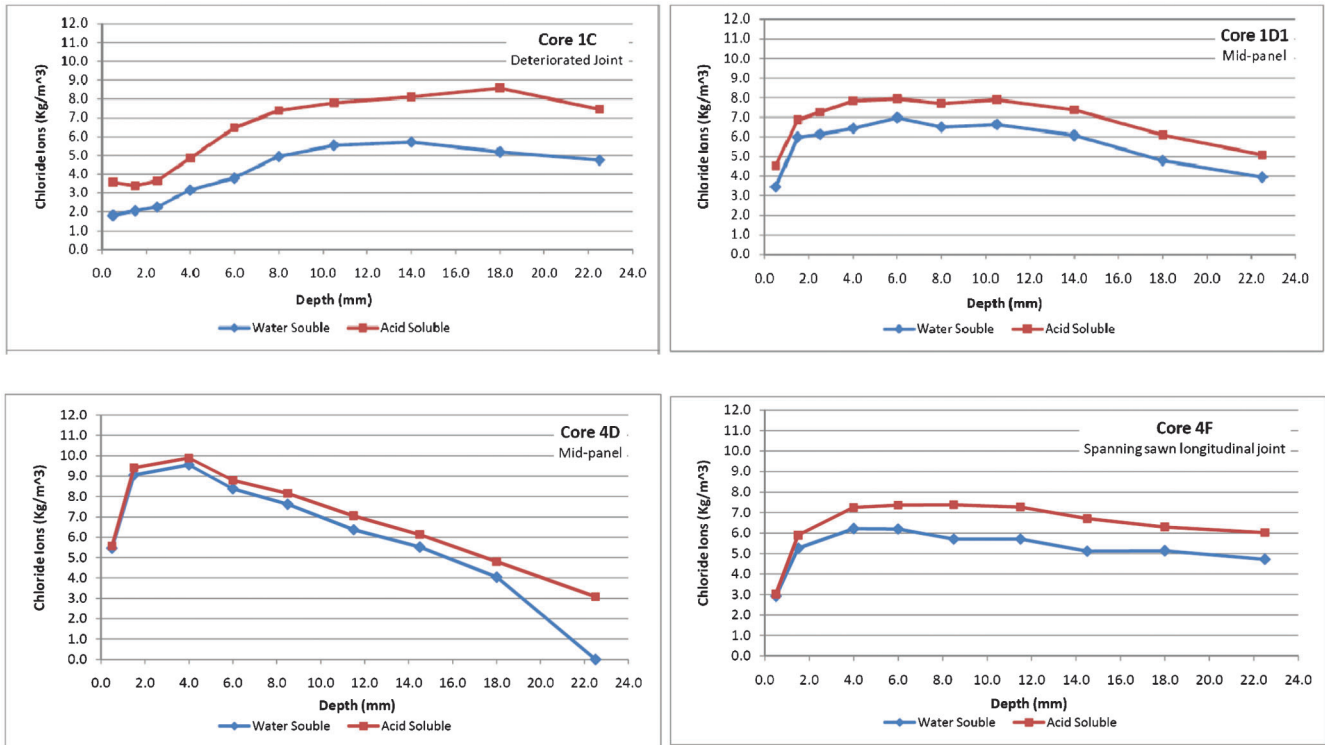


Figure 4.10 Examples of chloride concentrations in cores from Sections 1 and 4; chloride concentrations plotted against distance from joint face (1C and 4F) and from pavement surface (1D1 and 4D).

that replicated the modified point count method (3,4). The scanning and image analysis method provided objectivity and repeatability while providing a good level of accuracy, however it does not distinguish between entrained and trapped air voids.

A summary of the results of the air void system analysis are provide in Table 4.4. Aside from the percent total air or percent entrained air the key parameters that characterize an air void system that provides adequate protection from freezing and thaw-

ing damage are Specific Surface greater than or equal to 600 in.²/in.³, and Spacing Factor less than 0.008 in. (200 mm) (1,6).

Similar to the explanation provided in Part I of this report these concrete samples contained a certain amount of infilling of the air void system by secondary mineralization products which often were difficult to distinguish from the paste. The scanning and image analysis process identifies all infilled air voids as paste. Therefore the values given in Table 4.4 was the existing air void system and may not represent the initial air void system at the time of placement.

One striking feature of this analysis is that the existing air void system in the concrete placed in the panels near the deteriorated longitudinal joint had neither spacing factors or specific surface values within the range recommended for freeze-thaw durability (1C1, 1D1, 1J1, 1W1) and none of the concrete placed in the WB lanes (1998) had both a spacing factor and specific surface that met the PCA recommendations for adequate freeze-thaw resistance. Contrary to this, nearly all the concrete placed in the EB lanes, paved in 1997 had an adequate air void system at the time of sampling (core 5F1 being the exception).

TABLE 4.3
Freezing and thawing test results

Core	DF	Avg % mass loss
1D1	91.6	0.19%
1D2	96.4	0.08%
1F2	86.4	2.68%
1J1	93.1	0.38%
1S3	95.0	0.06%
1W1	93.0	0.08%
2D1	96.1	0.07%
2F1	90.5	0.381%
3D1	94.3	0.04%
3F1	96.5	0.13%
3J2	95.5	0.36%
3S3	96.6	0.12%
4D1	98.9	0.06%
4F1	95.3	0.26%
5D1	96.6	0.10%
5F1	95.9	0.58%
5W1	94.4	0.37%

4.8 Scanning Electron Microscopy Analysis (SEM)

Specimen selection and preparation for SEM followed procedures similar to those described in the full Part I report. Features similar to those identified and extensively shown in the original study also were

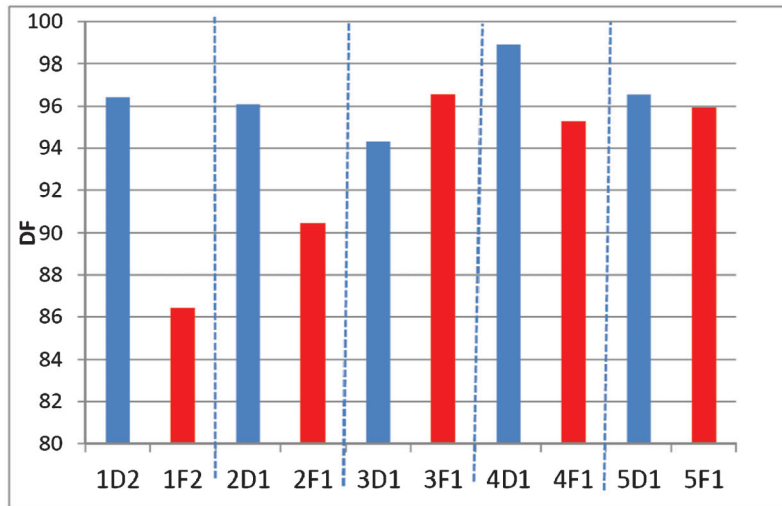


Figure 4.11 Average DF of F-T specimens taken at the sawn joint compared to corresponding mid-span of the same panel.

identified in these cores including air voids lined or filled with secondary mineralization products such as ettringite and Friedel's salt; and chlorides and Friedel's salt detected in the paste. Additional features noted in the I-94 specimens include poorly hydrated cement grains, fly ash particles, thaumasite and gypsum deposits (rare). SEM features identified are detailed for each specimen in Table 4.4 and some examples shown in Figures 4.13–4.14, and Appendix D (1,7,8,9,11).

Looking at the degree of infilling of the air voids in the SEM specimens there appeared to be a moderate to high level of infilling of the smaller voids in many of the samples from Section 1 (the section with the severely deteriorate longitudinal joint) and low to moderate infilling and lining of the voids in the other WB section, Section 2. Sample 5F had a moderate to high levels of infilling especially of the smaller voids, which is the one EB lane sample that also had an inadequate existing air void system. Generally the specimens from the joints

showed more infilling, lining and presence of ettringite and/or Friedel's salt than specimens from cores taken in non-joint areas. (Similar to figures shown in Part I of this report.)

The presence of unhydrated or poorly hydrated cement grains suggests poor curing (10). There were moderate to high occurrences of poorly hydrated cement grains in the very top few mm of the pavement surface and joint face in several Section 1 specimens (1C1, 1D1 and 1F2) and in some specimens from the other sections as well, suggesting curing conditions were less than optimal. It is uncertain to what extent, if any these 2–5 mm thin outer layers of poorly cured concrete may contribute to the overall durability of the concrete pavement, or the durability of the joint face, but it may be worth considering in further studies and investigations. The poorly hydrated cement grains at the sawn joint face of all sealed joints compared to a well-hydrated surface on the sawn joint face of the unsealed

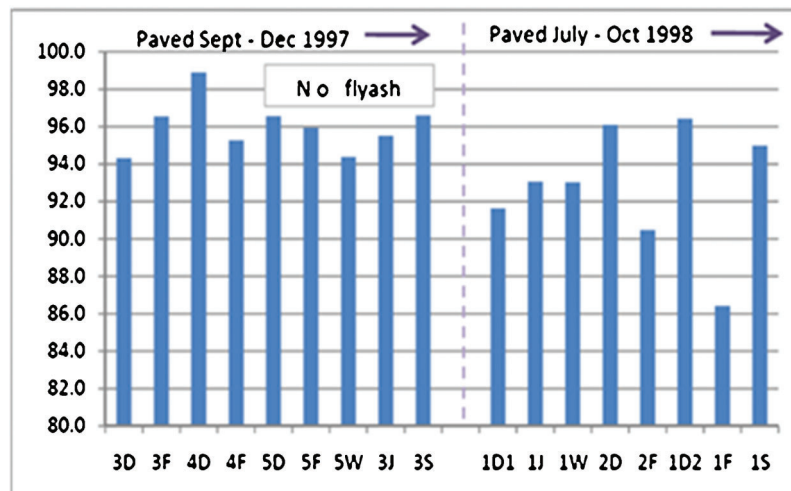


Figure 4.12 DF values for cores taken from pavement placed in 1997 (EB lanes) and 1998 (WB lanes).

TABLE 4.4
Summary of existing air void system analysis

Core	Total air (%)	Entrained air (%)	Specific surface (in. ² /in. ³)	Spacing factor (in.)	Infilled voids (SEM)	DF
1C1	2.9		554	0.011	Y	—
1D1	5.4	2.1	426	0.011	Y	91.6
1D2	7.9		480	0.007	—	96.4
1F2	3.5		517	0.011	Y	86.4
1J1	3.6		477	0.011	Y	93.1
1S3	7.0		548	0.007	VL	95.0
1W1	5.0		294	0.016	VL	93.0
2D1	9.1		489	0.006	Y	96.1
2F1	3.9		517	0.010	Y	90.5
3D1	5.0		693	0.007	VL	94.3
3F1	3.1		849	0.007	Y	96.5
3J2	6.3		619	0.006	—	95.5
3S3	5.6		702	0.006	N	96.6
4D1			—	—	N	98.9
4F1	5.0	3.0	665	0.007	N	95.3
5D1	6.3	3.8	605	0.006	Y	96.6
5F1	5.4	2.6	487	0.009	Y	95.9
5W1			—	—	N	94.4

NOTES:

Boldface = met target value recommended for good F-T durability.

N = no; Y = yes; VL = very low occurrence; — = not examined.

specimen examined (5F) suggests there may be a correlation between hydration of the concrete at a sawn joint face and the raggedness/smoothness of the joint face. Also sealing practices may be influencing the hydration of the joint face, but further examinations of more samples from unsealed and sealed joints are needed.

The SEM results indicate that all concrete sampled from the different sections contained fly ash. This does not coincide with our interpretation of the construction records. Section 5 and location 3S were supposed to represent no-fly ash mixes (Mix 2 or 6) but the SEM specimens for these locations contained fly ash. The appearance of fly ash in Section 5, and location 3S is a puzzle since these locations were supposedly paved late in the paving season. It is possible that some traces of fly ash can remain in the equipment or storage areas used for the cement and show up in trace amounts in the concrete. The amount of fly ash is extremely difficult to quantify in a well hydrated concrete (6,11). However, the amount of fly ash found in these SEM specimens suggests more than a trace accidental amount was part of the mix. The intent was to have some specimens that represented a no-fly ash concrete but it appears that this did not happen.

5. SUMMARY AND CONCLUSIONS

The I-94 section of pavement near Michigan City examined in the this study provided a unique combination of variables that provided insights into the concrete deterioration at the longitudinal joints apparent in one

section of the WB lanes (Section 1). Although built by one contractor in 1997 and 1998 using a similar structural design, mixture designs and materials throughout, the performance of the concrete varied dramatically. The focus of this study was to compare and contrast samples from the deteriorated section of I-94 to non-deteriorated concrete at the same site and at different sites along this I-94 project near Michigan City. The final objective of this study was to investigate the cause of the concrete deterioration found at these longitudinal joints.

A total of 18 cores were retrieved from five different pavement sections along I-94 between exits 34 and 40, and where feasible, the base material was sampled and the drainage observed at each core hole. The base sampling and drainage observations suggest that at some places the base was no longer granular and was not draining as adequately as designed. In sections in which enough drainage information was collected the drainage was measurably reduced at joints compared to non-joint areas (Section 1 with deteriorated joints and Section 2 with no signs of concrete deterioration).

The edges drains were examined using a drain camera where possible. Some drains were blocked and the camera could not penetrate more than a few feet into the drain, other drains were passable but sections were filled with water while some drains seemed to be functioning well with a small flow of water at the bottom. Sediment and precipitate coated some screens and drain edges. It was obvious that not all the drains were functioning properly and even some blocked, but more precise or direct correlations could not be made

Location	Core	Sample	Distant from top/jt face	unhydrated cement	Fly ash	void sz	voids filled	voids lined	Etringite	Friedal Salt	Cracks	carbonate d paste	Comments	
1	C	j	0 - 2mm	++++			+++	++++	+++	+++			Cl- and Sulfur found randomly in paste (ett and Friedal salt?)	
		~bottom of saw cut	2 - 4 mm	+++		≥ 4 μm	+++	++++	+++	+++				
		t	0 - 2mm	+++		most	++	+++	+++	++	+++			
		-50 mm from joint face	2 - 5 mm	++		8-50 μm	++	+++	+++	++	+++			
1	D1	t	0-15mm+	+++	Y		+++	+++	+++	+		?	Lt Gry paste around some empty voids (leached?) Poor ITZ near top. Voids <15μm often filled	
		m	~ 250mm	+			+++	+++	+++	na			Specimen from mid-depth. Well hydrated paste, smallest voids often lined or filled w/ ett., no Cl- found	
		F	40mm below print surface	++++		L: most 5 - 10 μm sz filled	+++	+++	+++	+	++		Specimen from below sealer. Poorly hydrated cement grains common within 2mm of joint face. Some areas have voids are < 10 microns, filled w/ ett and a little Friedal salt and difficult to see.	
		J	~100 mm	+			+++	++++	+++	+			Many voids filled or lined w/ ett; possibly some thaumasite (Ca-Si-S-CO3). Friedal Salt found in one spot only. Some roots of sample with poor polish.	
2	S	t	0-3 mm	+	Y	10-200 μm	+	++	++	++			Size of air-voids varies from 30 to 500 μm but most common are ± 100 μm	
		t	>3 mm	+	Y	30-500 μm	++	++	++	+++			Many empty air-voids, very few filled with ettringite; some thaumasite	
		t	0-3 mm	+	Y	10-100 μm	+	+	+++	+			Size of air-voids varies from 30 to 200 μm but the most common are ± 100 μm	
		t	>3 mm	+	Y	30-200 μm	+	+	+++	+			Unreacted Fly ash particle (rare)	
3	F	t	0 - 15mm+	++++	Y		++	++	++	++	+		Poor polish & epoxy embedment. Features less distinct, difficult to quantify. Open air void (>20 μm) common. Air voids <20 μm filled w/ ettringite & difficult to see. Si-enriched ett common (sample prep problem?)	
		tj	0 - 15mm+	++	Y		++	+++	+	+	+++		Abundant air voids (spacing factor often <100 microns) only some of the smallest voids filled, a couple of fly ash particles, no Cl- found	
		m	~100 mm	+++			+	++	++	na			Specimen from near saw cut bottom. Cl- in paste very common from face to several mm into paste, ett at joint face, nearly all voids filled within 5mm of joint face (ett w/ some Cl- peaks). A few cracks contain ett.	
		j	0-5 mm from jt face	+++		10-100 μm most common	++++	+++	+++	++	+++		Air-voids filled with gypsum, in the cover zone very few traces of S and Cl; poorly hydrated cement grains Friedal's salt observed in all specimen	
4	S	t	0-2 mm	++++	Y	30-150 μm	+	+	-	-	++		The absence of ettringite in air-voids in top surface (0-2 mm) and the presence in deeper regions of specimens suggest the carbonation zone in the cover zone. Friedal's salt observed in all specimen.	
		t	> 2 mm	+	Y	50-100 μm	-	-	+	++++			Empty cracks near the surface, parallel to the surface, the orientation suggest the freezing and thawing cycles, traces of S and Al present in cover zone. Friedal's salt observed in whole specimen	
		t	0-2 mm	++++	Y	30-100 μm	-	-	-/+	++	+		Etringite is rarely present, only in smaller air-voids (~10 μm). Friedal's salt observed in all specimens	
		t	> 2 mm	+	Y	10-100 μm	-	-	+	++	++		Several of the smallest voids filled (≤ 10μm). Cl- found randomly in paste and voids	
5	F	t	0 - 2mm	+++	Y		++	+	++	++			Unexpected Fly ash. Cl- measurable but not abundant. Ett filled voids common/abundant near jt face. Some Friedal Salt. Unhydrated cement grains rare and small	
		j	0 - 2mm	+	Y		+++	+++	+++	+	+++		Lack of ettringite and presence of Friedl's salt	
		j	≥ 3mm	+	Y		++++	+++	+++	+++	++		Air-voids are randomly distributed, very few about 500 μm diameter, a few empty micro-crack are located in the matrix, lack of ettringite and presence of Friedal's salt	
		t	0-3 mm	++++	Y	20-200 μm	-	-	-	+++	+			
5	W	t	> 3 mm	+	Y	30-150 μm	-	-	-	-	++	+		
		t	> 3 mm	+	Y	30-150 μm	-	-	-	-	-	++	+	

++++ High occurrence +++ Moderate ++ Low occurrence + Very Low occurrence - negligible to none na none observed
t = top of core j = joint face m = mid-depth

Figure 4.13 Features observed in specimens analyzed using SEM.

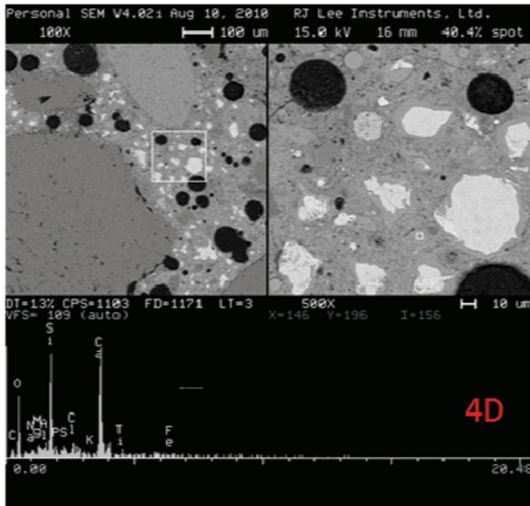


Figure 4.14 Presence of poorly hydrated cement grains (bright angular particles with strong Si and Ca peaks) common in the top 0–2 mm of many specimens and at the sawn joint face.

between the functioning of the drains and observed pavement performance.

By examining the cores megascopically it was determined that the concrete material was in sound condition with no obvious flaws. A close look at the sawn joints revealed a difference between the joint face of the sealed joints compared to the unsealed joints. Although most of the sawn joints appeared to be in good condition from the pavement surface (except for the deteriorated joints), looking at the joints in cross section (along the vertical surface of the core) suggested otherwise. The concrete on the saw cut faces of sealed joints were smooth and in good condition for the first couple inches, but 2–3 in. below the pavement surface the saw cut face appeared more ragged, with microcracks running parallel to the joint face. Sometimes the point at which the sawn face changed from smooth to ragged seemed to match the level of the backer rod and

sometimes it did not. In contrast the sawn joint faces of the unsealed joints were smooth and undamaged through the entire 4–5 in. depth.

The chloride content from each core was measured; from the pavement surface to 1-in. depth for all non-joint cores and from the sawn joint face to 1 in. back from the joint face into the concrete for cores at joints. Elevated chlorides were measured in all samples with the highest chlorides measured in the non-joint cores in the WB lanes. The deteriorated joint had the highest chlorides of all cores from joints but overall the chlorides were lower at the joints than in the top 1 in. of non-joint cores (D, W, S). The unsealed joints had slightly higher chloride levels than the sealed, non-deteriorated joints. Overall it appears that the chlorides move more readily into the concrete from the top down than in from the joint face.

Unlike the water soluble chloride measurements, the acid soluble chlorides would include measurements of chlorides bound in the paste and in secondary products such as Friedel's salt. It was theorized that the difference between the water soluble and acid soluble chlorides might reflect the amount of chlorides that were tied up in compounds such as Friedel's salt. The differences in water and acid soluble chlorides measurements for each sample were compared to the presence and abundance of Friedel's salt identified in the SEM analysis, but no direct, consistent correlation was obvious between these features.

All specimens passed the freezing-thawing test (F-T) with all Durability Factor (DF) >90, except for 1F2 that tested at DF = 86 (some consider DF >60, others consider DF >80 indicates durable F-T resistant concrete). Although these test results suggest durable F-T resistant concrete at all locations there are some interesting trends. Nearly all concrete at joints had a DF lower than the concrete from the nearby mid-span, especially in the WB lanes. Also, the lowest DF were in concrete from the WB lanes.

The lower DF of concrete from the WB lanes coincides with marginal to inadequate air void system parameters (specific surface and spacing factor) when compared to PCA recommendations for good freeze thaw protection (although the DF were all greater than 80). All but one core from the EB lanes had specific surface and spacing factor values that were considered adequate for effective F-T resistance. Any air voids filled with a secondary mineralization such as ettringite were not counted as an air void but were counted as paste, therefore these values do not necessarily represent the original air void system but may represent the existing air void system that is available for future F-T resistance.

Looking at the degree of infilling of the air voids in the SEM specimens there appeared to be a moderate to high level of infilling of the smaller voids in many of the WB lane samples, and of sample 5F from the EB lane. Specimen 5F also is the one EB lane sample that had an inadequate measured air void system. 5D and 5F came from the same concrete panel so it is reasonable to

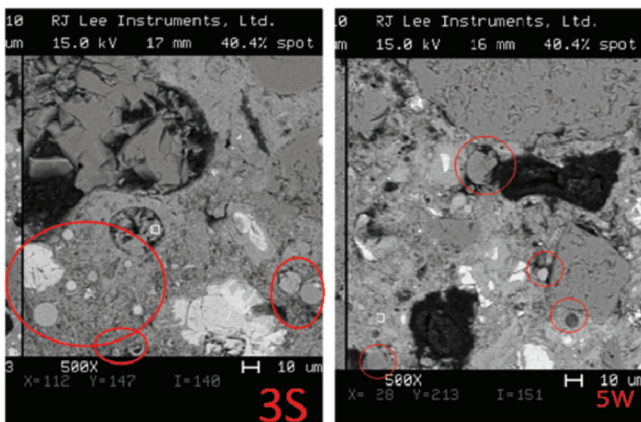


Figure 4.15 Fly ash particles identified unexpectedly in specimens from Section 5 and specimen 3S (round particles inside red circles).

assume that their original air void systems were similar. Yet unlike 5F sample 5D had a low occurrence of infilling of voids and an adequate air void system. It is likely that the infilling of air voids seen in 5F is at least partially responsible for the reduced air void system. Infilling may explain some of the reduced air void parameters in some specimens but not all. For example 1W had the worst spacing factor and specific surface values for this study, but very little infilling or lining of the air voids was seen under the SEM. Infilling and lining of the air voids did have some influence on reducing the measured air void system in some specimens.

REFERENCES

1. Arribas-Colon, M. "Investigation of Premature Distress around Joints in PCC Pavements." MSCE thesis, Purdue University, West Lafayette, Indiana, 2008.
2. Neville, A. M. *Properties of Concrete*, 4th ed. Longman Group, Ltd., London, 1995, 884 pages.
3. Carlson, J., L. Sutter, T. J. Van Dam, and K. R. Peterson. Comparison of Flatbed Scanner and RapidAir 457 System for Determining Air Void System Parameters of Hardened Concrete. *Transportation Research Record, Journal of the Transportation Research Board*, No. 1979, Transportation Research Board of the National Academies, Washington, D. C., 2006, pp. 54–59.
4. Pade, C., U. H. Jakobsen, and J. Eisen. A New Automatic Analysis System for Analyzing the Air Void Systems in Hardened Concrete. *Proceedings of the 24th International Conference on Cement Microscopy*, San Diego, California, 2002, pp. 204–213.
5. Peterson, K. W., R. A. Swartz, L. L. Sutter, and T. J. Van Dam. Hardened Concrete Air Void Analysis With a Flatbed Scanner. *Transportation Research Record, Journal of the Transportation Research Board*, No. 1775. Transportation Research Board of the National Academies, Washington, D. C., 2001, pp. 36–43.
6. Kosmatka, S. H., B. Kerkhoff, and W. C. Panarese. *Design and Control of Concrete Mixtures*, 14th ed. Portland Cement Association, Skokie, Illinois, 2002, 372 pages.
7. St. John, D. A., A. B. Poole, and I. Sims. *Concrete Petrography: A Handbook of Investigative Techniques*. John Wiley & Sons, Inc., New York, 1998.
8. Van Dam, T. J., L. L. Sutter, K. D. Smith, M. J. Wade, and K. R. Peterson. *Guidelines for Detections, Analysis and Treatment of Materials-Related Distress in Concrete Pavements—Vol. 2*. Publication FHWA-RD-01-164, Washington D. C., 2002.
9. Sutter, L. L., K. R. Peterson, T. J. Van Dam, and K. Smith. Using Epifluorescence Optical Microscopy to Identify Causes of Concrete Distress. *Transportation Research Record: Journal of the Transportation Research Board*, No. 1798, Transportation Research Board of the National Academies, Washington, D. C., 2002, pp. 22–30.
10. Bentz, D. P., and P. E. Stutzman. Curing, Hydration, and Microstructure of Cement Paste. *ACI Materials Journal*, Vol. 103, No. 5, Sept.–Oct. 2006, pp. 348–356.
11. Walker, H. N., D. S. Lane, and P. E. Stutzman. *Petrographic Methods of Examining Hardened Concrete: A Petrographic Manual*, Revised 2004. Publication FHWA-HRT-04-150, U.S. Department of Transportation, Turner-Fairbank Highway Research Center, McLean, Virginia, 2006.

APPENDIX A. DRAINAGE AND DRAINAGE LAYER OBSERVATIONS AND TESTING

DRAINAGE AND SUBBASE SAMPLING

Subbase Drainage

Table A.1 summarizes the drainage observed in the core hole and related subbase information.

Subbase Sampling

The drainage layer immediately underlying the pavement was constructed of #8 sized aggregate and was sampled in several locations by scooping out material from the bottom of the core hole by hand or with a metal scoop. The material was comprised primarily of slag aggregate, except at core 3J which was a quarried carbonate aggregate (shown in Figure A.2.). Some of the slag aggregate had fused together into more massive chunks as seen in samples from 1C, 2F, 3D, 4F and 4D in Figures A.1 through A.3. At core holes 1C, 1J and 3F little to no granular material was obtained before a solid massive layer was hit that made it impossible to sample.

Edges Drains

The general locations of the drains examined are plotted on Figure 4.2. Drain 1 is approximately 160 ft east of the Section 1 cores and slants to the east, away from the coring site. The screen was in place at the drain opening with a small amount of damp sediment approximately an inch deep against the screen. The camera went 75' into the edge-drain. No obstructions were encountered although a small amount of vegetation was occasionally seen (as shown in Figure 4.4). The camera went through a pocket of water where the drain was completely submerged for about 2 ft, a few feet in from the screen near the pavement edge and still in smooth (PVC) pipe. The only other water encountered were small patches of water approximately 1 in. deep (as seen in Figure 4.4, right).

Drain 2 is approximately 340 ft west of Section 1 cores. The first section of the drain is smooth PVC pipe and completely submerged (as shown in Figure A.5, left). Further in the drain is a corrugated pipe that had about 1 in. of water at bottom (Figure A.5, photo on right). The corrugated pipe takes a turn at about 63 ft in that was too tight to get the camera past. It was theorized that this drain crosses under pavement and joins the drainage system under the medium. A connection to an edge drain a few feet in from the screen was expected but not seen. It may have been in the area where the pipe was completely submerged and cloudy water obscured the view of a connection.

TABLE A.1
I-94 Michigan City drainage and base information

Core		Length	Location	Drainage	Base condition	Notes
#	#					
1J1	4	14 in.	STA 24+600 WB lane	Slow	~2 in. granular then solid	± 2 in. of fine material in bottom of hole then hard layer; could not dig through with hand or spoon
1D2	2	16 in.		Granular	Granular slag aggregate; no notes about drainage	
1F2	1	15.3 in.		Very slow		No base sampled
1C1	5	15.2 in.		Extremely slow	Hard and solid	No drainage; WL same in core hole after 20 min; chunks and some granular attached to/from core; in hole too hard and solid to sample
1D1	3	15.2 in.		Good	Granular	Quick drainage; granular base; nearby shoulder joint drained quickly
1W1	6	14.75 in.		Good	Granular	Quick drainage; base sampled, granular
1S3	7	15.2 in.		Good		Drained quickly. No water remained in hole after drilling
2F1	8	15 in.	STA 23+900 WB lanes	Moderate to slow	Larger chunks of cement particles	Moderately slow drainage (8 in. of water in hole after drilling, drop to 4.5 in. after 15 min); water poured at joint drained very slowly
2D1	9	15.2 in.		Moderate		Moderate drainage; 5 in. of water in hole after drilling
3J2	10	12.5 in.	STA 23+900 EB lanes	Moderate	Granular limestone aggregate	Moderate drainage; most of water drained from hole in 10 min
3F1	11	15 in.		Moderate to slow	Granular slag	Moderate to slow drainage; 4 in. of water in hole drained to 3.8 in. after 5 min; granular w/slag smell
3D1	12	15.2 in.			Granular w/larger chunks	Base ~granular with cemented chunks
3S3	13	14.75 in.			Granular	Sampled base, granular
4F1	14	15.6 in.	STA 25+000		granular w/larger chunks	Base granular with larger chunks of cemented material
4D1	15	15 in.		Good	Granular w/larger chunks	Very good drainage; <1 in. water in hole after drilling
5F1	16	14.5 in.				
5D1	17	14.5 in.		Good	Granular	Good drainage; water 1–2 in. hole after drilling
5W1	18	14.5 in.			Granular	Granular slag aggregate

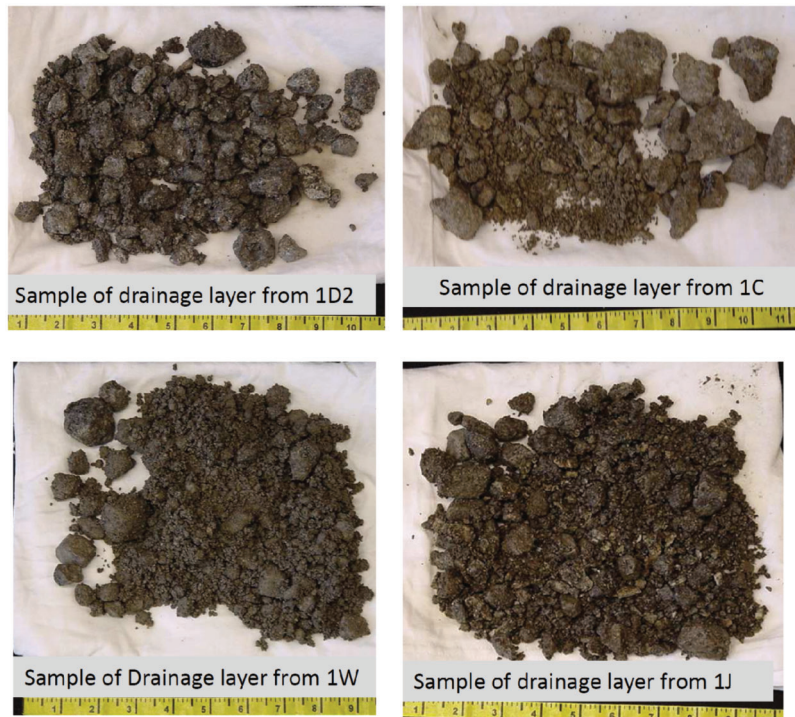


Figure A.1 Drainage layer samples from I-94, Section 1.

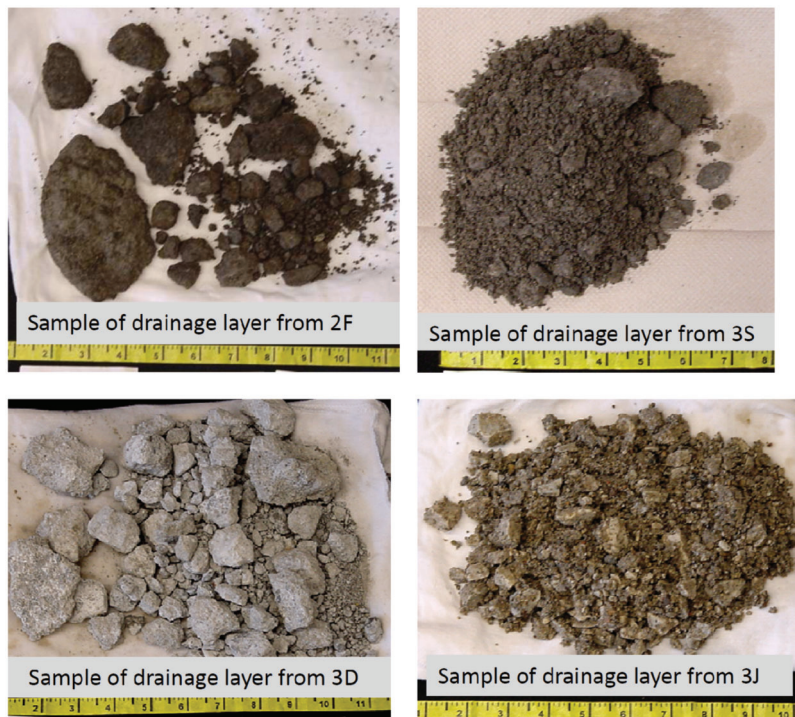


Figure A.2 Aggregate drainage layer sampled at core holes in Sections 2 and 3.

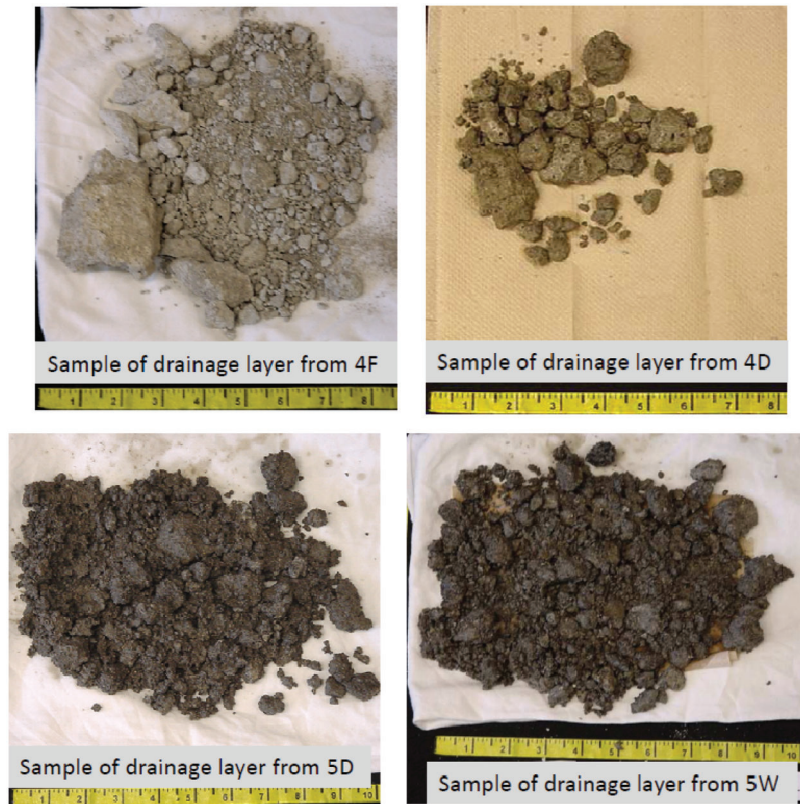


Figure A.3 Samples from drainage layer at core holes in Sections 4 and 5.

Drain 3 is approximately 375 ft west of Drain 2. The outlet and screen for this drain was clogged with sediment (as seen in Figure 4.5). The water ran free out of drain after disturbing the sediment (i.e., kicking the screen). An obstruction was encountered in this drain about 3 ft in that the camera could not pass and a 1-in. dowel could not get through. In the first 3 ft of pipe the camera images showed sediment built up around the inside of the drain pipe.

Section 2, Non-Deteriorated Concrete (WB Lanes Just West of Johnson St. Overpass) Drain 4 was near the

Section 2 coring location but the outlet was buried in a ditch filled with cattails, soils and water and not accessible. Water in the ditch was draining towards the east and the pavement surface slopes east and downward, towards the overpass.

Section 3, Non-Deteriorated Concrete, EB Lanes The pavement surface was sloping east towards the Johnson St overpass. Water was running out of the nearby Drain 5, but the screen was covered with sediment and the inside of the drain was encrusted with sediment that was light brown and flakey, similar to material collected at Drain 3. The camera could penetrate only 5 to

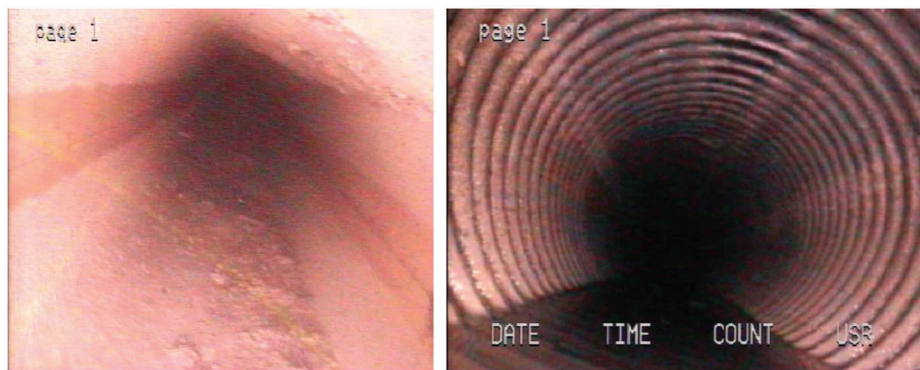


Figure A.4 Drain 2. Initial PVC section completely submerged (left) and corrugated pipe further in with 1 in. of water (right).

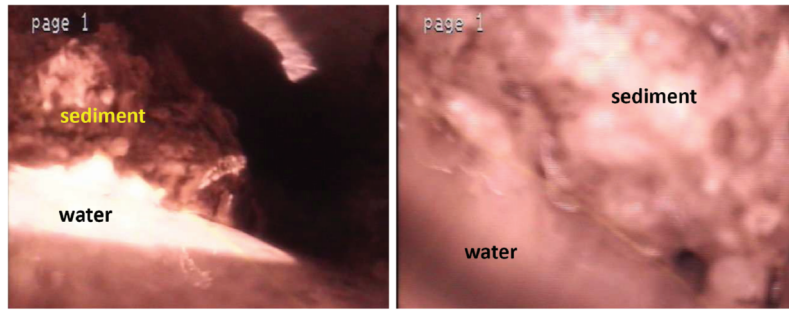


Figure A.5 Drain 5 appears nearly clogged with sediment but still allows some water to pass.

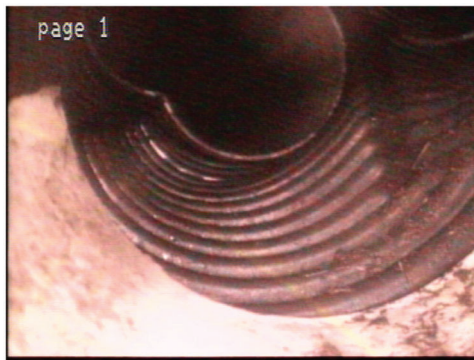


Figure A.6 Drain 6, at transition joint from corrugated to smooth PVC pipe approximately 10 ft into the pipe.

6 ft into the drain. Photos indicate that sediment clogged the drain but a small amount of water was still trickling over/past the sediment (shown in Figure A.5).

Section 4, EB Lanes, Unsealed Joints Drain 6 was open, the screen was clear, a patch of grass was growing about a foot in front of the opening and a bright green slime covered the bottom of the PVC outlet pipe. We could not get the camera past the joint/bend in the pipe as it goes from PVC to corrugated, approximately 10 ft in from the outside edge of the pavement (joint shown in Figure A.6).

Section 5 EB Lanes, Unsealed Joints Concrete in this area had some corner cracks. Drain 7, which was closest to and just west of the coring site, was the last drain west of an overpass. The pavement surface slopes very slightly to the east, towards the overpass. The screen was clear and the outlet drain pipe had a thin layer of damp sediment < 1/2 in. deep but no flowing water. However, much of the first 40 ft of the drain was filled with water. At approximately 50 ft the camera encountered a joint/turn and could not pass. This drain probably crosses under the road and intersects with the drainage system under the medium. No intersection was visible for the outside shoulder edge drain, which should have been at approximately 10 ft. The intersection with the first edge drain may have been obscured by cloudy water. Images on the camera were not very clear when the camera was submerged and the water cloudy.

APPENDIX B. I-94 PAVEMENT CORES

COLLECTION OF CORES

A total of 18 cores were taken from various locations along the EB and WB lanes of I-94 near Michigan City. The coring locations were identified by the research team with input from INDOT and the industry representatives. The coring was completed by INDOT Office of Research with traffic control provided by the INDOT sub-district of LaPorte. The LaPorte Operations Manager was very cooperative and all the proposed cores were retrieved. Policy and safety concerns related to this I-94 corridor limited the extent and duration of traffic control, limiting the time for base sampling and drainage tests.

Standardized coring locations established in the initial project, were used. As described below and shown in Figure B.1, cores at locations J, W and S were added. Specimens were labeled according to the following nomenclature, depending on their location. (NOTE: No cores were taken from locations A, B or E.)

Damaged Concrete

A—damaged area of a transverse joint

B—damaged area of a longitudinal joint near the junction of longitudinal and transverse joint

C—damaged area of a longitudinal joint away from the transverse joint

Undamaged Concrete

D—mid-span of the slab, undamaged section

E—undamaged transverse joint adjacent to the damaged transverse joint

F—undamaged area of the longitudinal joint away from the transverse joint

J—next to construction joint, undamaged (<1 in. from joint)

TABLE B.1

Core locations—a cross-reference of the preliminary numbering system and standardized system

Preliminary core no.	Established core no.	Location
1	1F2	STA 24+600 WB lane
2	1D2	
3	1D1	
4	1J1	
5	1C1	
6	1W1	
7	1S3	
8	2F1	STA 23+900 WB lanes
9	2D1	
10	3J2	STA 23+900 EB lanes
11	3F1	
12	3D1	
13	3S3	
14	4F1	STA 25+000 EB lane
15	4D1	
16	5F1	STA 125 EB lane
17	5D1	
18	5W1	

W—wheel path (>2 ft from transverse joint)

S—shoulder (>2 ft from joints)

At the time of coring the cores were labeled sequentially and later identified with the appropriate alphanumeric code. Table B.1 is a cross-reference of this labeling system. Figure B.2 is the photo-log of all the cores taken along I-94 for this project. The images include side, top and bottom views of all 18 cores.

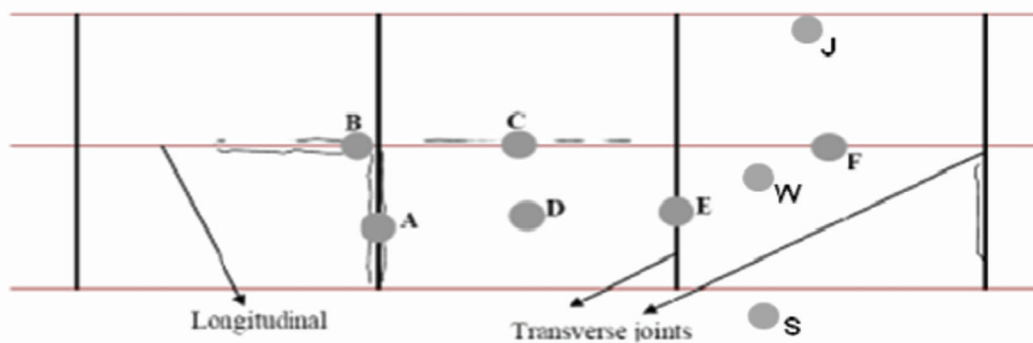


Figure B.1 Standardized coring locations—revised.

SECTION 1

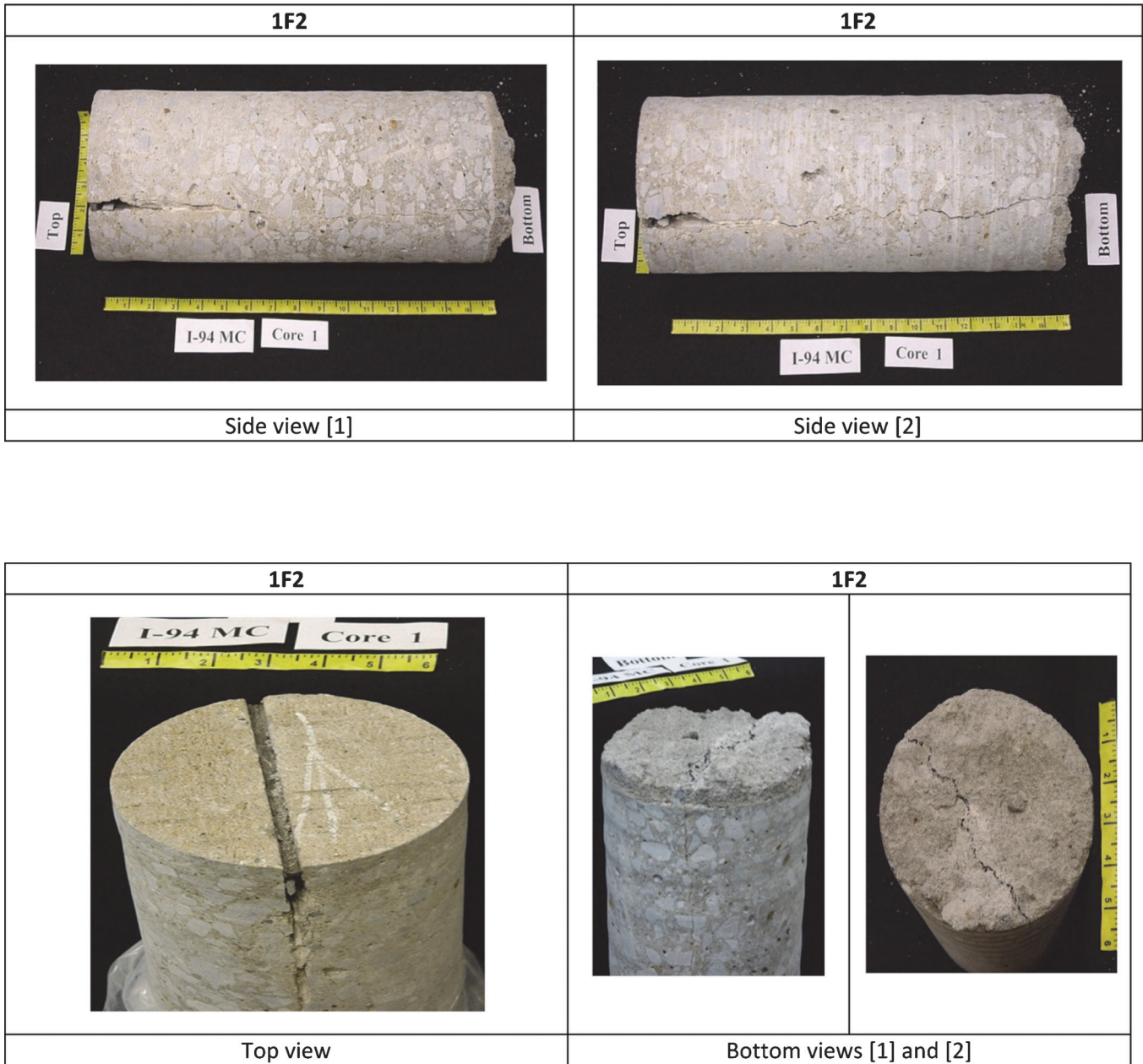


Figure B.2 Collection of cores.

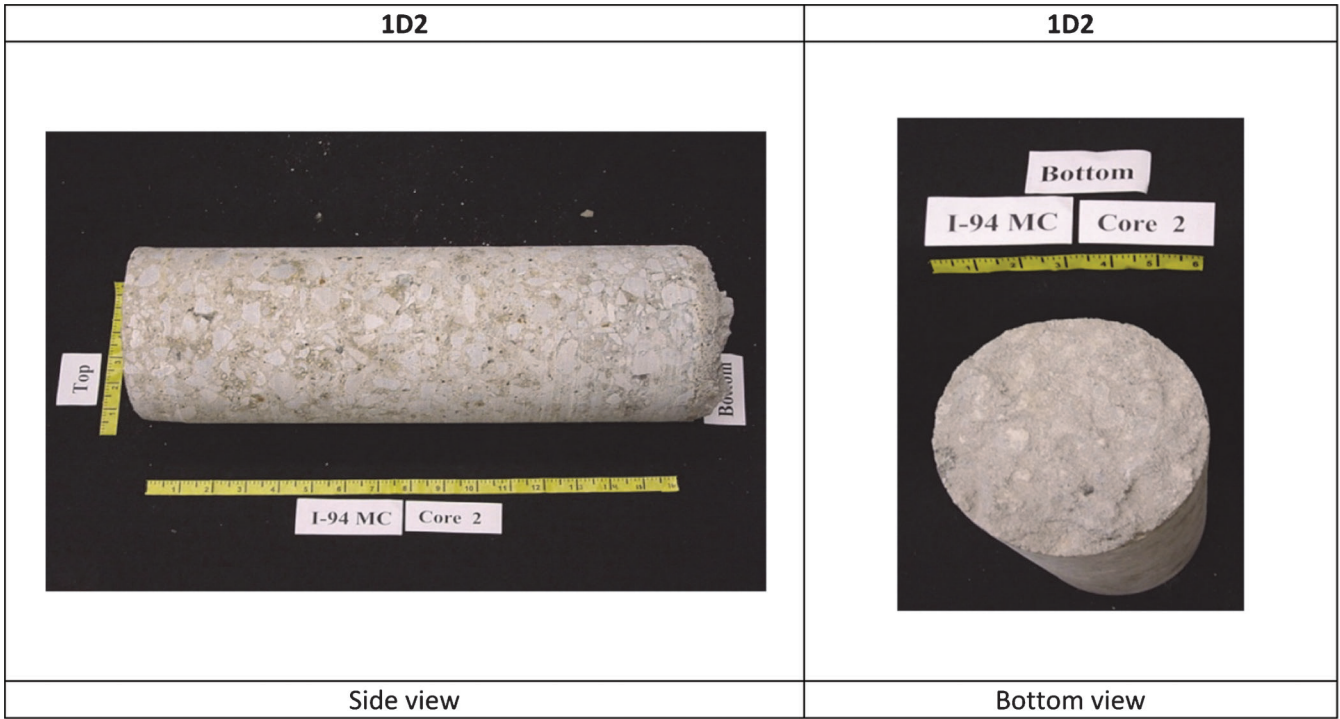
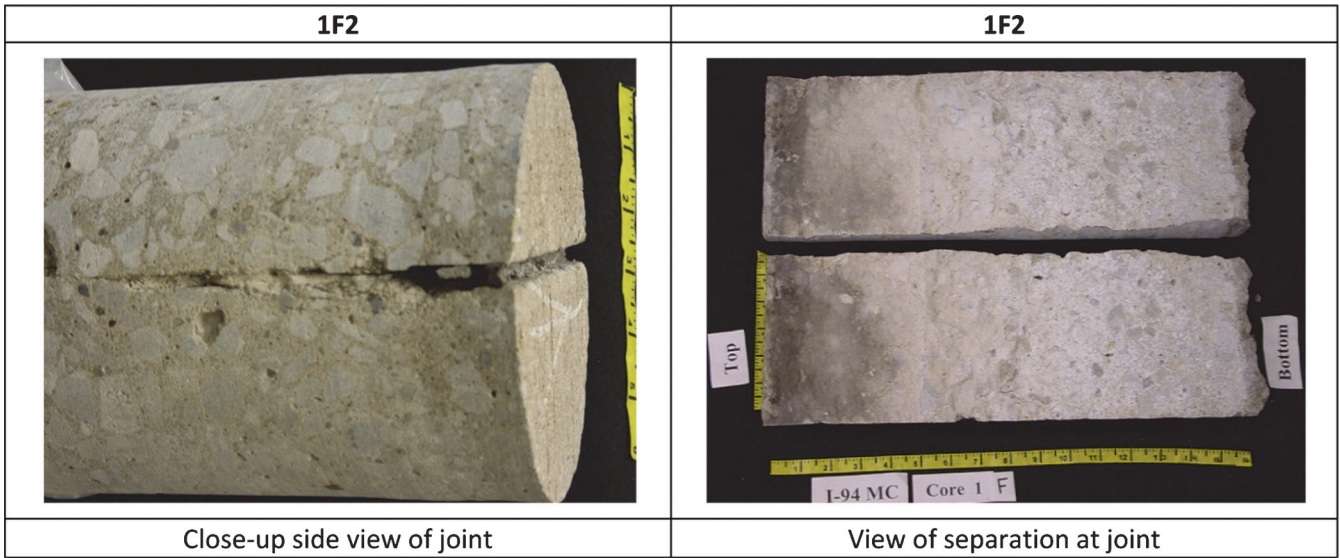


Figure B.2 Continued.

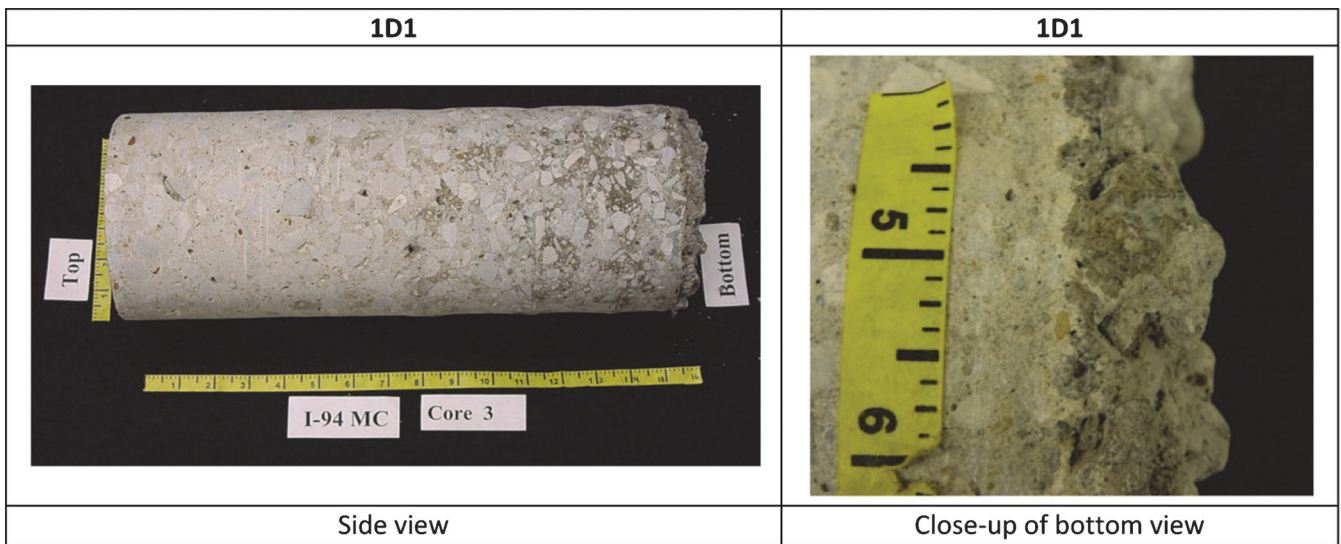
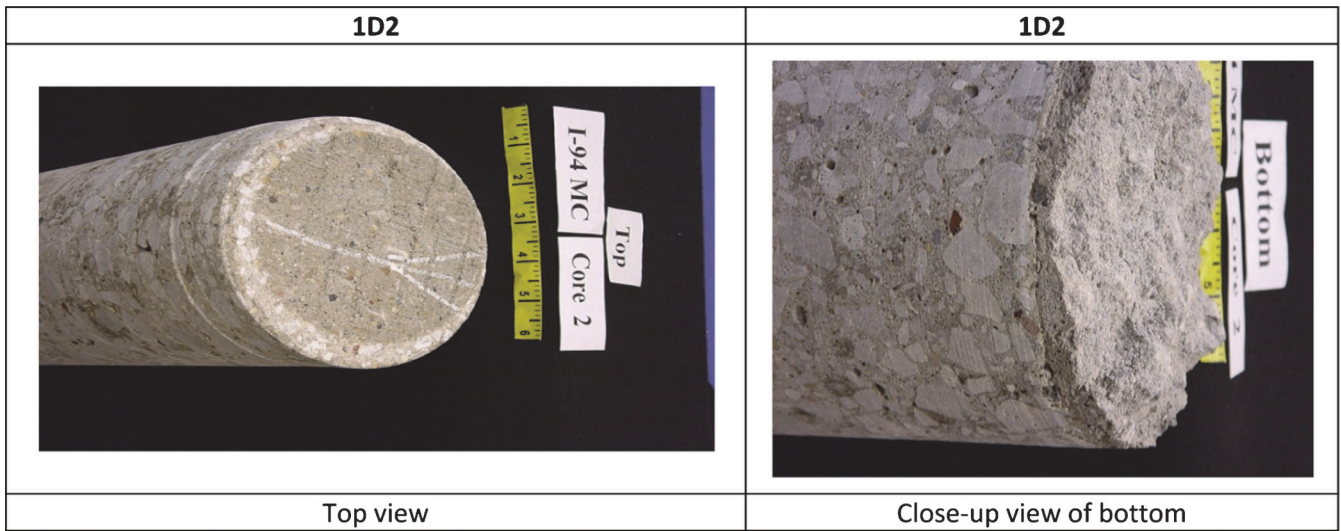


Figure B.2 Continued.

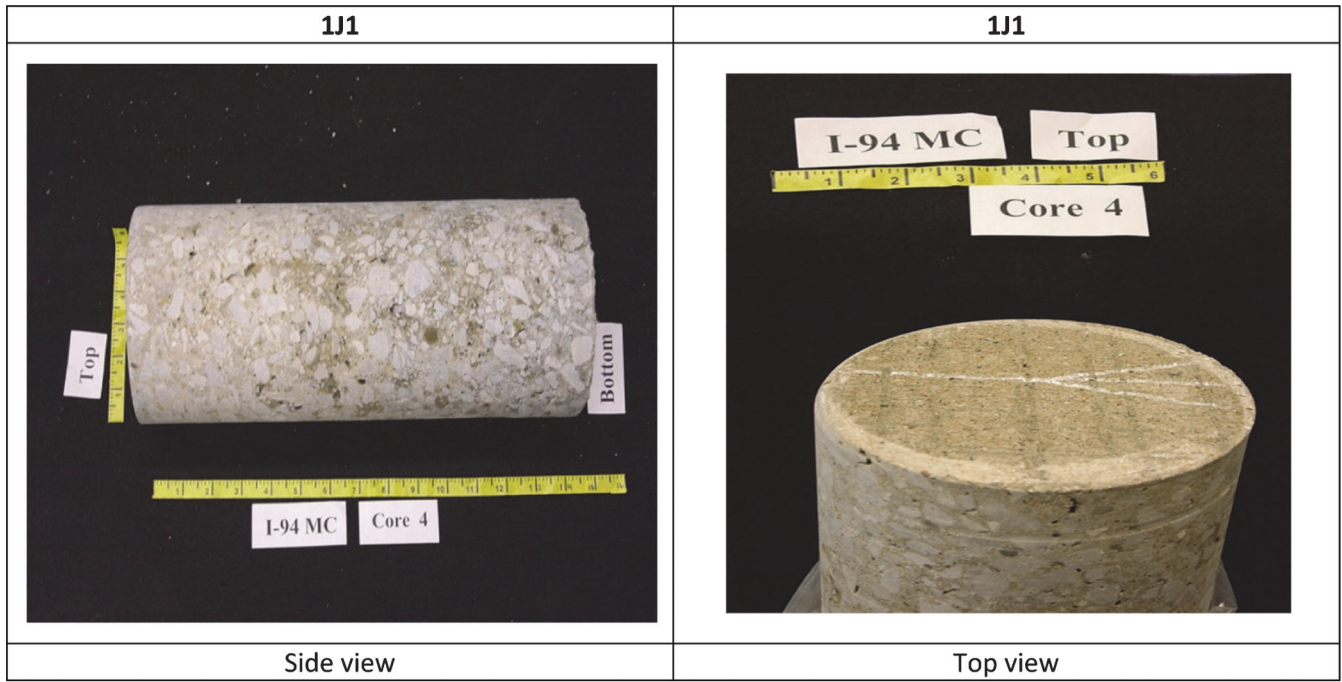
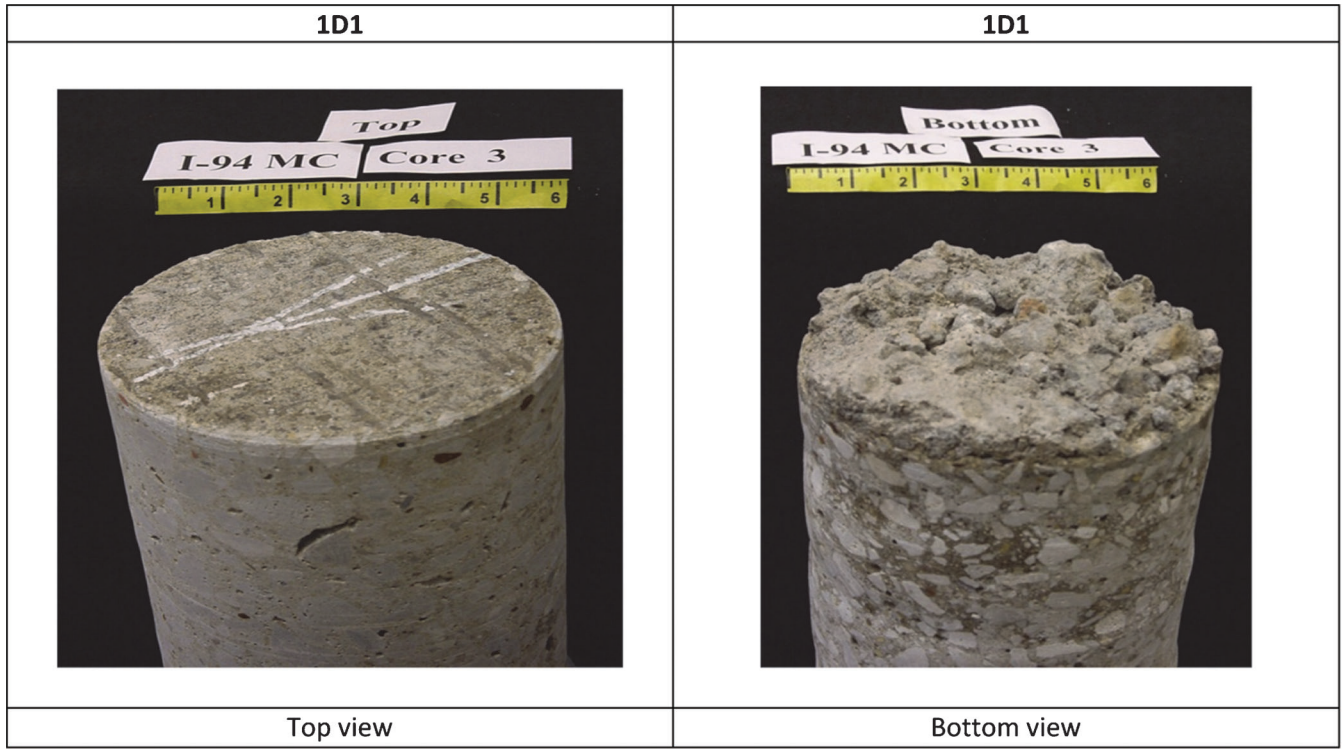


Figure B.2 Continued.

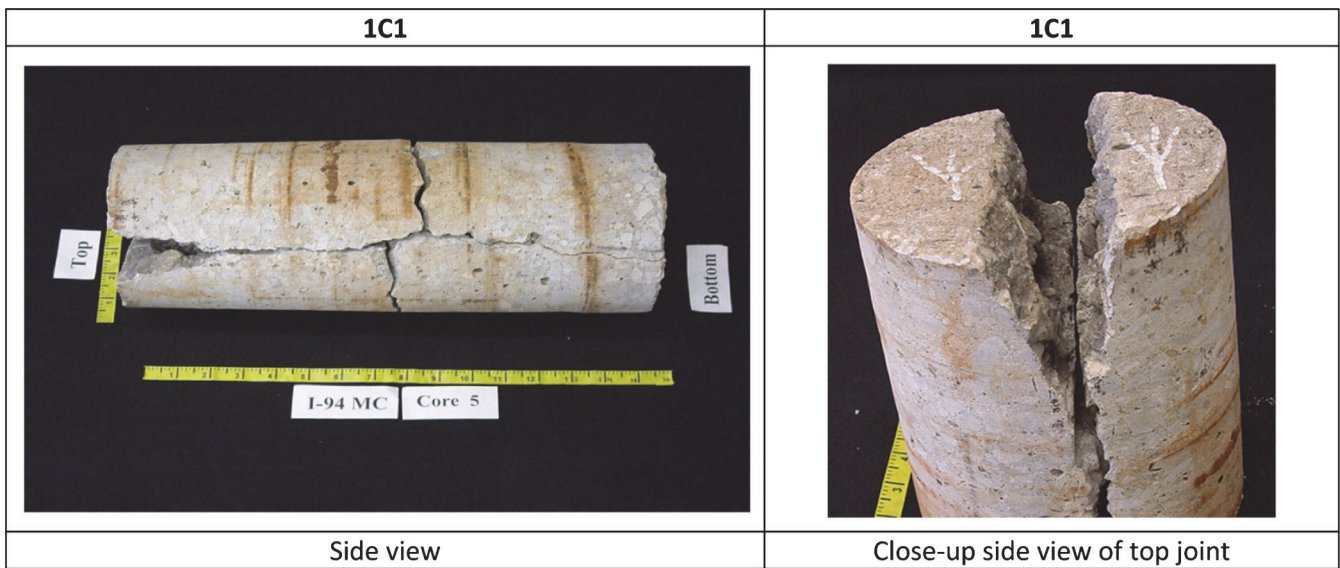
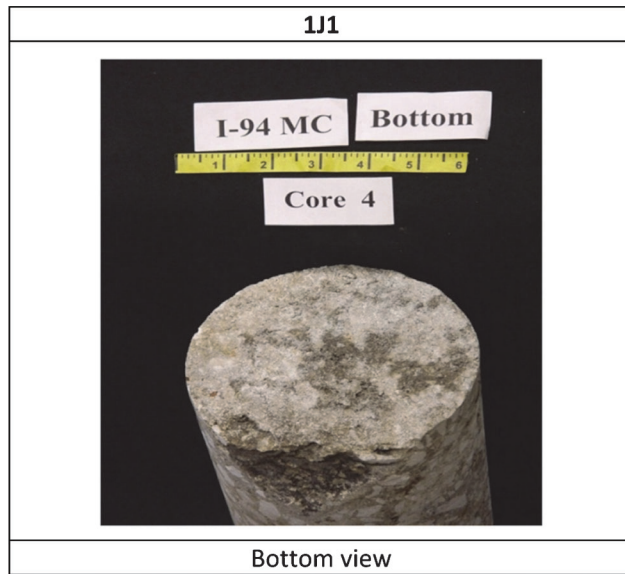


Figure B.2 Continued.

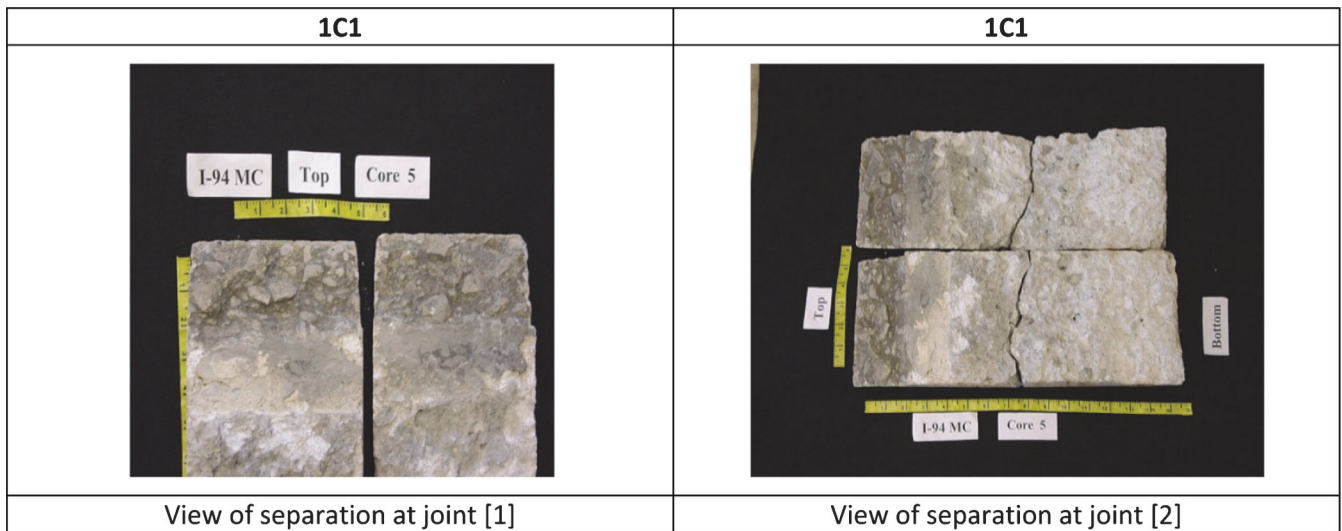
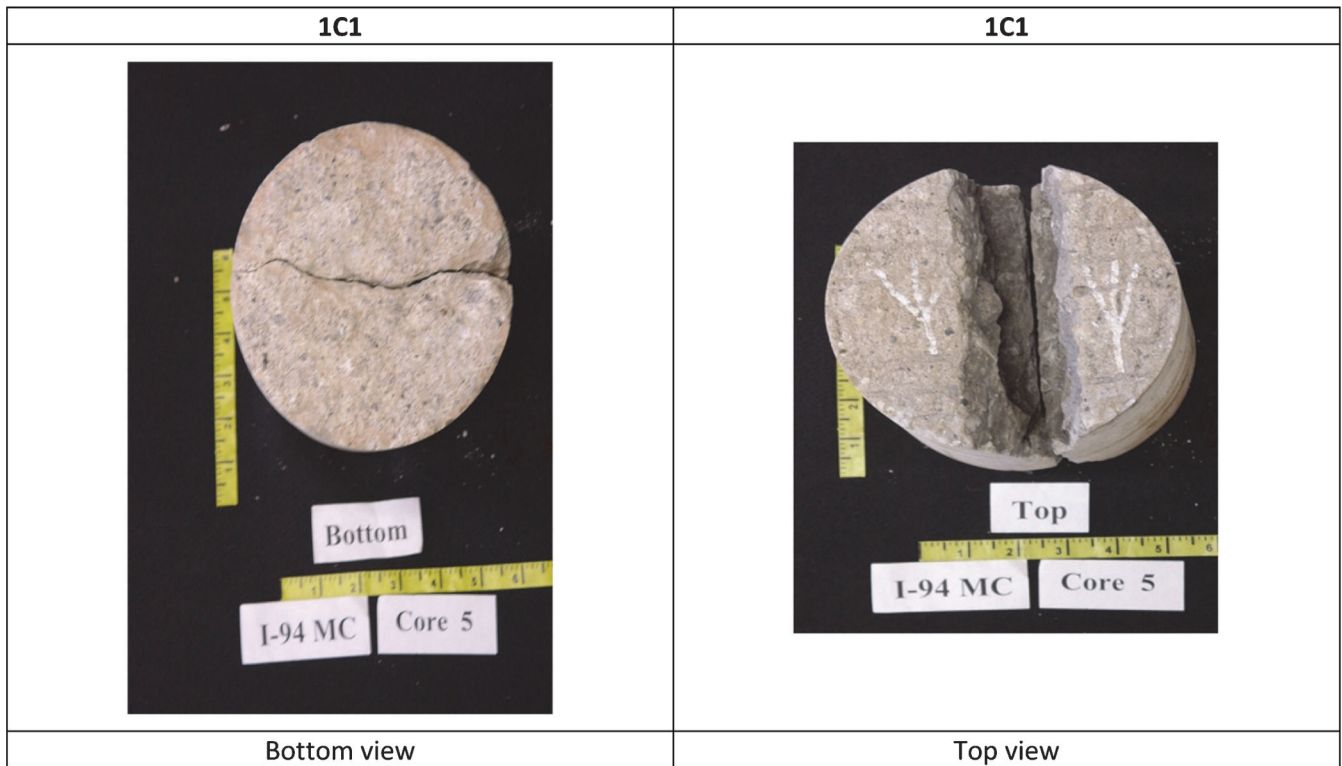


Figure B.2 Continued.

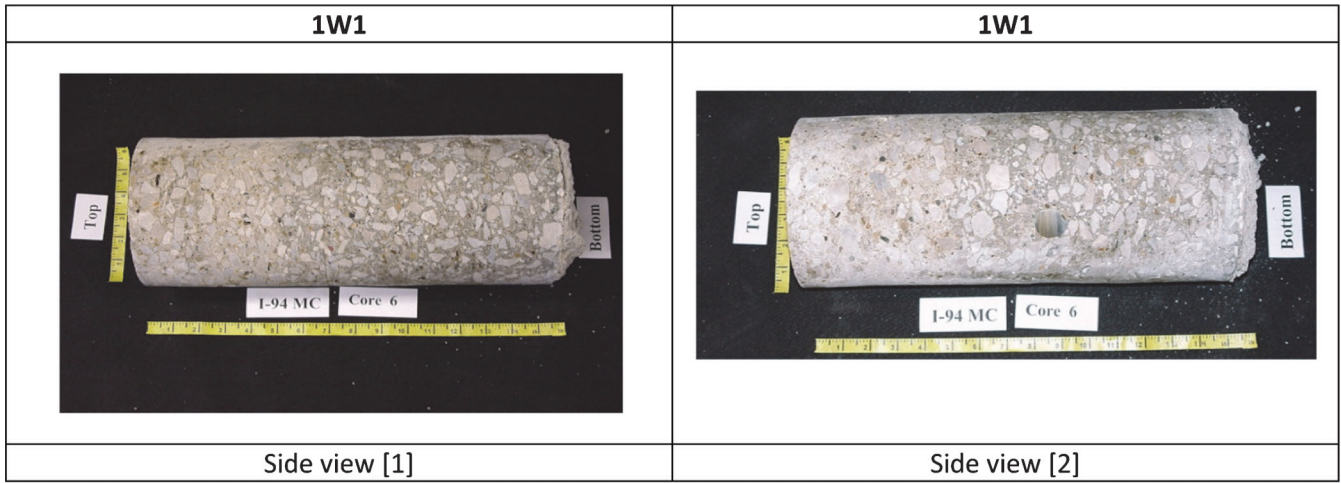


Figure B.2 Continued.

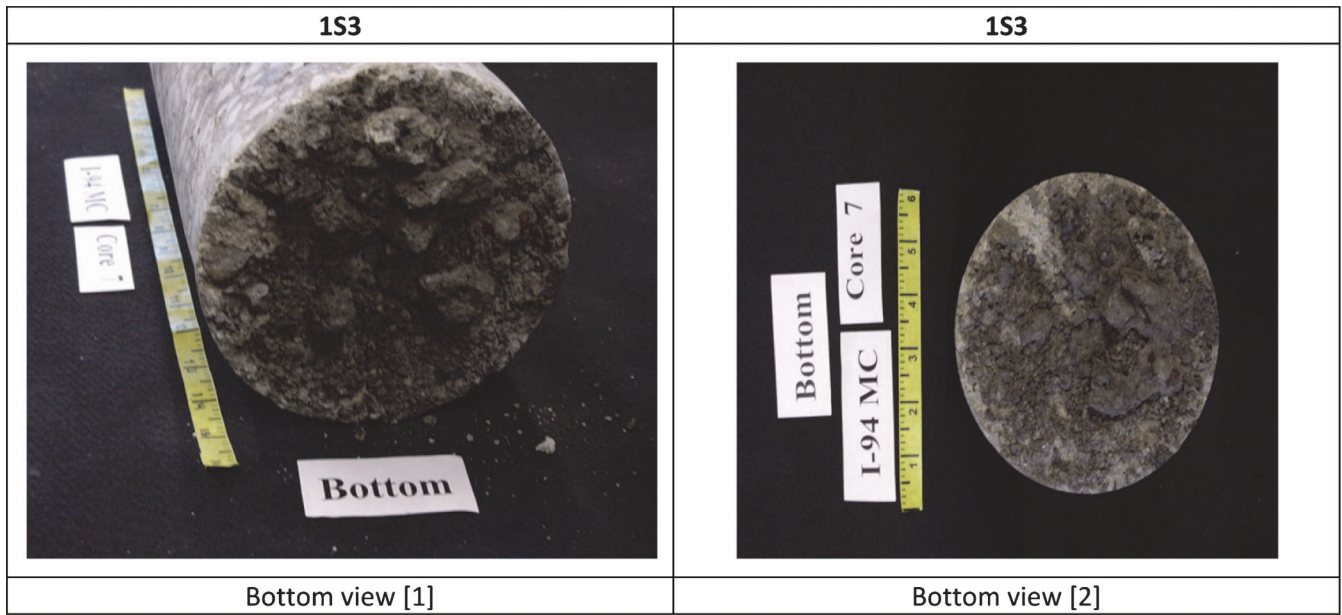
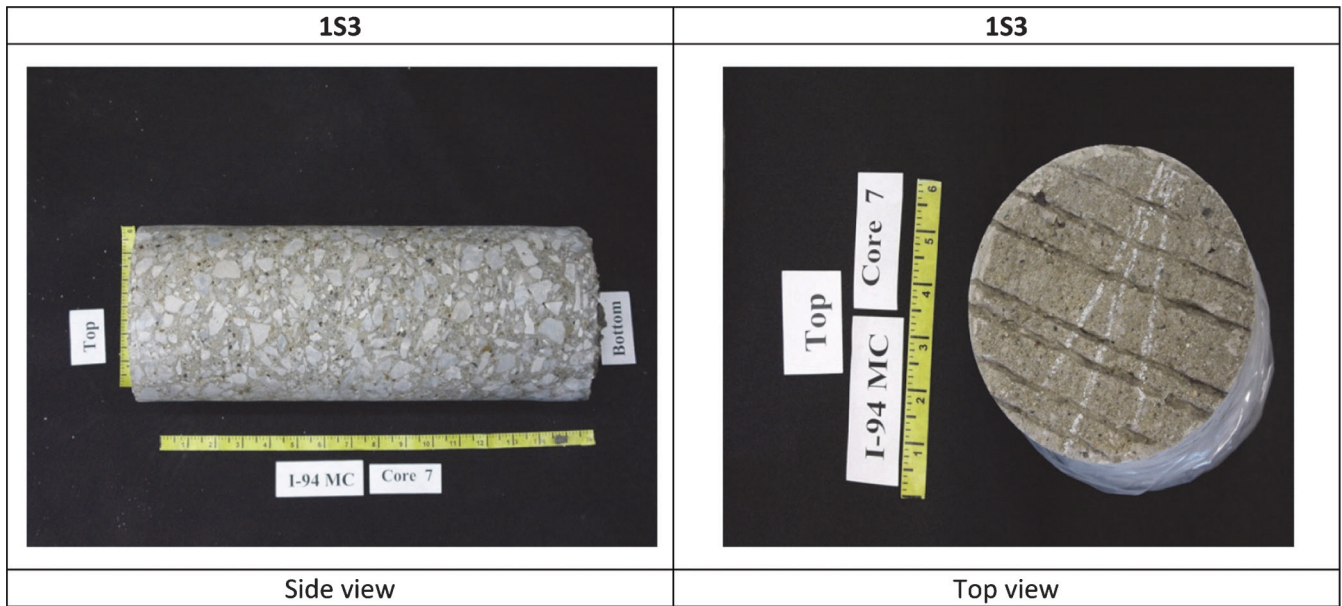


Figure B.2 Continued.

SECTION 2

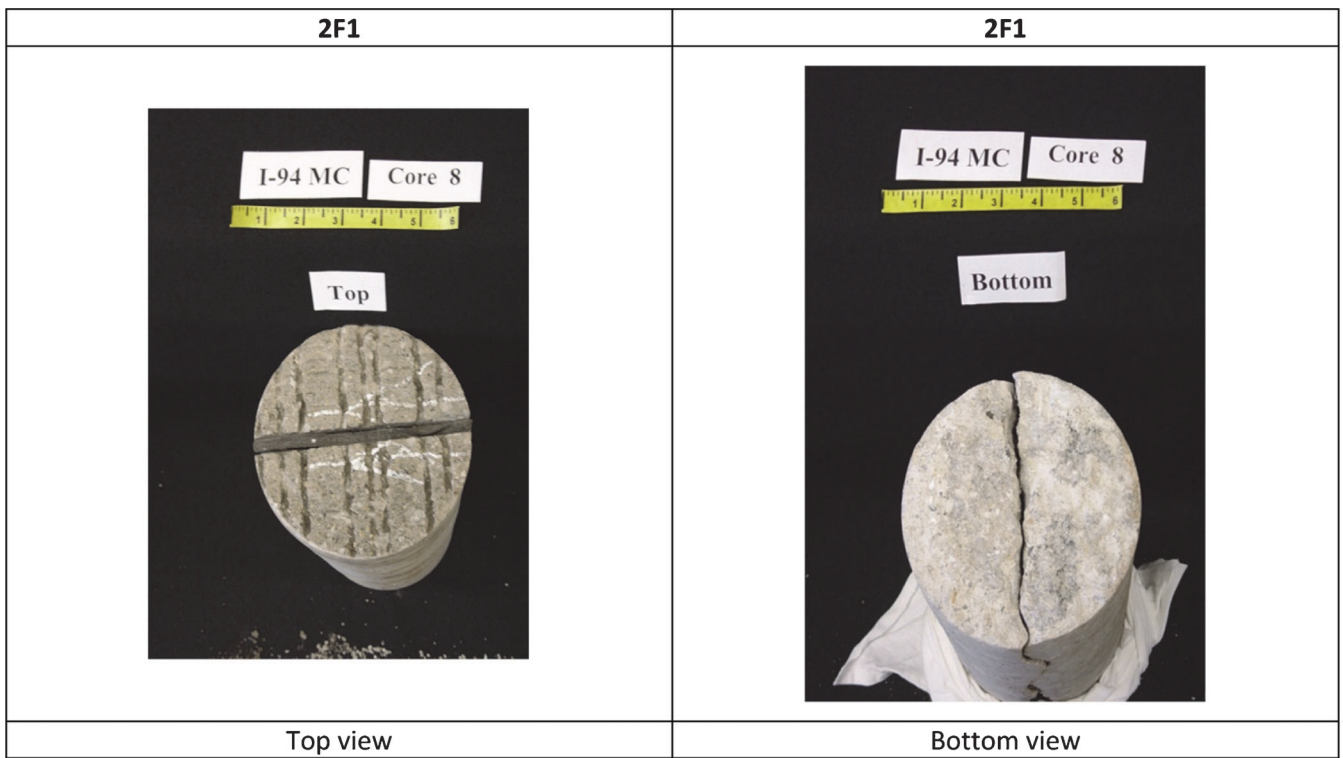


Figure B.2 Continued.

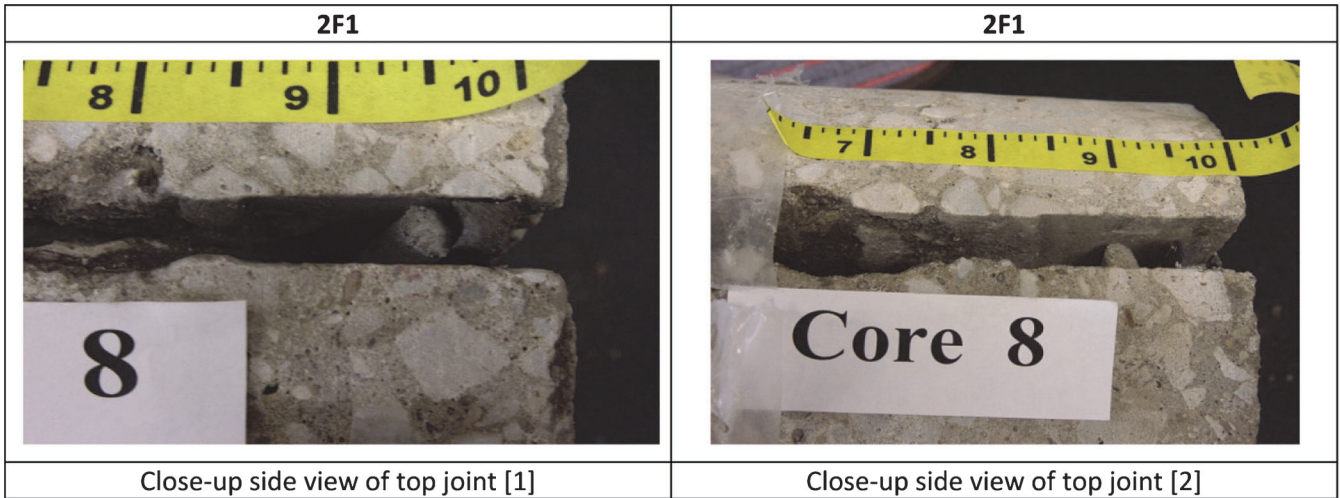


Figure B.2 Continued.

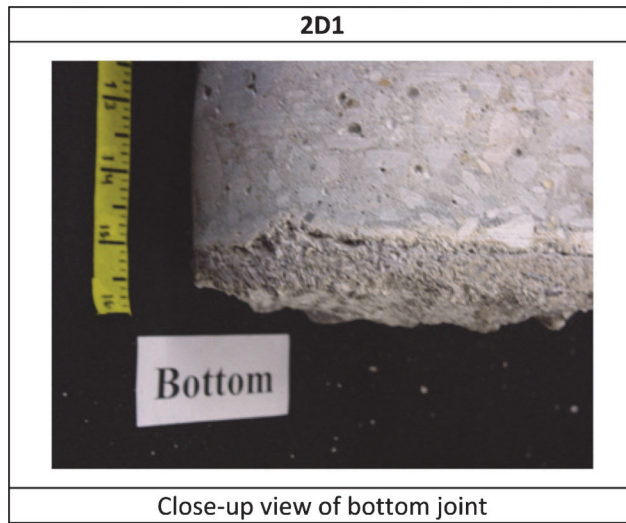
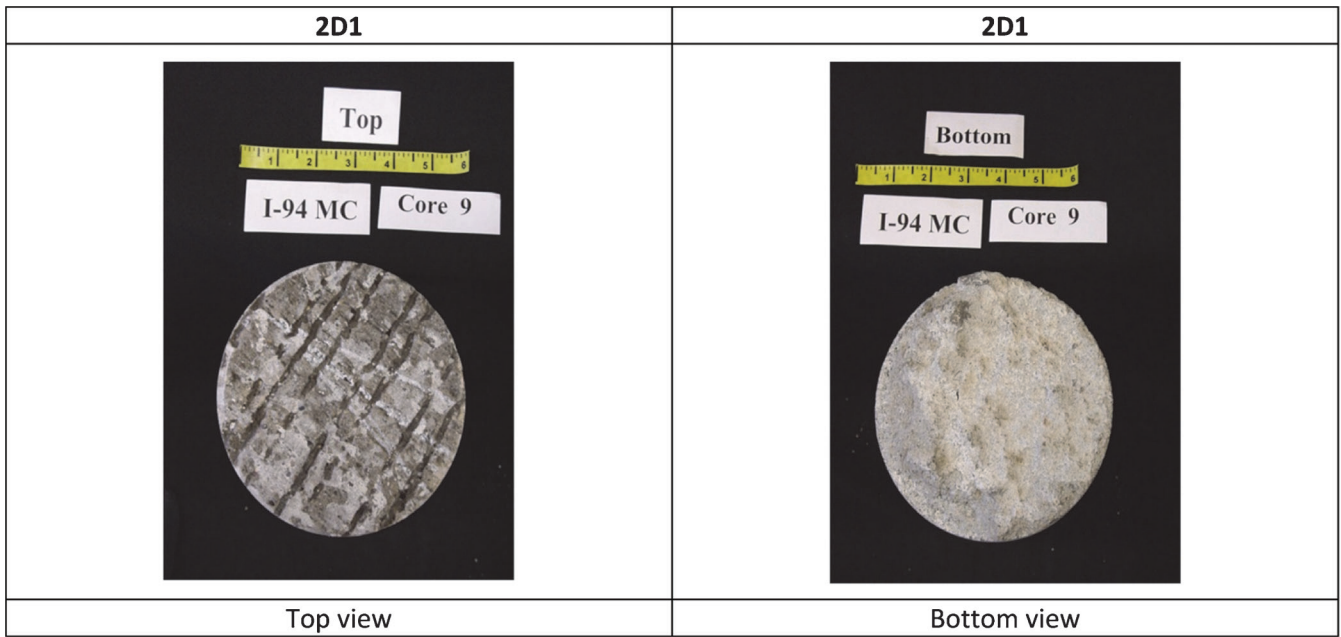


Figure B.2 Continued.

SECTION 3

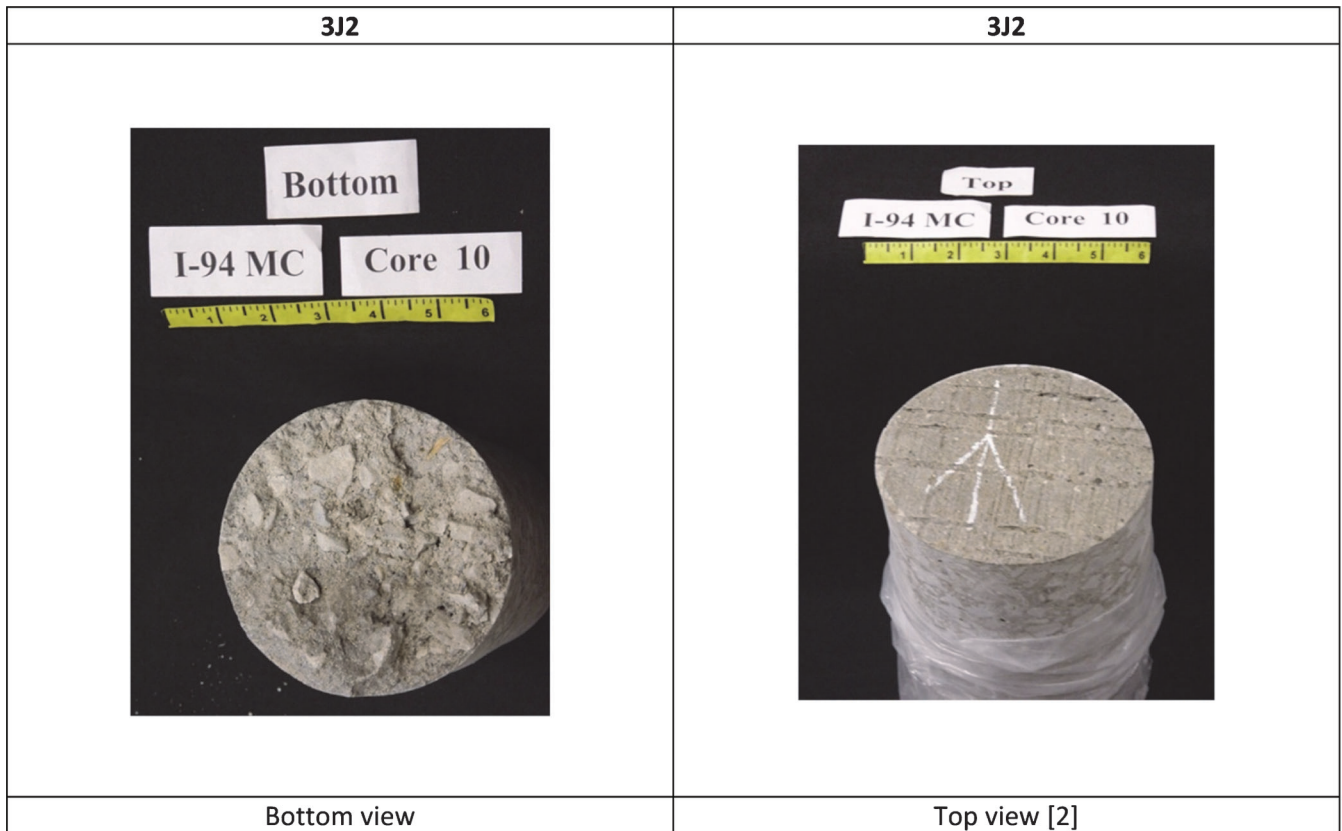
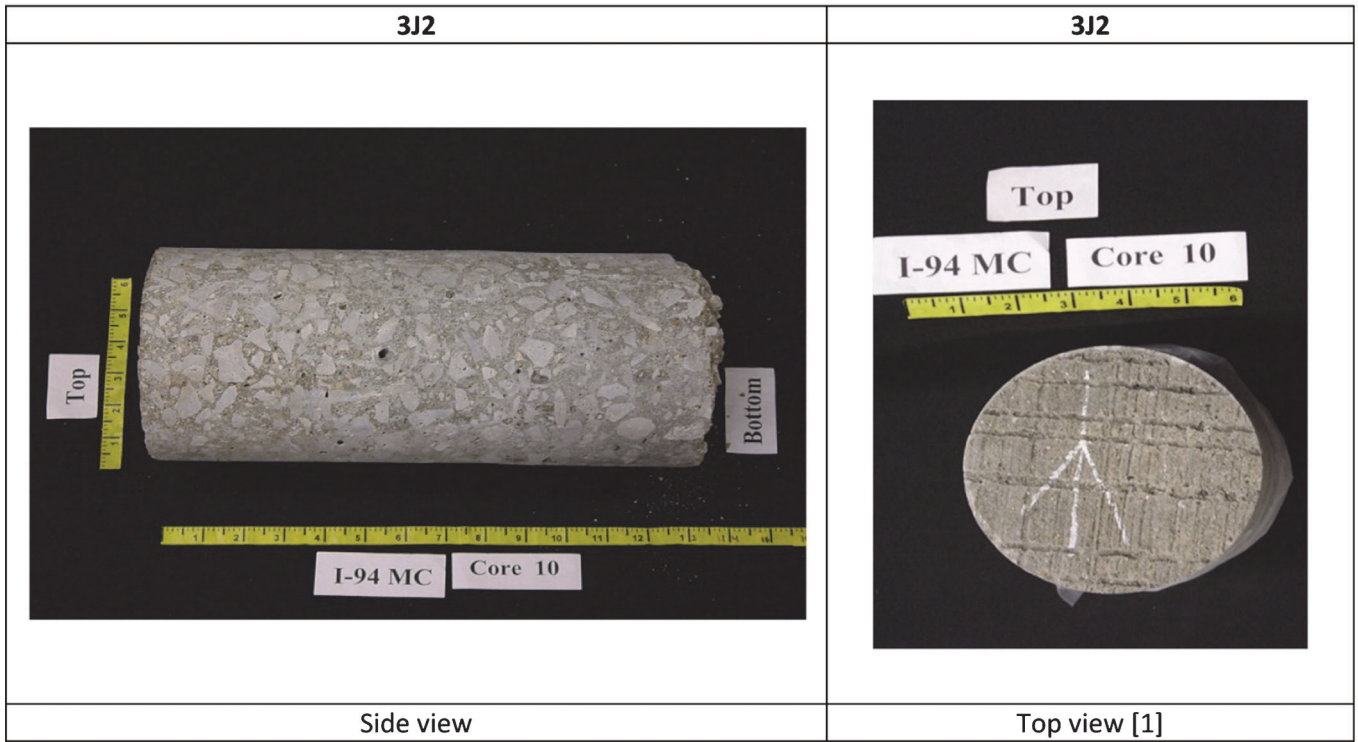


Figure B.2 Continued.

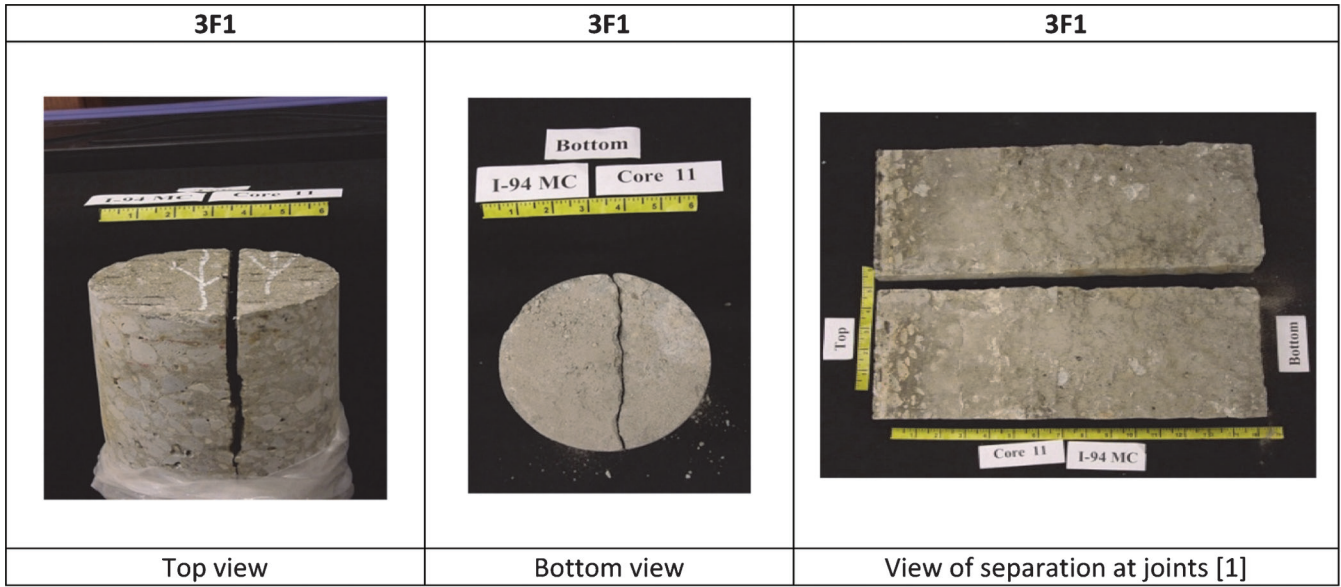


Figure B.2 Continued.

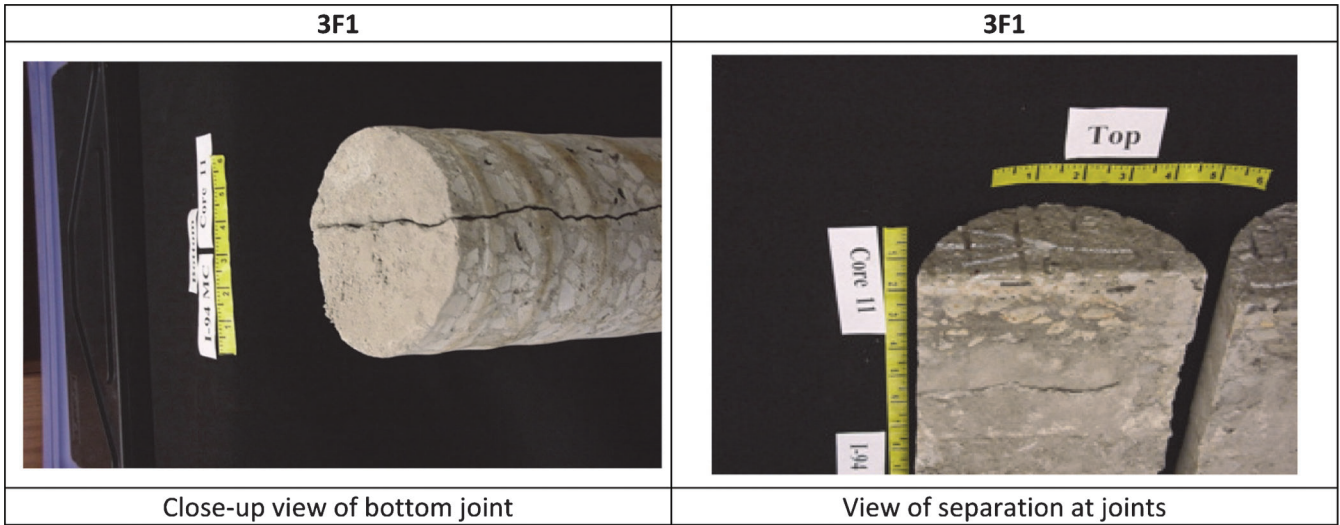


Figure B.2 Continued.

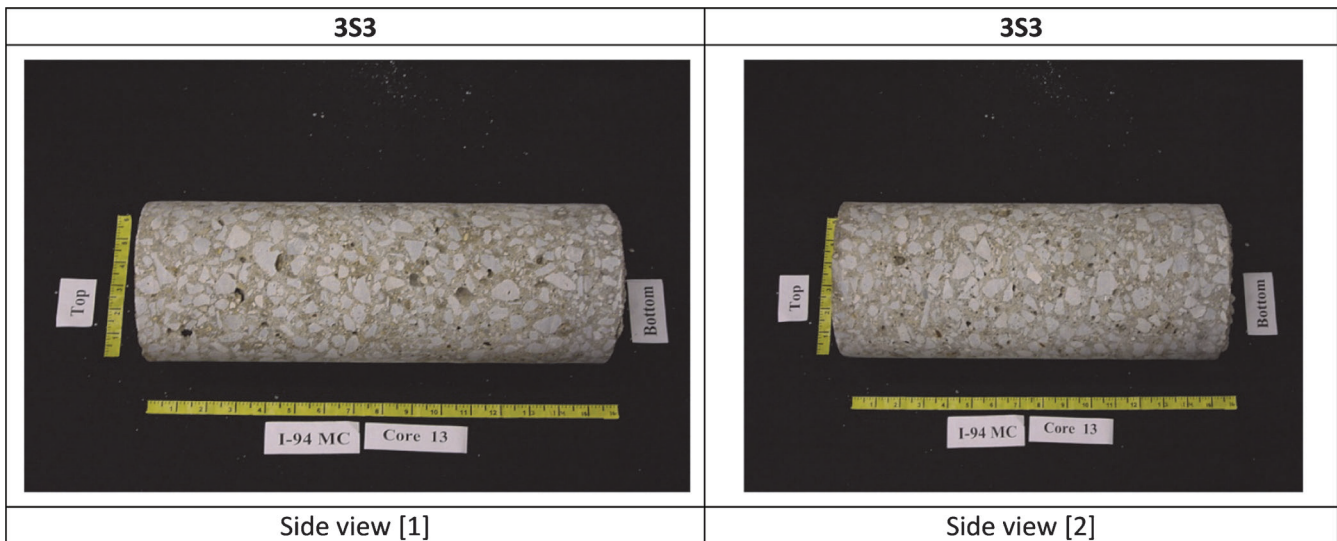
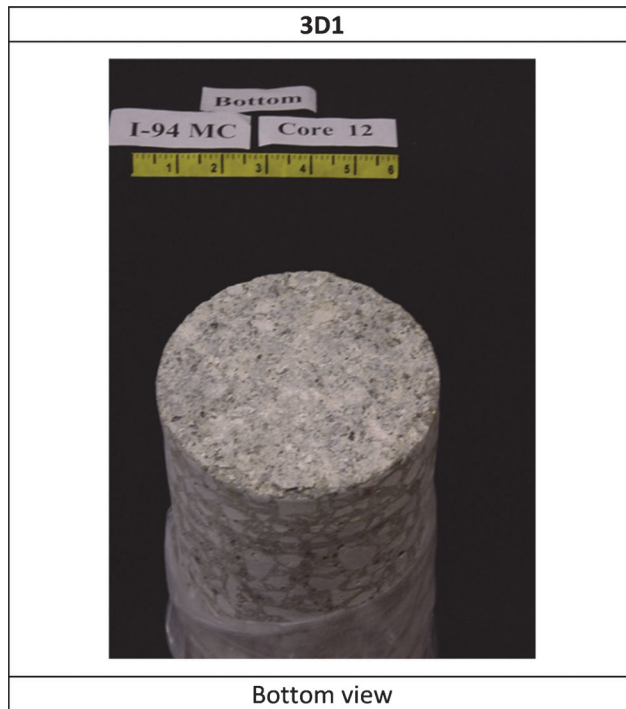
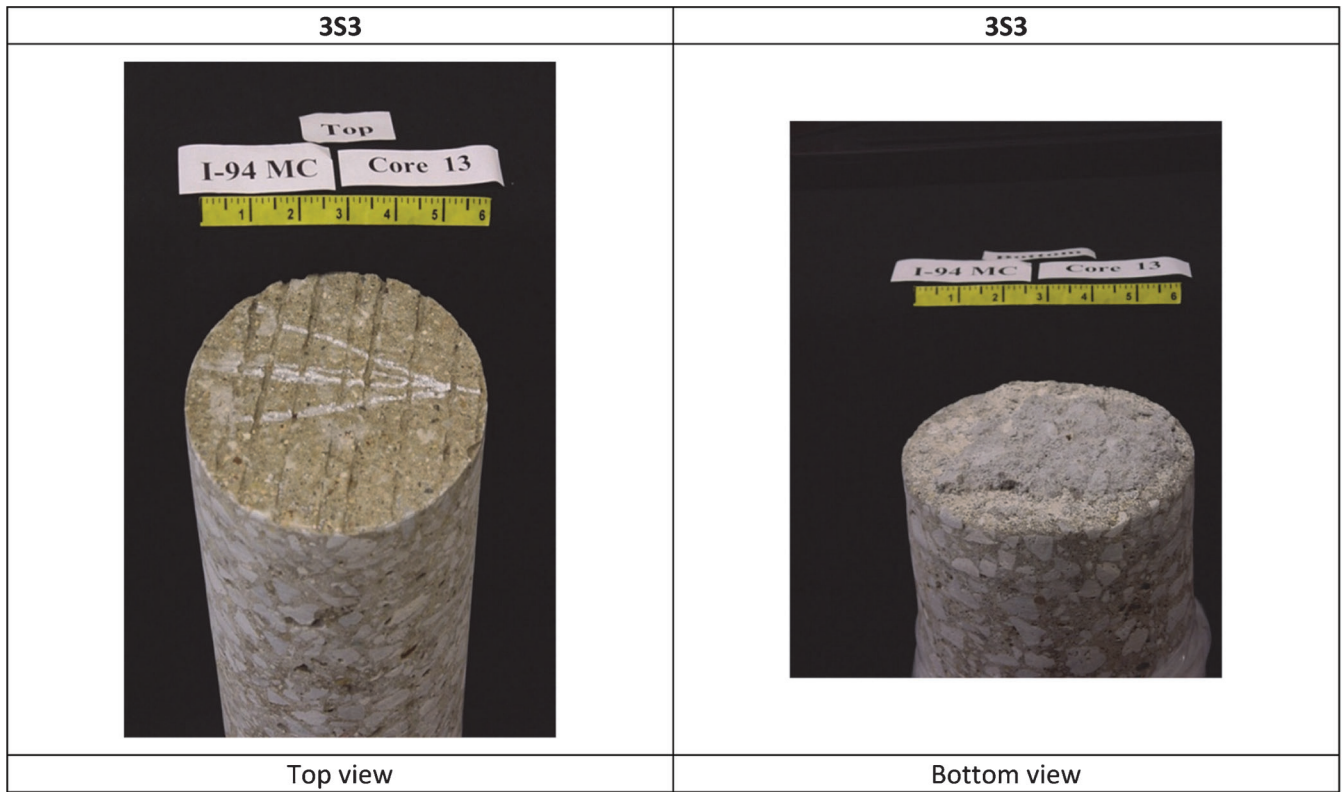


Figure B.2 Continued.



SECTION 4

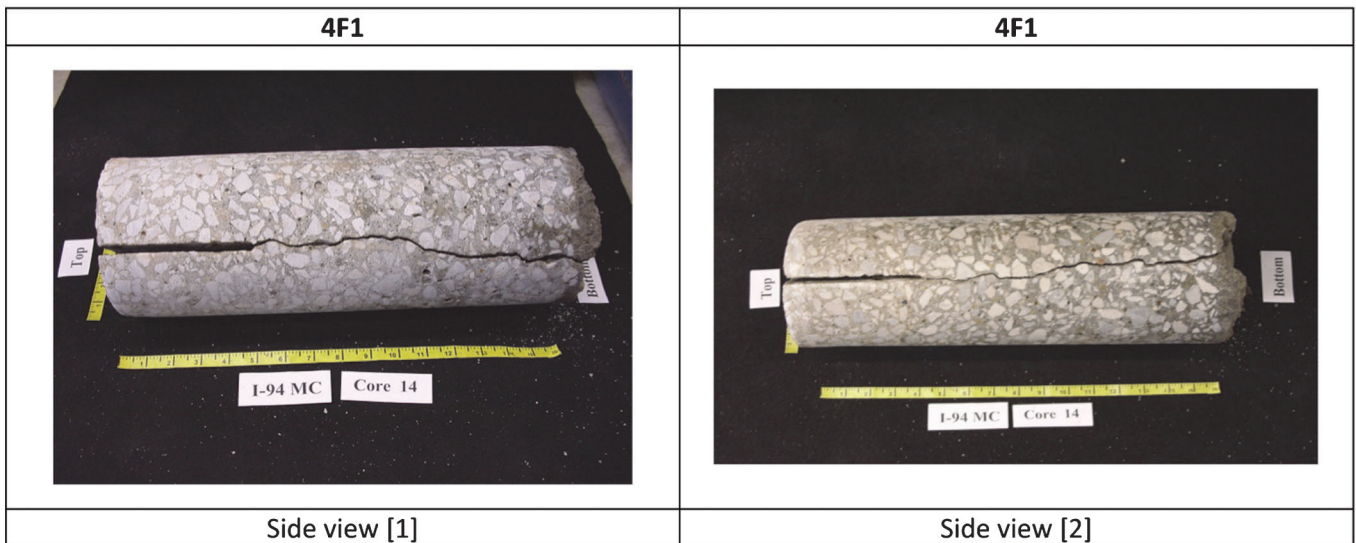


Figure B.2 Continued.

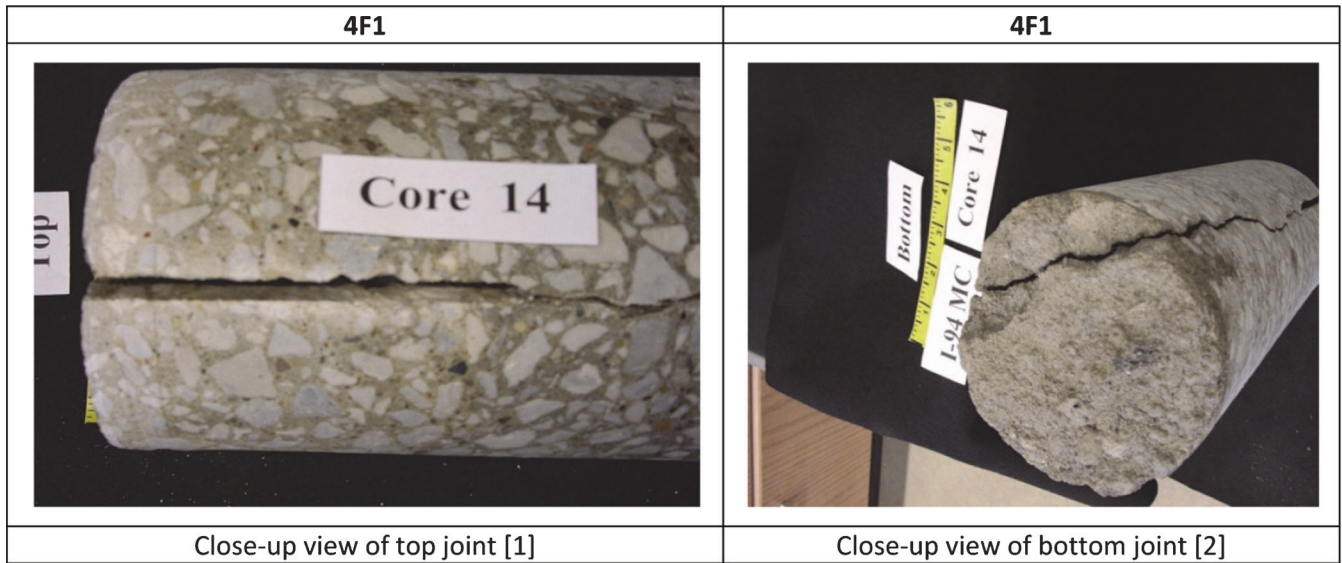
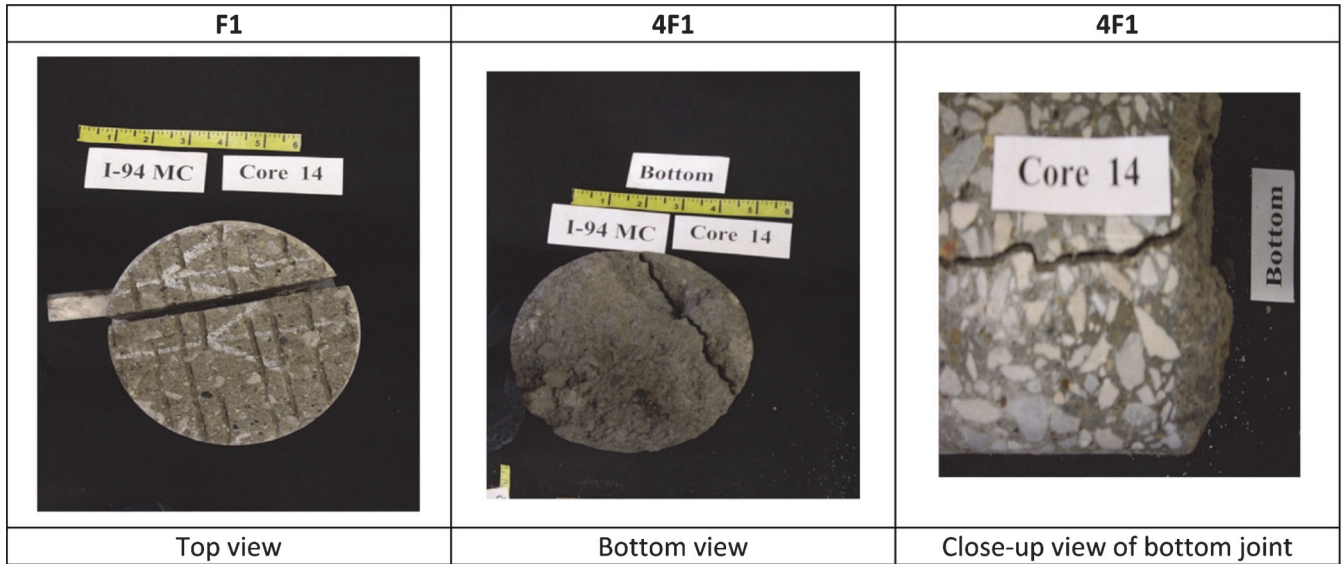


Figure B.2 Continued.

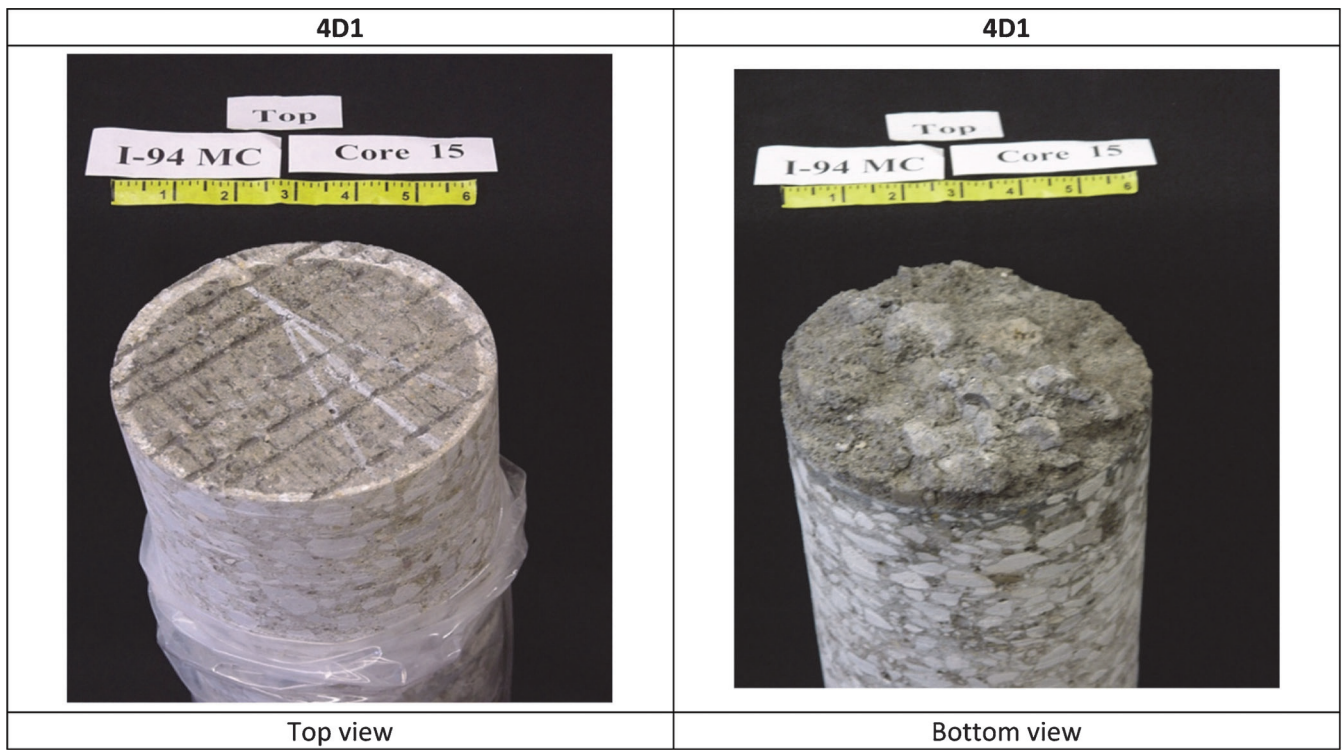
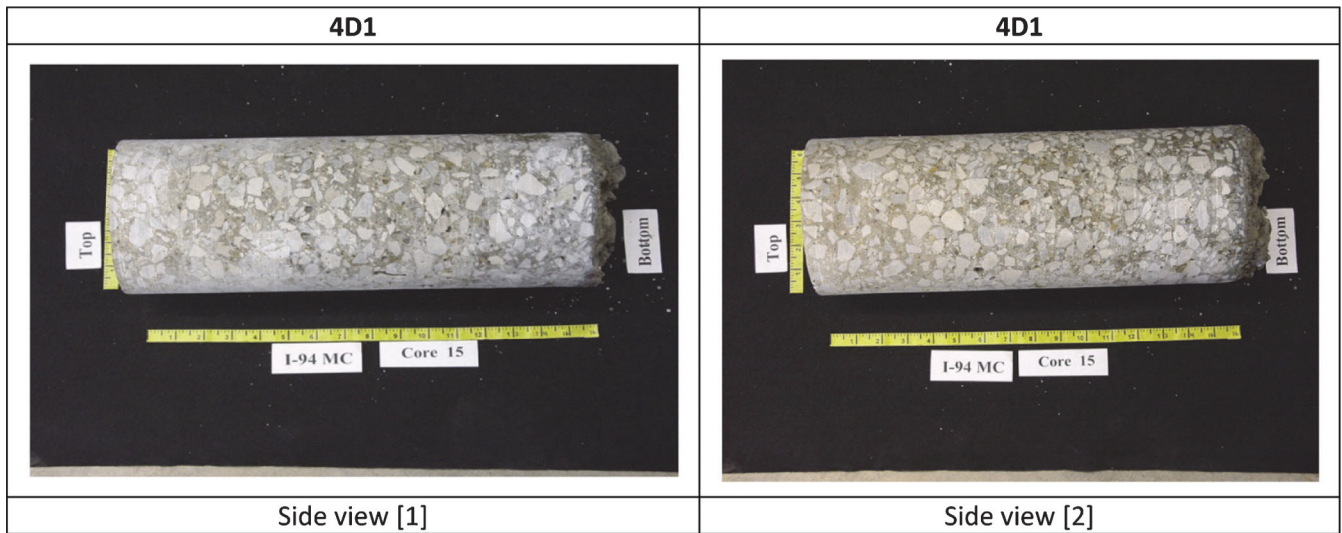


Figure B.2 Continued.

SECTION 5

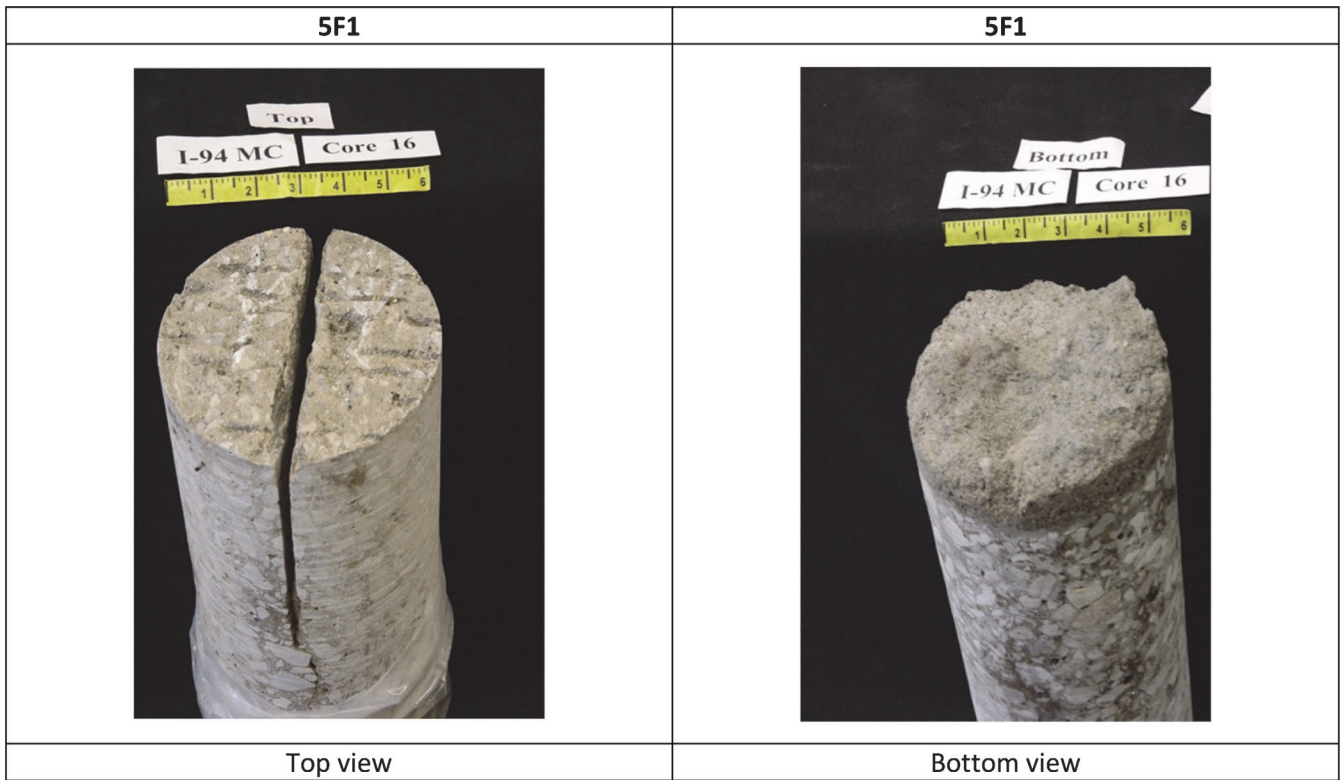
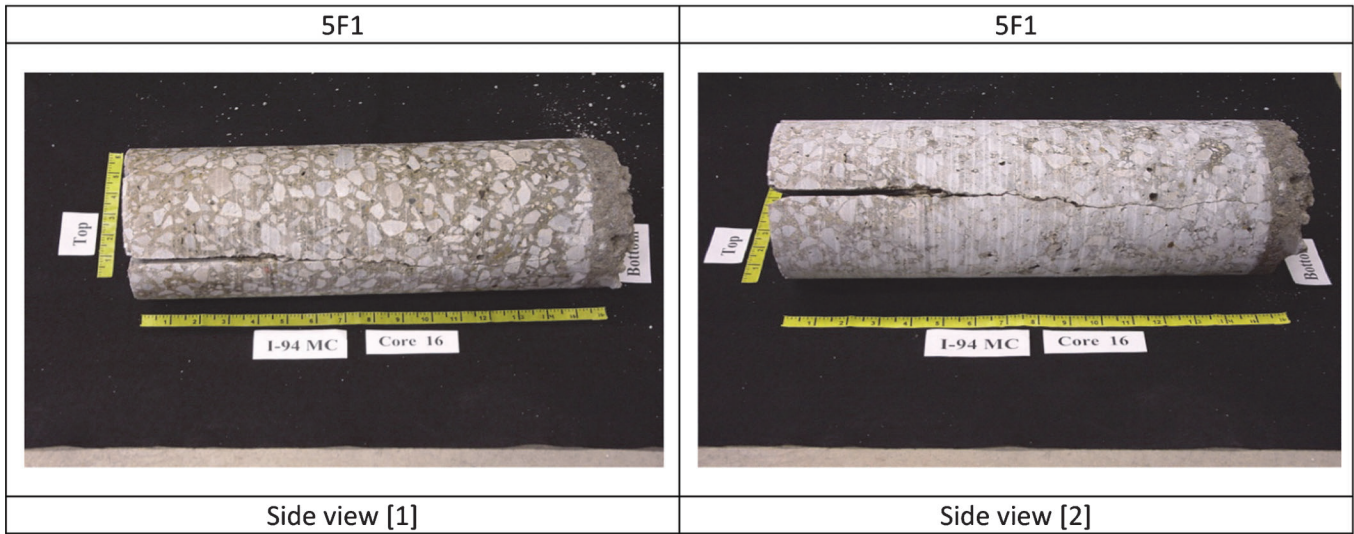


Figure B.2 Continued.

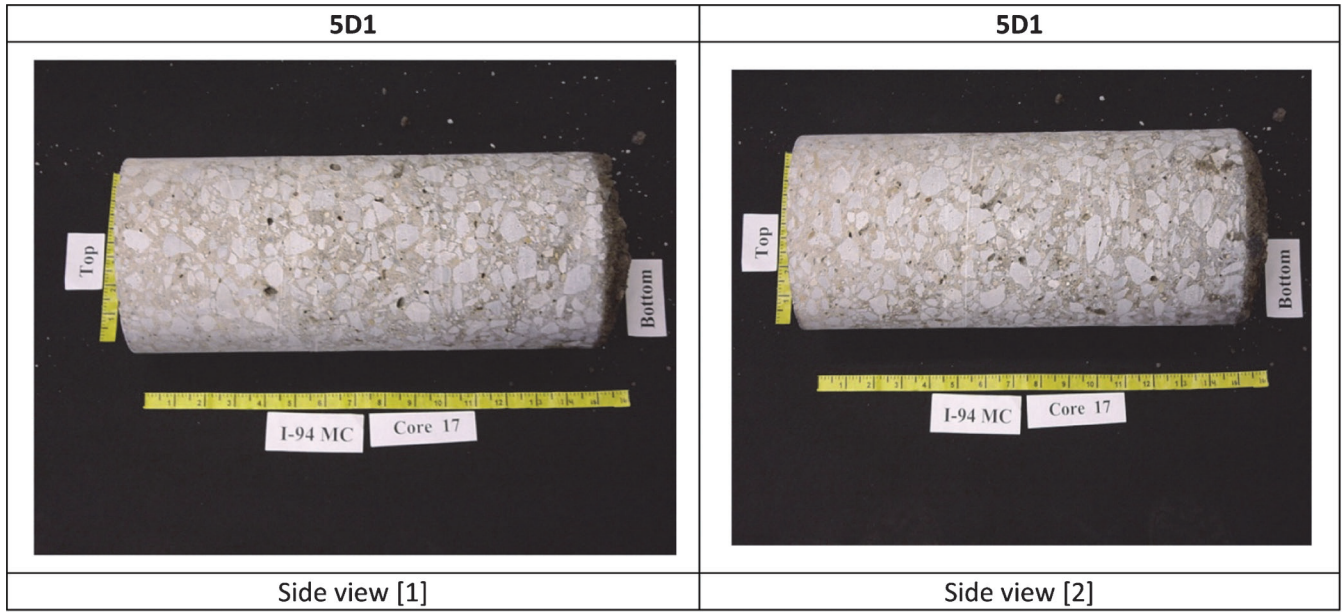
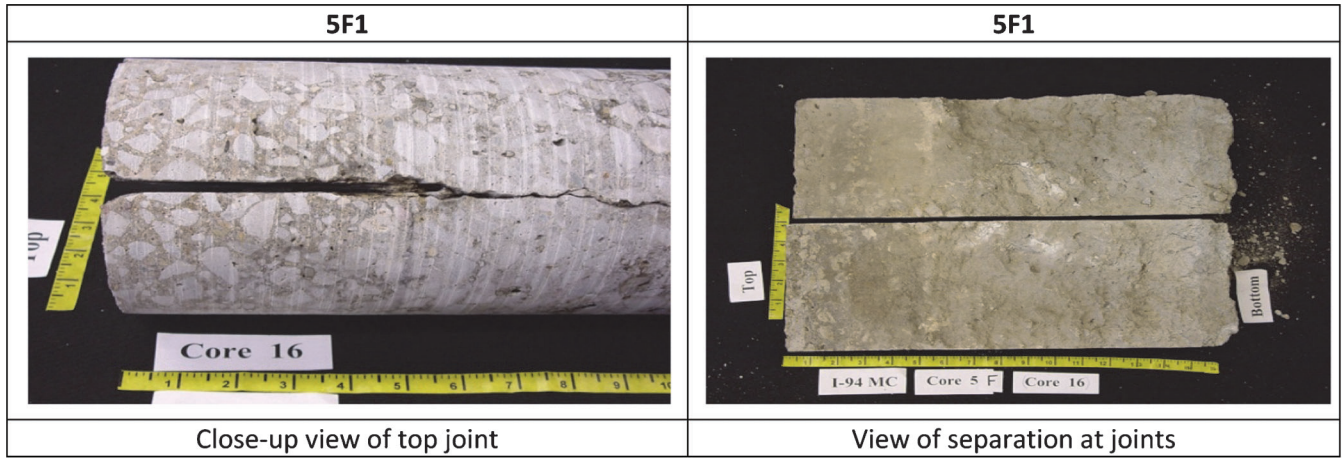


Figure B.2 Continued.

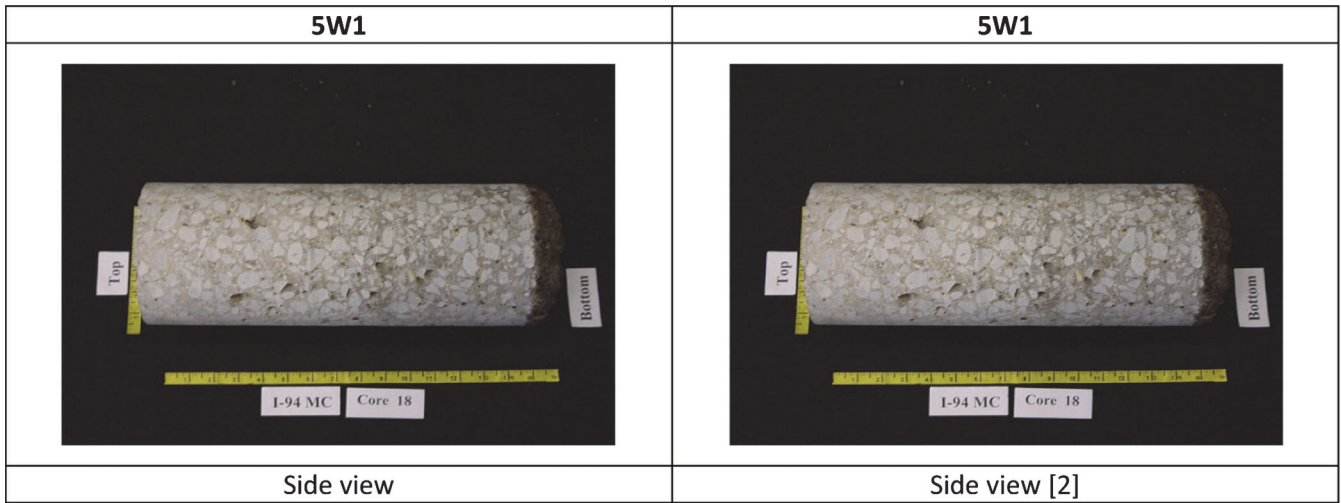
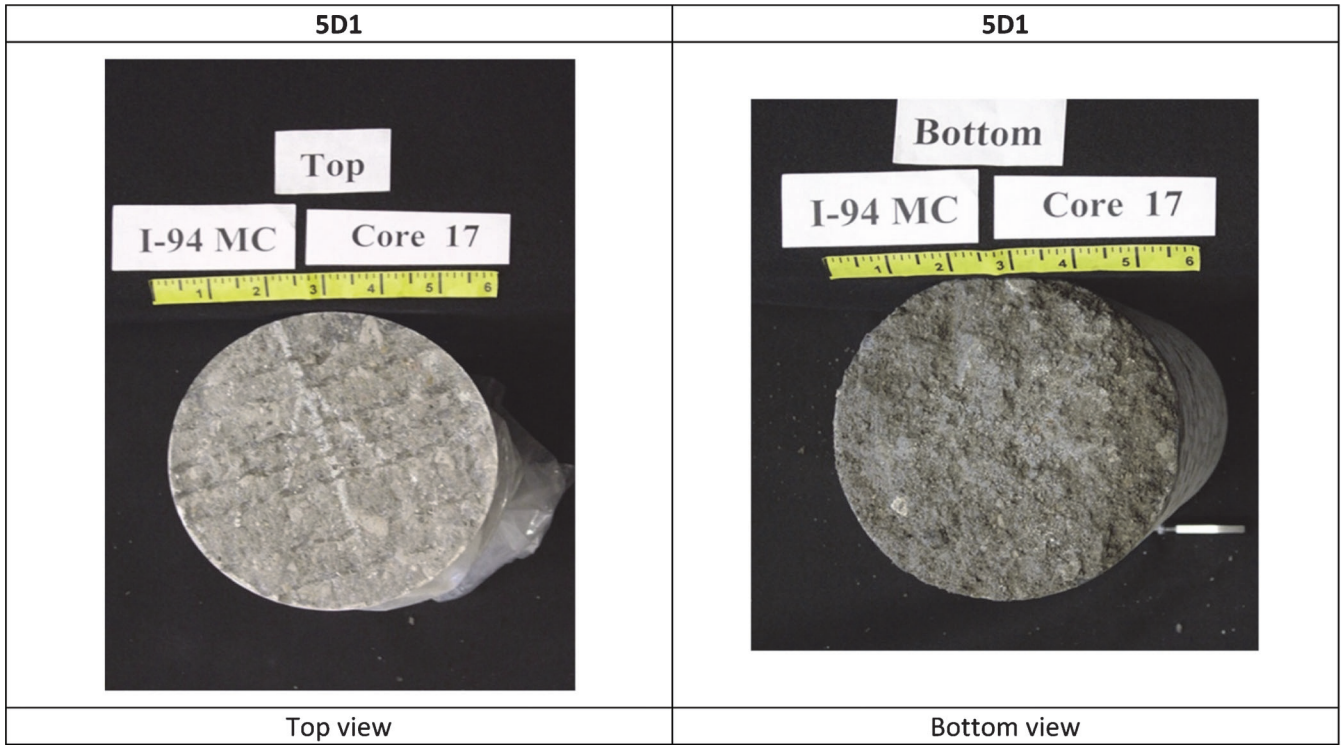


Figure B.2 Continued.

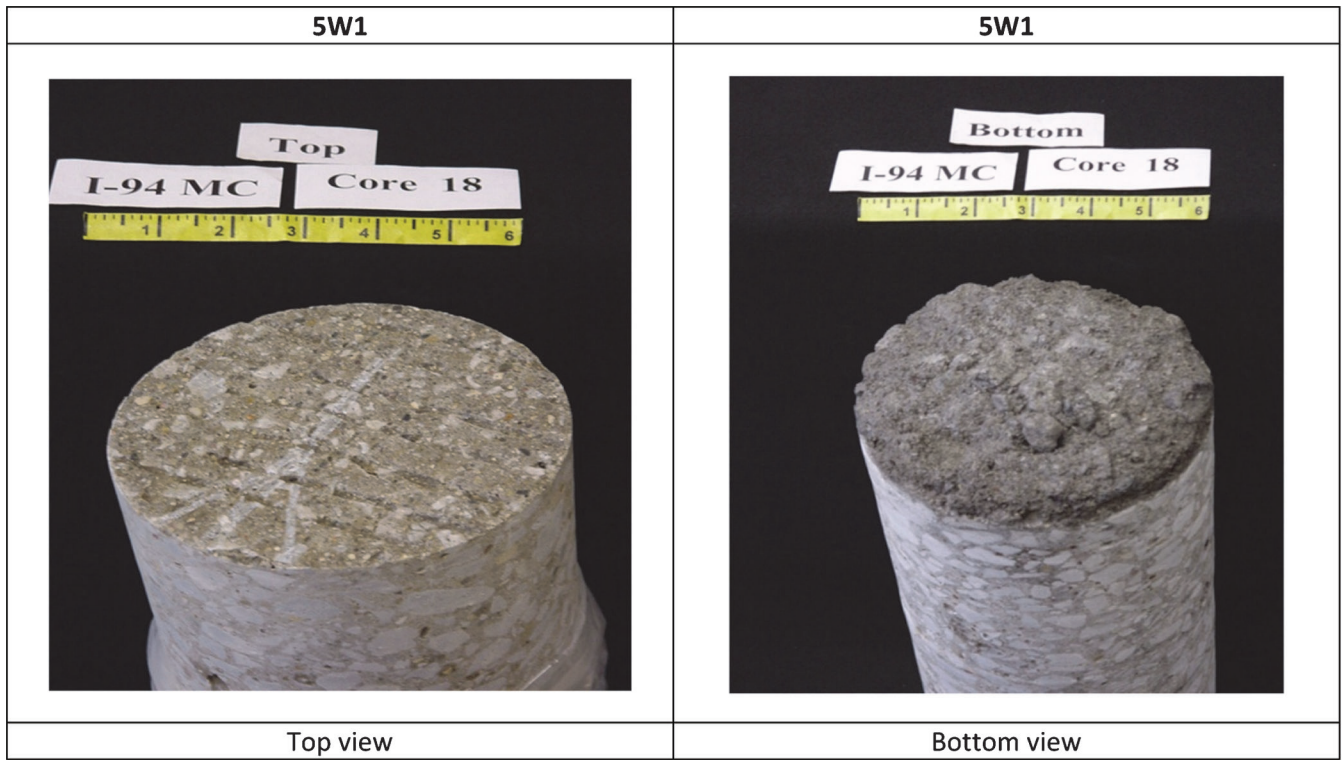


Figure B.2 Continued.

APPENDIX C. TESTS AND TESTING RESULTS

TESTS AND TEST SPECIMENS

Initial testing included megascopic examinations, chloride analysis and air void analyses. All cores were examined megascopically and under low magnification noting any cracks, segregation or obvious differences in the aggregate or paste within the core and between cores. All cores were tested for chloride contents (per ASTM C 1556) developing a chloride concentration profile in the horizontal direction parallel from the joint face inward for near-joint cores and in the vertical direction (with depth) for all other cores.

The existing air void system was evaluated in all cores taken in the mid-panel and at or near joints following ASTM C457 (cores 1–6, 8–12, 14–17). Sample prep of 15 polished slabs for air void analyses were completed and the air void system parameters were identified using an automated image analysis system on processed scanned images of the polished slabs per a technique developed at Michigan Technological University and practiced at Purdue. This image analysis system simulates a linear traverse according to the criteria established in ASTM C457, Modified Point Count Method. The more traditional, manual method for the modified point count method was completed on four of the samples, for comparison, which was similar to the procedure used in the original Part I study. Test procedures and sample preparation were as followed and documented for Part I (1).

Micro-analyses initially included SEM and XRD analysis: Of these 2 tests the SEM examination provided the most insights into

the microstructure of the paste and air void system. Besides looking at the basic microstructure the SEM was used to determine if the air void system was compromised by infilling with secondary minerals and if so what those minerals were (e.g., ettringite, Friedel's salt or other products). XRD was performed on some samples and results were very similar to results of samples from the original study. Because these results provided no additional insights that were not already provided in more detail from the SEM examinations the XRD analysis was discontinued in favor of more extensive SEM work. The test procedures and sample preparation were similar to the original study and details can be found in Arribas-Colon, 2008 MS thesis (1).

Freeze-thaw testing (F-T) of samples from mid-panel cores and cores from other locations within the slab were compared to samples taken at the joints in order to better understand the F-T durability of the concrete at different locations within the project and within the slab, and to better understand how the existing air void system or possibly other variables may have related to the remaining F-T durability of the concrete. The test procedures and sample preparation were similar to the original study and details can be found in Arribas-Colon, 2008 MS thesis (1).

ADDITIONAL DATA COLLECTION AND ANALYSIS

Chloride Analysis included measuring both the water soluble and acid soluble chloride content. The acid soluble chloride content is sometimes referred to as the total chlorides. All test results are shown in figures C.1 and C.2.

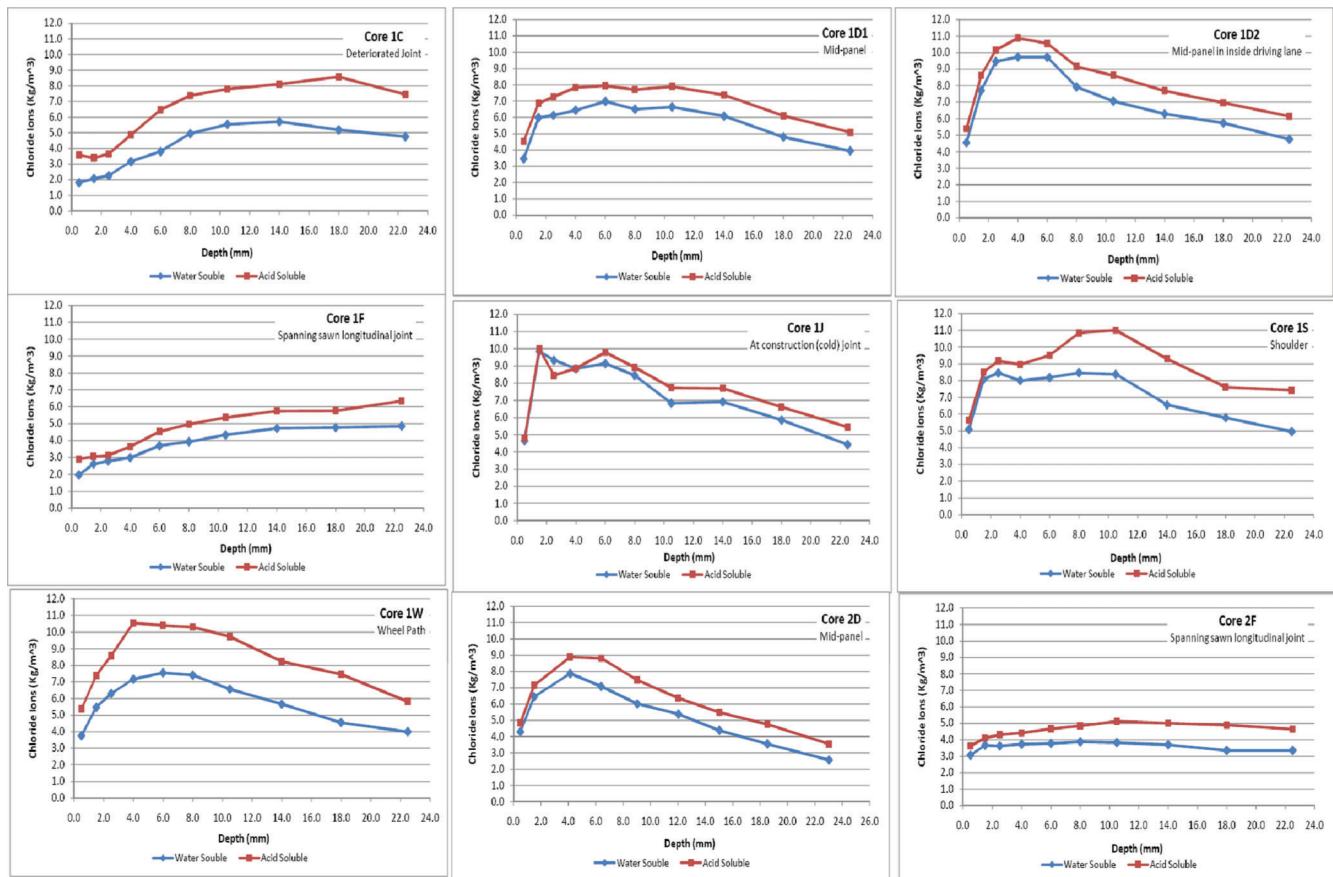


Figure C.1 Chloride analyses for cores taken in Sections 1 and 2.

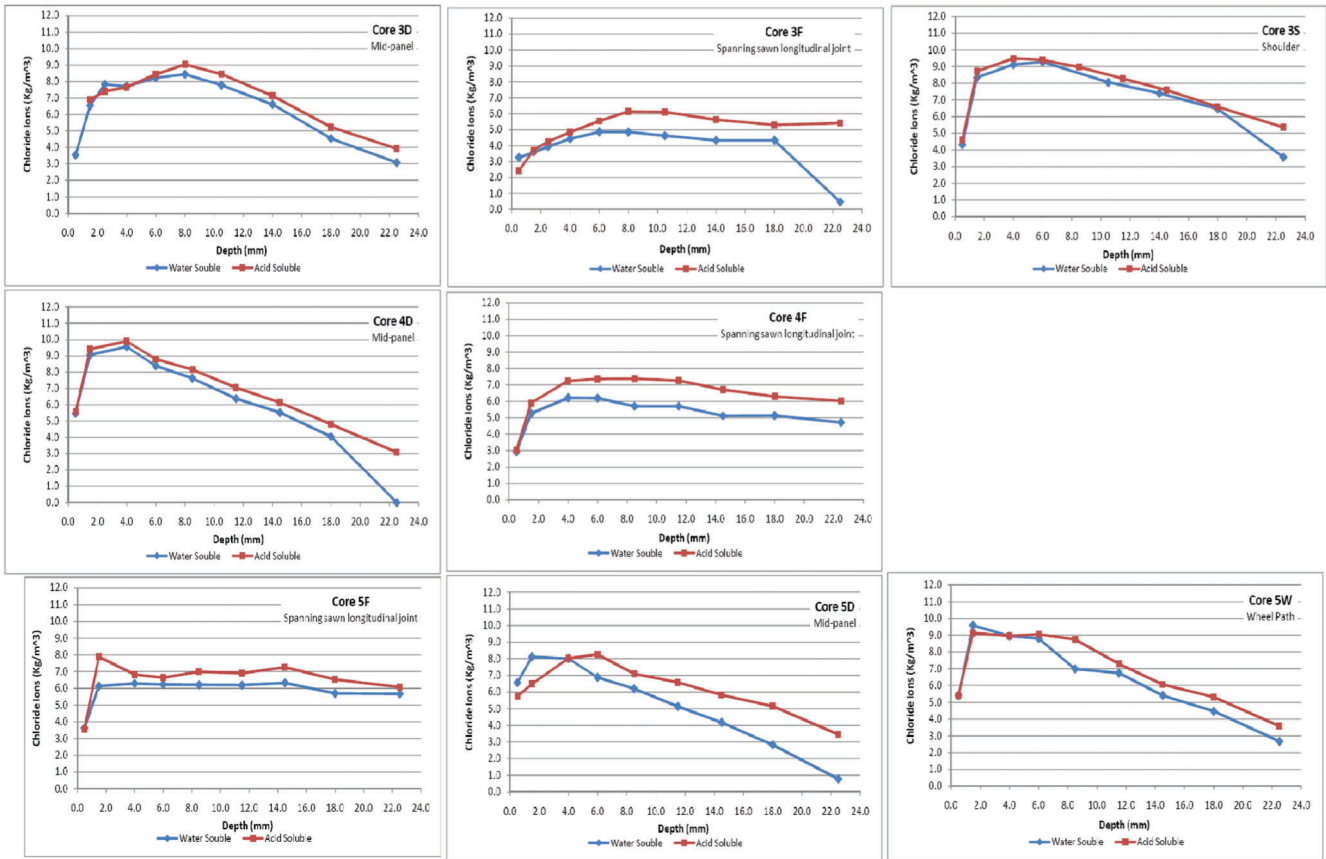


Figure C.2 Chloride analyses for cores taken in Sections 3, 4 and 5.

FREEZE-THAW TEST RESULTS

The freeze-thaw test results for all specimens are summarized in Figure C.3. The “B” and “T” used in the alpha-numerical sample designations indicate if the test sample was cut from near the top of the core (T) or bottom of the core (B).

Location	Core	Sample	Rel Dym Mod	Avg Rel Dyn Mod	%mass loss	Avg %mass loss	
1	C	NA					
	D1	B1	90.5	91.6	0.04%	0.19%	
		B2	91.8		0.32%		
		T1	87.0		0.26%		
		T2	97.2		0.13%		
	D2	B1	96.8	96.4	0.06%	0.08%	
		B2	96.7		0.06%		
		T1	96.9		0.12%		
		T2	95.3		0.09%		
	F	B1	88.2	86.4	3.10%	2.68%	
		T1	81.1		4.94%		
		T2	89.9		2.26%		
	J	B1	93.8	93.1	0.35%	0.38%	
		B2	92.7		0.25%		
		T1	93.5		0.29%		
		T2	92.3		0.68%		
	S	B1	95.0	95.0	0.04%	0.06%	
		B2	91.6		0.10%		
T1		95.9	0.04%				
T2		97.5	0.07%				
W	B1	92.8	93.0	0.11%	0.08%		
	T1	96.8		0.39%			
	T2	89.5		0.05%			
2	D	B1	94.0	96.1	0.076%	0.07%	
		B2	96.0		0.068%		
		T1	96.3		0.086%		
		T2	98.1		0.064%		
	F	B1	94.9	90.5	0.425%	0.381%	
		B2	75.4		0.202%		
		T1	94.7		1.112%		
		T2	94.1		0.126%		
T3	93.3	0.038%					

Location	Core	Sample	Rel Dym Mod	Avg Rel Dyn Mod	%mass loss	Avg %mass loss
3	D	B1	87.9	94.3	0.125%	0.04%
		T1	97.7		0.000%	
		T2	96.4		0.000%	
		T3	95.3		0.022%	
	F	B1	96.7	96.5	0.061%	0.13%
		T1	96.9		0.197%	
		T2	98.0		0.021%	
		T3	94.5		0.232%	
	J	T1	96.1	95.5	0.188%	0.36%
		T2	96.6		0.284%	
		T3	94.1		0.458%	
		T4	95.2		0.517%	
	S	B1	96.2	96.6	0.211%	0.12%
		B2	97.7		0.000%	
		B3	95.7		0.067%	
		3S	95.6		0.152%	
T1		98.8	0.251%			
c	95.9	0.050%				
4	D	B1	97.2	98.9	0.161%	0.06%
		T1	101.6		0.075%	
		T2	99.4		0.022%	
		B2	97.4		0.000%	
	F	T1	96.0	95.3	0.337%	0.26%
		T2	95.8		0.244%	
		T3	94.1		0.179%	
5	D	B1	98.3	96.6	0.065%	0.10%
		B2	95.3		0.166%	
		T1	96.5		0.045%	
	F	T2	96.2	95.9	0.110%	0.58%
		B1	95.8		0.054%	
		T1	95.2		0.494%	
	W	T3	96.8	94.4	1.103%	0.37%
		B1	97.8		0.000%	
B2		97.9	0.046%			
T1		86.0	1.335%			
T2	95.9	0.118%				

Figure C.3 Freeze-thaw test results of all specimens tested.

APPENDIX D. SEM RESULTS

SEM specimens were made from concrete from 14 of the 18 pavement cores retrieved. The features described in this appendix are from five concrete specimens and represent all of features observed. The first number in samples 1, 3, 4 or 5 indicated the pavement section from which the samples came. The letters indicate the following:

D = mid-panel
W = wheel path
S = shoulder

The specimens were prepared according to proper techniques for Scanning Electron Microscope analysis with Energy Dispersive X-ray spectroscopy (SEM/EDX). More specifically, the samples for SEM/EDX investigation were cut using a slow speed diamond saw cooled with mineral oil. The samples were then dried in an oven at 50°C for 3 days, vacuum-impregnated with a low-viscosity epoxy, lapped and polished using a special procedure. A strip of conductive copper tape was then attached to each polished sample, after which they were coated with a thin layer of palladium for about a minute using a Hummer®6.2 sputter coater.

Each specimen was prepared in such a way that the polished face examined was a cut made perpendicular to the pavement

surface and the top of the polished surface was the top of the original pavement surface.

Each of the samples was thoroughly examined using Aspex®LLC personal Scanning Electron Microscope (SEM) in the backscatter mode using an acceleration voltage of 15 kV. Between examinations, the specimens were stored in a vacuum desiccator to protect them from laboratory humidity.

Terms used in this report include:

Ettringite (Candlot's salt) - $3\text{CaO} \cdot \text{Al}_2\text{O}_3 \cdot 3\text{CaSO}_4 \cdot 32\text{H}_2\text{O}$.

Gypsum - $\text{CaSO}_4 \cdot 2\text{H}_2\text{O}$.

Friedel's salt - $3\text{CaO} \cdot \text{Al}_2\text{O}_3 \cdot \text{CaCl}_2 \cdot 10\text{H}_2\text{O}$.

Thaumasite - $\text{Ca}_3[\text{Si}(\text{OH})_6] \cdot \text{CO}_3 \cdot \text{SO}_4 \cdot 12\text{H}_2\text{O}$ or $\text{Ca}_6[\text{Si}(\text{OH})_6]_2(\text{CO}_3)_2(\text{SO}_4)_2 \cdot 24\text{H}_2\text{O}$.

Figure D.1 shows nine images of features seen in specimen 1S, from the core taken in the shoulder in Section 1. Figure D.2 shows nine images of features seen in specimen 1W from the core taken in the wheel path in Section 1. Figure D.3 shows eight images of features seen in specimen 3S from the core taken in the shoulder in Section 3. Figure D.4 shows nine images of features seen in specimen 4D from the core taken in the mid-panel Section 4. Figure D.5 shows ten images of features seen in specimen 5W from the core taken in the wheel path, Section 5.

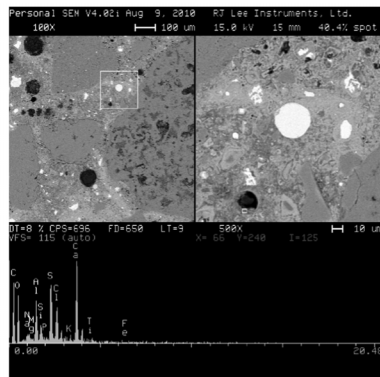


Fig. 1S-1
Mix of ettringite and Friedel's salt in empty air-void, anhydrous cement grains, x500

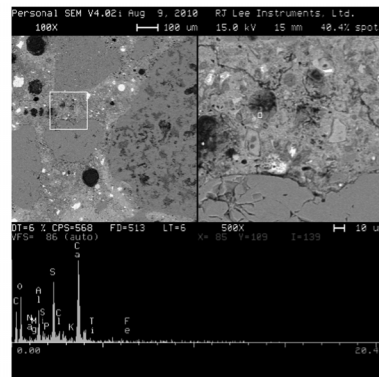


Fig. 1S-2
Needles of ettringite in air-void, dense microstructure, a few empty microcrack, empty air-voids, x500

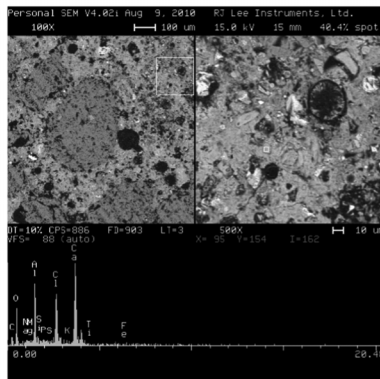


Fig. 1S-3
Friedel's salt in cement matrix, ettringite in air-void, x500

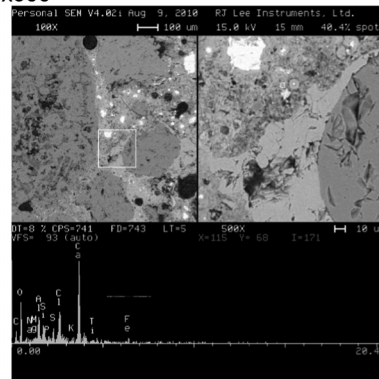


Fig. 1S-4
Friedel's salt in a matrix, traces of S (small amount of ettringite), dense ITZ, x500

Figure D.1 Specimen 1S.

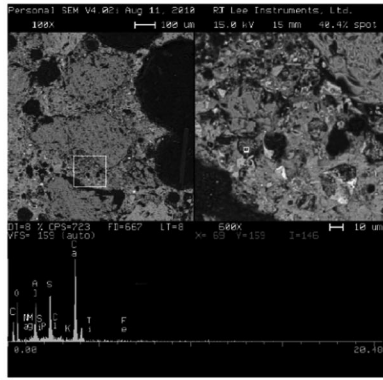


Fig. 1S-5,
Ettringite located in a small air-void (10 μm), x 600

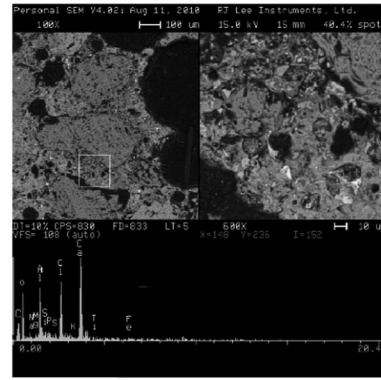


Fig. 1S-6
Friedl's salt, x600

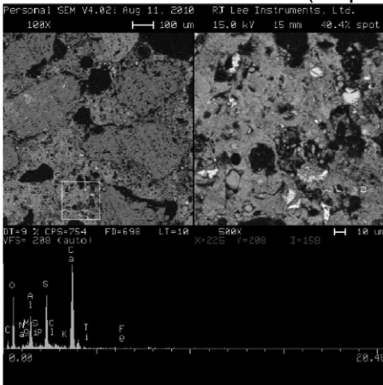


Fig. 1S-7
Ettringite in matrix, x500

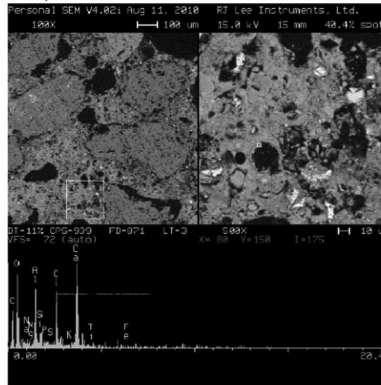


Fig. 1S-8
Friedl's salt in empty air-void (15 μm), x500

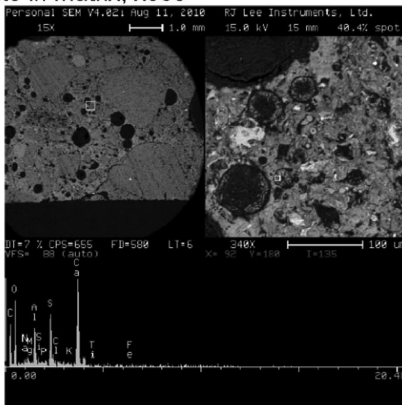


Fig. 1S-9
Ettringite fills the empty air-voids, x 500

Figure D.1 Continued.

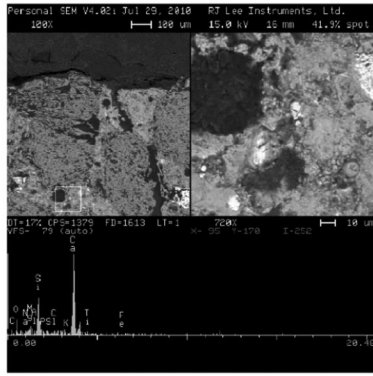


Fig. 1W-1
Top of the specimen, fly ash particle, empty air-void, partially reacted cement grain, empty crack between aggregate, x720

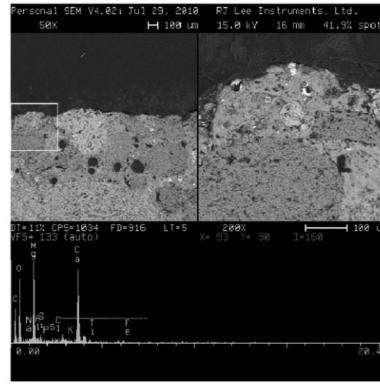


Fig. 1W-2
Dolomite particle on the surface of the specimen, x200

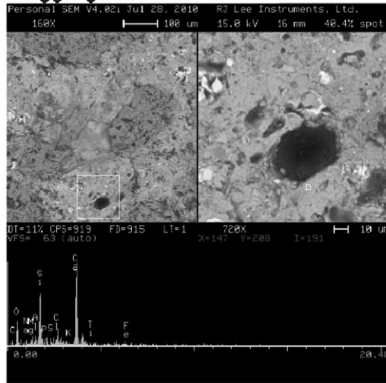


Fig. 1W-3
Empty air-void, dense matrix built with C-S-H, a few anhydrous cement grains, x720

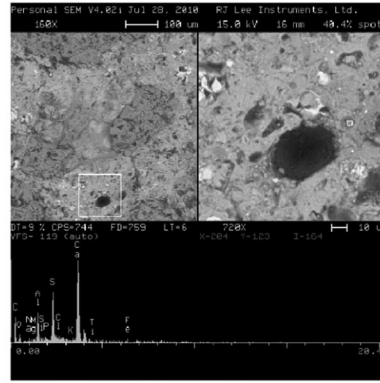


Fig. 1W-4
The same structure as on Fig.1W-3 but the ettringite in air-void is visible, x720

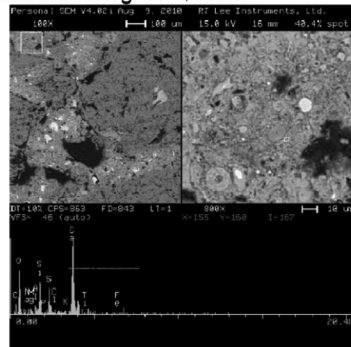


Fig. 1W-5
Porous coarse aggregate, traces of thaumasite, many anhydrous cement grains, x 800

Figure D.2 Specimen 1W.

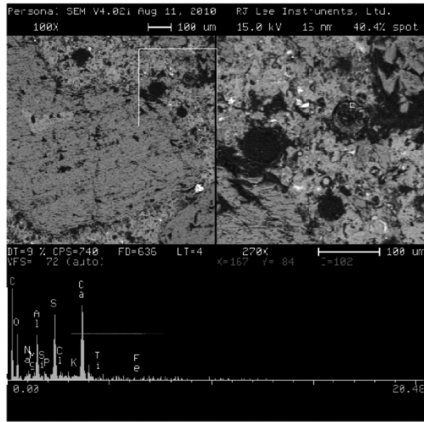


Fig. 1W-6
Ettringite in air-void (50 μm), a few unreacted cement particles, x270

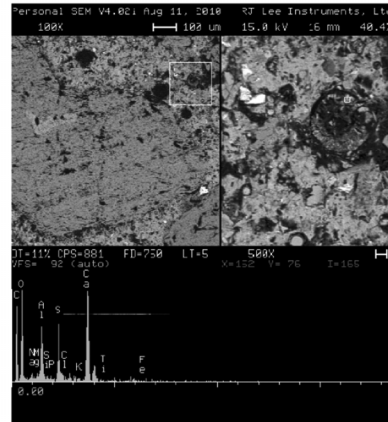


Fig. 1W-7
The same area as Fig. 1W-6, fly ash parti visible, magnification x500

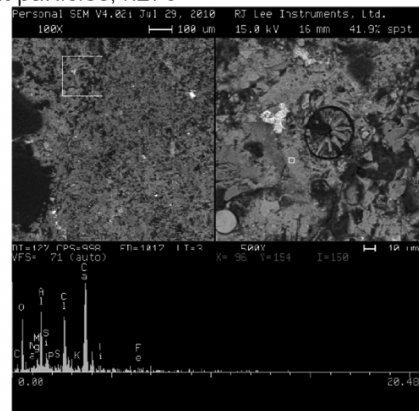


Fig. 1W-8
Friedl's salt in a matrix, x 500

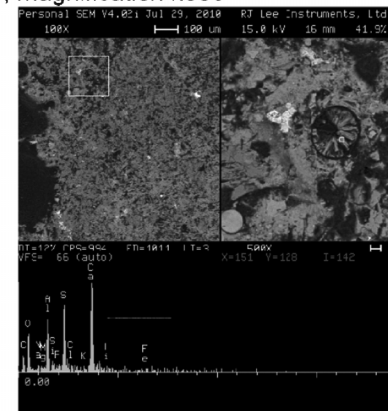


Fig. 1W-9
The same area as Fig. 1W-8, air-void filled ettringite, x 500

Figure D.2 Continued.

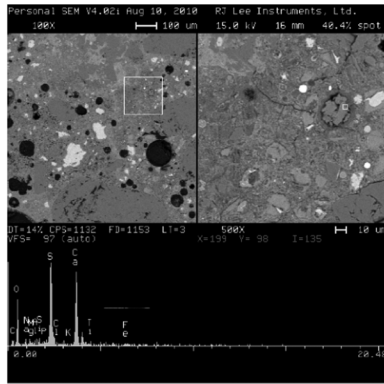


Fig. 3S-1
Gypsum in air-void, many empty air-voids, small empty micro-crack in the matrix, x 500

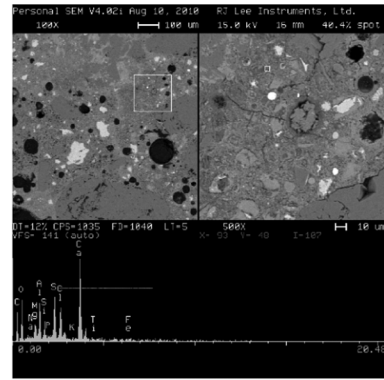


Fig. 3S-2
Traces of ettringite and Friedl's salt, x500

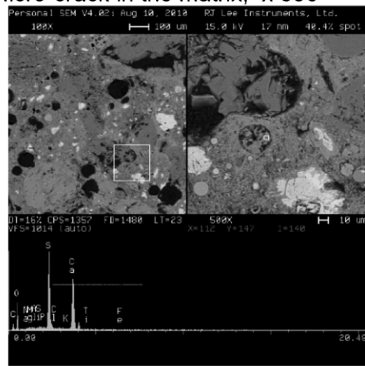


Fig. 3S-3
1 mm from the surface, presence of gypsum in air-void, many fly ash particles, x500 (picture from the left - many of unhydrated cement grains)

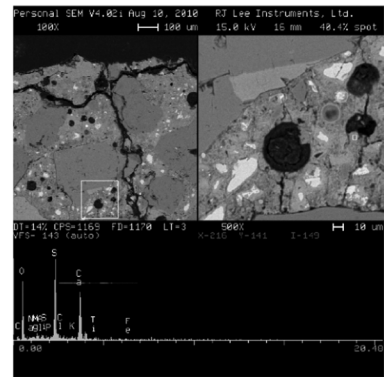


Fig. 3S-4
Air-void partially filled with gypsum, empty cracks near the surface, x 500

Figure D.3 Specimen 3S.

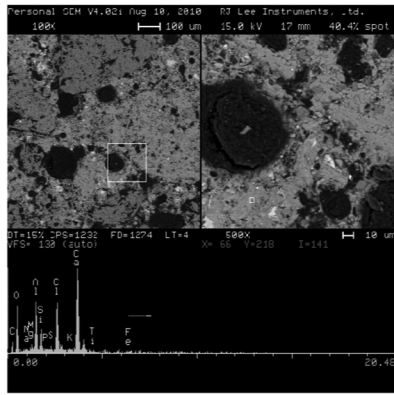


Fig. 3S-5
Friedl's salt in a matrix, porous cement matrix,
a few unhydrated cement grains, x 500

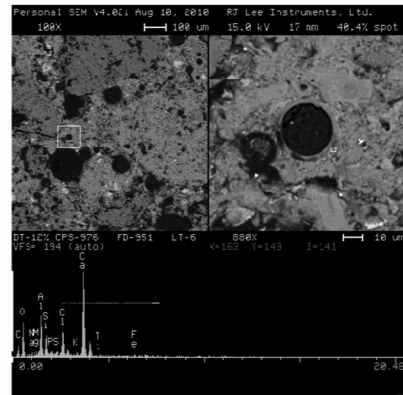


Fig. 3S-6
Friedl's salt around the empty air-void, x 500

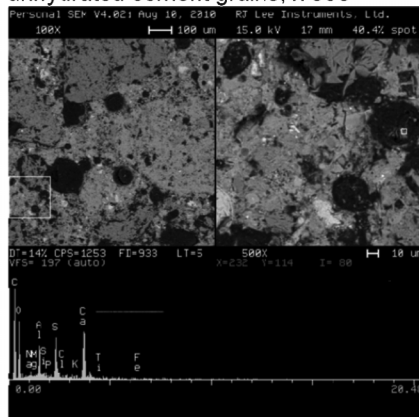


Fig. 3S-7
Ettringite located on the bottom of the air-void,
x 500

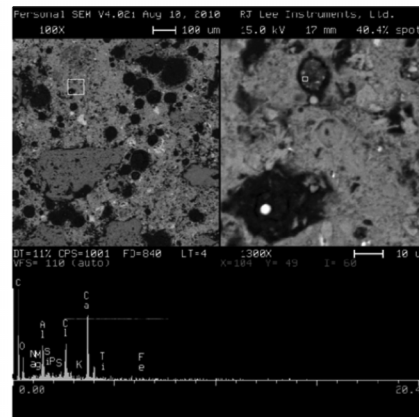


Fig. 3S-8
Friedl's salt located in the small (5 μm) air-void,
x 1300

Figure D.3 Continued.

Distance from surface 0-2 mm

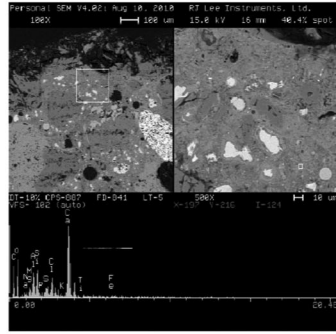


Fig. 4D-1
Surface of the specimen, traces of the Cl and Al – Friedl's salt, traces of the Al and S – ettringite, many unhydrated cement grains, x 500

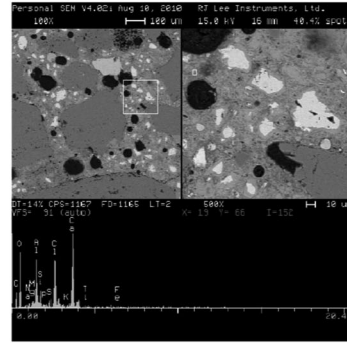


Fig. 4D-2
Friedl's salt in a matrix, many unhydrated cement grains, x 500

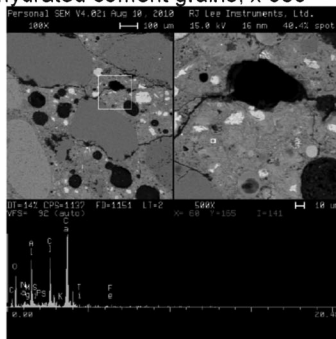


Fig. 4D-3
Another location of Friedl's salt in a matrix, empty air-voids, x 500

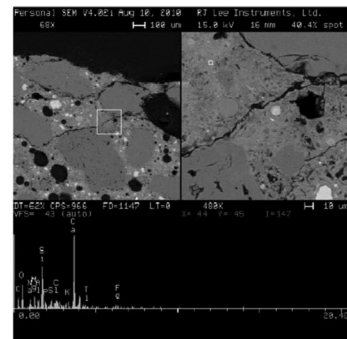


Fig. 4D-4
Empty cracks parallel to the surface (probably caused by freezing and thawing).

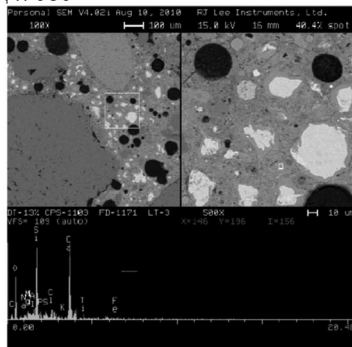


Fig. 4D-5
Many anhydrous cement grains, empty air-voids, x 500

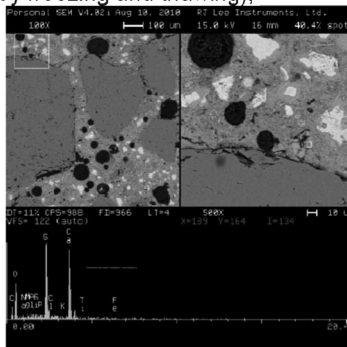


Fig. 4D-6
Gypsum near the coarse aggregate, x 500

Figure D.4 Specimen 4D.

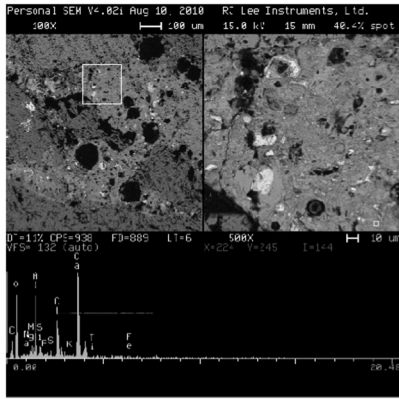


Fig. 4D-7
Friedl's salt in a matrix, a few anhydrous cement grains, x 500

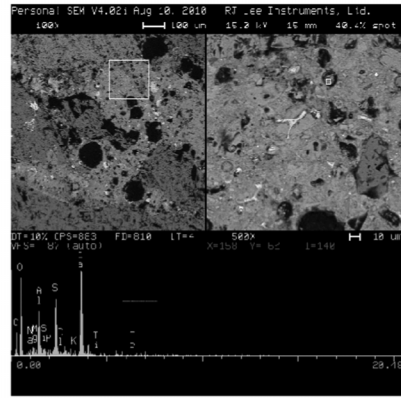


Fig. 4D-8
Ettringite in small (10 µm) air-void, x 500

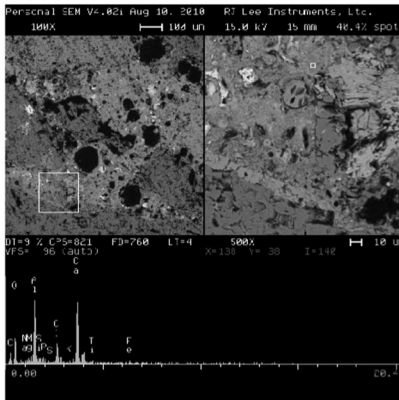


Fig. 4D-9
Friedl's salt in a matrix, x 500

Figure D.4 Continued.

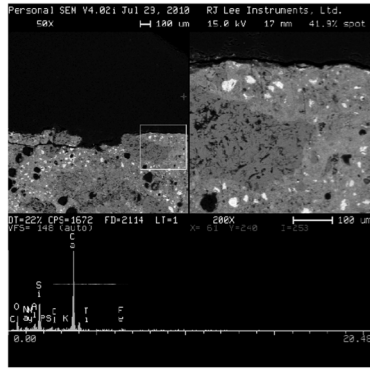


Fig. 5W-1
Surface of the specimen, many unreacted cement grains, dense microstructure, x 200

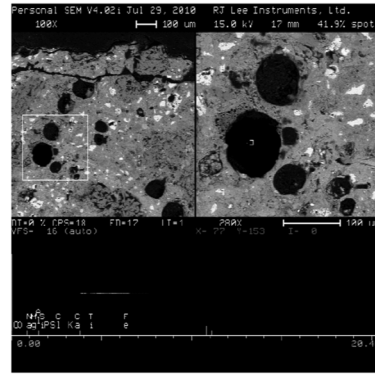


Fig. 5W-2
Empty air-voids, empty crack propagates parallel the surface, x 280

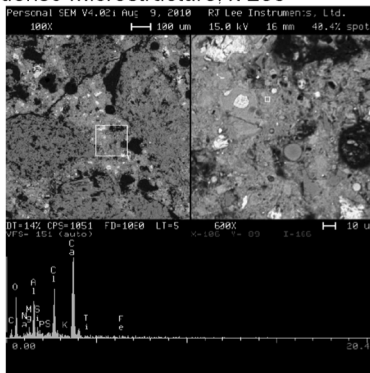


Fig. 5W-3
Friedl's salt in a matrix, empty microcrack, fly ash particle, x 600

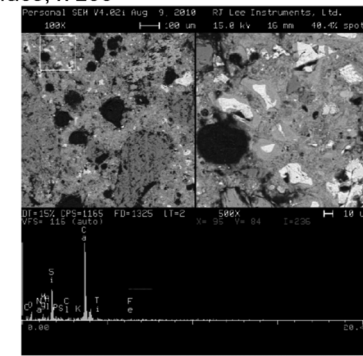


Fig. 5W-4
Many unhydrated cement grains, x 500

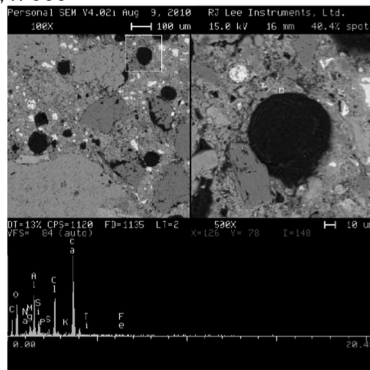


Fig. 5W-5
Friedl's salt around empty air-voids, x500

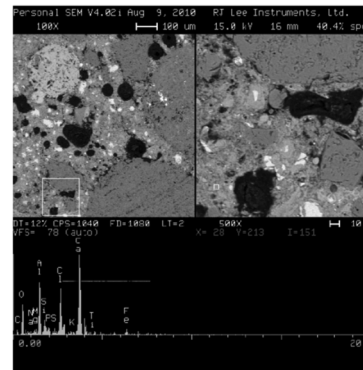


Fig. 5W-6
Friedl's salt, x 500

Figure D.5 Specimen 5W.

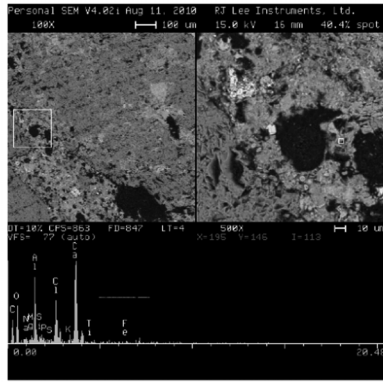


Fig. 5W-7
Friedl's salt between empty air-voids, x 500

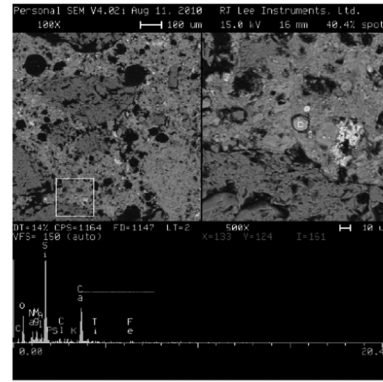


Fig. 5W-8
Fly ash particle (about 10 µm), x 500

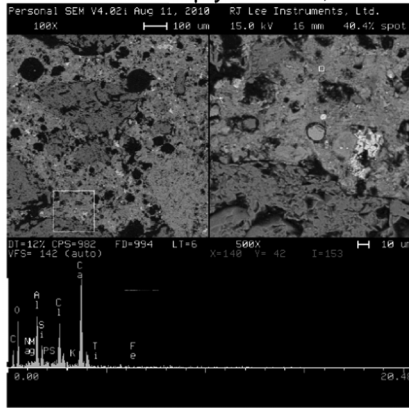


Fig. 5W-9
Friedl's salt with traces of Si, x 500

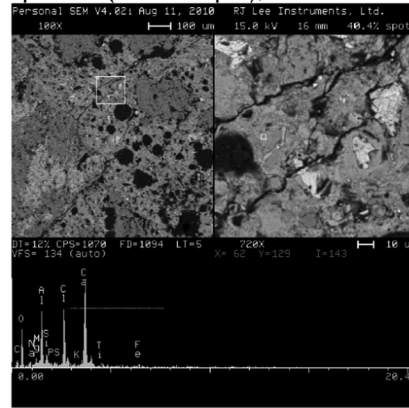


Fig. 5W-10
Friedl's salt in a matrix, empty cracks propagated only through the matrix not through the aggregate, x 720

Figure D.5 Continued.